Calhoun
Institutional Archive of the Naval Postgraduate School

Calhoun: The NPS Institutional Archive

DSpace Repository

Theses and Dissertations | Thesis and Dissertation Collection

1978-06

Mass, salt, and heat transport across seven latitude circles in the North Atlantic Ocean: a description of the general circulation based on geostrophic calculations from international geophysical year and adjacent data

Baker, Timothy L.

Monterey, California. Naval Postgraduate School

http://hdl.handle.net/10945/18488

Downloaded from NPS Archive: Calhoun

http://www.nps.edu/library

Calhoun is a project of the Dudley Knox Library at NPS, furthering the precepts and goals of open government and government transparency. All information contained herein has been approved for release by the NPS Public Affairs Officer.

Dudley Knox Library / Naval Postgraduate School
411 Dyer Road / 1 University Circle
Monterey, California USA 93943

MASS, SALT, AND HEAT TRANSPORT ACROSS SEVEN LATITUDE CIRCLES IN THE NORTH ATLANTIC OCEAN: A DESCRIPTION OF THE GENERAL CIRCULATION BASED ON GEOSTROPHIC CALCULATIONS FROM INTERNATIONAL GEOPHYSICAL YEAR AND ADJACENT DATA

Timothy L. Baker

Report Number--NPS68-78-004

NAVAL POSTGRADUATE SCHOOL
Monterey, California

THESIS

MASS, SALT, AND HEAT TRANSPORT ACROSS SEVEN LATITUDE CIRCLES IN THE NORTH ATLANTIC OCEAN: A DESCRIPTION OF THE GENERAL CIRCULATION BASED ON GEOSTROPHIC CALCULATIONS FROM INTERNATIONAL GEOPHYSICAL YEAR AND ADJACENT DATA

by

Timothy L. Baker

June 1978

Thesis Advisor: Glenn H. Jung

Approved for public release; distribution unlimited.

Prepared for:

Office of Naval Research
Code 481
NSTL Station, MS 39529

T184044

NAVAL POSTGRADUATE SCHOOL
Monterey, California

Rear Admiral Tyler F. Dedman
Superintendent

Jack R. Borsting
Provost

This thesis is prepared in conjunction with research supported in part by OFFICE OF NAVAL RESEARCH under WR #N00014-78-WR-80032 issued 1 October 1977.

Reproduction of all or part of this report is authorized.

Unclassified

SECURITY CLASSIFICATION OF THIS PAGE (When Data Entered)

REPORT DOCUMENTATION PAGE

READ INSTRUCTIONS BEFORE COMPLETING FORM

1. REPORT NUMBER: NPS68-78-004	2. GOVT ACCESSION NO.
3. RECIPIENT'S CATALOG NUMBER	
4. TITLE (and Subtitle): Mass, Salt, and Heat Transport Across Seven Latitude Circles in the North Atlantic Ocean: A Description of the General Circulation Based on Geostrophic Calculations from International Geophysical Year and Adjacent Data	5. TYPE OF REPORT & PERIOD COVERED: Master's Thesis; June 1978
	6. PERFORMING ORG. REPORT NUMBER
7. AUTHOR(s): Timothy L. Baker	8. CONTRACT OR GRANT NUMBER(s)
9. PERFORMING ORGANIZATION NAME AND ADDRESS: Naval Postgraduate School, Monterey, California 93940	10. PROGRAM ELEMENT, PROJECT, TASK AREA & WORK UNIT NUMBERS: N00014-78-WR-80032
11. CONTROLLING OFFICE NAME AND ADDRESS: Naval Postgraduate School, Monterey, California 93940	12. REPORT DATE: June 1978
	13. NUMBER OF PAGES: 124
14. MONITORING AGENCY NAME & ADDRESS (if different from Controlling Office): Naval Postgraduate School, Monterey, California 93940	15. SECURITY CLASS. (of this report): Unclassified
	15a. DECLASSIFICATION/DOWNGRADING SCHEDULE

16. DISTRIBUTION STATEMENT (of this Report)

Approved for public release; distribution unlimited.

17. DISTRIBUTION STATEMENT (of the abstract entered in Block 20, if different from Report)

18. SUPPLEMENTARY NOTES

19. KEY WORDS (Continue on reverse side if necessary and identify by block number)

North Atlantic Ocean, general circulation, heat transport, mass transport, salt transport, geostrophic ocean currents, level of no motion.

20. ABSTRACT (Continue on reverse side if necessary and identify by block number)

This report using data from a five year period, including the International Geophysical Year (1954-1959), presents a detailed analysis of several aspects of the physical oceanography of the North Atlantic Ocean.

Assuming the geostrophic approximation to be valid, a level of no motion was established by satisfying the requirement of mass and salt continuity across seven latitude sections extending from 8°N to 48°N, with each latitude

DD FORM 1 JAN 73 1473 (Page 1)

EDITION OF 1 NOV 65 IS OBSOLETE

S/N 0102-014-6601

Unclassified

SECURITY CLASSIFICATION OF THIS PAGE (When Data Entered)

20.

section providing comprehensive temperature and salinity data extending from coast to coast and from the sea surface to the ocean floor.

Based on this level of no motion, net meridional heat transport values were determined for each latitude section and compared with those of previous studies for the North Atlantic Ocean and the Northern Hemisphere. The results of this comparison indicate that the inclusion of the heat transported in the bottom peripheral areas of the latitude sections did not affect the overall flux of heat to any appreciable degree when compared to results proposed by Jung (1974-1976) using the same data ignoring the bottom area. Also, it is seen that the meridional heat transport during the I.G.Y. was anomalously low when compared to values taken from 1955-1973.

Lastly, a general circulation pattern is developed from mass transport values for each of three layers of water: Upper Water, Intermediate Water, and Deep and Bottom Water. These circulation patterns are also compared with past descriptions of the general circulation; most notably, those of Sverdrup et al. (1942), Jung (1955), and Worthington (1976). The circulation patterns find good support with all three authors in the Upper and Intermediate Waters, but sharp contrasts exist between the deep and bottom circulation and that proposed by Worthington for his Deep Layer. Strong support for the pattern developed in this study is provided, however, by the works of Schmitz (1977), and Tucholke, Wright, and Hollister (1973).

Approved for public release; distribution unlimited.

Mass, Salt, and Heat Transport Across Seven Latitude Circles in the North Atlantic Ocean: A Description of the General Circulation Based on Geostrophic Calculations From International Geophysical Year and Adjacent Data

by

Timothy L. Baker
Lieutenant, United States Navy
B.S., Villanova University, 1971

Submitted in partial fulfillment of the
requirements for the degree of

MASTER OF SCIENCE IN OCEANOGRAPHY

from the

NAVAL POSTGRADUATE SCHOOL
June 1978

ABSTRACT

This report using data from a five year period, including the International Geophysical Year (1954-1959), presents a detailed analysis of several aspects of the physical oceanography of the North Atlantic Ocean.

Assuming the geostrophic approximation to be valid, a level of no motion was established by satisfying the requirement of mass and salt continuity across seven latitude sections extending from $8^{o}N$ to $48^{o}N$, with each latitude section providing comprehensive temperature and salinity data extending from coast to coast and from the sea surface to the ocean floor.

Based on this level of no motion, net meridional heat transport values were determined for each latitude section and compared with those of previous studies for the North Atlantic Ocean and the Northern Hemisphere. The results of this comparison indicate that the inclusion of the heat transported in the bottom peripheral areas of the latitude sections did not affect the overall flux of heat to any appreciable degree when compared to results proposed by Jung (1974-1976) using the same data ignoring the bottom area. Also, it is seen that the meridional heat transport during the I.G.Y. was anomalously low when compared to values taken from 1955-1973.

Lastly, a general circulation pattern is developed from mass transport values for each of three layers of water: Upper Water, Intermediate Water, and Deep and Bottom Water. These circulation patterns are also compared with past descriptions of the general circulation; most notably, those of Sverdrup et al. (1942), Jung (1955), and Worthington (1976).

The circulation patterns find good support with all three authors in the Upper and Intermediate Waters, but sharp contrasts exist between the deep and bottom circulation and that proposed by Worthington for his Deep Layer. Strong support for the pattern developed in this study is provided, however, by the works of Schmitz (1977), and Tucholke, Wright, and Hollister (1973).

TABLE OF CONTENTS

LIST OF FIGURES

LIST OF TABLES

I. INTRODUCTION

For centuries it has been recognized that the heat budget of the earth is characterized by a net surplus of solar radiation received in the tropics, and a net loss of heat in the polar regions. However, since the temperature regimes of these regions has not undergone a progressive change, it must be assumed that the excess heat received in the tropics is transported poleward by some mechanism(s) of energy transfer. Presumably the solid earth, via conduction, is not responsible for this transfer; therefore the atmosphere and world ocean - the earth's fluid envelope, must be the mechanism for this meridional transfer of energy. Originally it had been thought that the ocean was the principal vehicle of transfer; this idea was discarded in the early twentieth century in favor of the atmosphere being the dominant mode of energy transfer, with the oceanic contribution considered negligible.

In 1952 Jung proposed that the oceans, with their systems of currents, might be of far greater importance in the transfer of heat energy than had been considered. He pointed out that previous works such as that of Sverdrup (1942) had considered only the standing horizontal eddy, that is the Gulf Stream system and its return currents, in their calculations. Jung then proposed that closed vertical circulations in meridional planes conceivably could transport large quantities of energy, even though the velocities involved are quite small. This was followed by his detailed study in 1955 to determine the heat transported by geostrophic ocean currents in the North Atlantic Ocean using data from the Meteor Atlases.

Since that time many studies of the oceanic contribution to the meridional transfer of heat have been made (Budyko, 1956; Sverdrup, 1957; Bryan, 1962; Sellers, 1965; Vander Haar & Oort, 1973); but generally these studies have not used synoptic or nearly synoptic data for an entire ocean.

This study using a computer program developed by Greeson in his 1974 master's thesis, and seven nearly synoptic latitude sections of oceanographic data from the International Geophysical Year and adjacent years (1954-1959), was undertaken to determine the general geostrophic circulation and values of net heat flux for the North Atlantic Ocean.

II. BACKGROUND

A. ENERGY TRANSPORT

In dealing with energy transport within a fluid, be it the atmosphere or the ocean, we should begin with a general equation which applies to all fluid motion:

$$T^* = \int_S \overset{(a)}{(\rho U} + \overset{(b)}{\rho c^2/2} + \overset{(c)}{\rho \phi} + \overset{(d)}{P)}\ V_n\ dS \qquad (1)$$

where T^* is the total meridional energy transferred normal to a vertical wall encircling the earth at a particular latitude, ρ is density, U is the internal energy per unit mass, c is the magnitude of the fluid velocity, ϕ is the potential energy per unit mass, P is pressure, V_n is the component of the fluid velocity normal to the latitude wall at a given level in either air or ocean and dS is the differential area of the wall.

This equation simply states that the total amount of energy transferred across a complete latitude circle is equal to the sum of the transport due to advection of internal energy (a), the transport of kinetic energy (b), the transport of potential energy (c), and rate of work done by pressure forces (d).

According to Jung (1952) the transport of kinetic energy (b) is negligible when compared to the other terms and can therefore be ignored.

Within the oceans, the transfer of energy is accomplished by the ocean currents. The simplifying assumption of geostrophic equilibrium usually is made to facilitate the determination of the magnitude of these currents. Also, the assumption of hydrostatic equilibrium in the vertical usually is

made, eliminating terms (c) and (d) from our general equation. Therefore, in the ocean, equation (1) reduces to :

$$T^*_o = \int_o \rho_s U_s V_{ns} \, dO$$

where the subscript s stands for seawater, and O is that part of our latitude wall, S, cutting through the oceans. If we now neglect the compressibility effects in water we may write $U_s = C_{ps} T_s$ where C_{ps} is the specific heat at constant pressure of sea water and T_s is the temperature of sea water. Our equation now may be written:

$$T_o^* = \int_o \rho_s C_{ps} T_s V_{ns} \, dO \qquad (2)$$

In the atmosphere certain simplifying assumptions also may be made. Term (d) of our general equation (1) may be replaced by $\rho_a RT_a$ where R is the gas constant for dry air (.287 joules g^{-1} $^oK^{-1}$), T_a is the absolute temperature of air (the subscript a indicates air) if we assume the ideal gas law for the atmosphere (White, 1950). From term (a) we may write $U_a = C_{va} T_a + qL$, which states that the internal energy of the atmosphere is equal to the internal energy of dry air plus the latent energy contained in the water vapor. Here C_{va} is the specific heat at constant volume for dry air which may be considered a constant to a very good degree of approximation, q is the specific humidity, and L is the latent heat of condensation. Equation (1) now may be written as:

$$T_a^* = \int_a (C_{va} T_a + qL + \phi_a + RT_a) \rho_a V_{na} \, dA;$$

from the first law of thermodynamics for an isobaric process we have $C_{pa} = C_{va} + R$ (Haltner and Martin, 1957); therefore:

$$T_a^* = \int_a (C_{pa} T_a + qL + \phi_a) \rho_a V_{na} \, dA, \qquad (3)$$

where A is that part of the latitude wall, S, which cuts through the atmosphere.

The determination of the total energy transport in the atmosphere - ocean complex now simply reduces to adding the advection of sensible heat of the atmosphere and oceans with the advection of water vapor and potential energy of the atmosphere. Therefore, the total transfer of energy is:

$$T^* = T_o^* + T_a^* = \int_o \rho_s \, C_{ps} \, T_s \, V_{ns} \, dO + \int_a (C_{pa} \, T_a + qL + \phi a) \, \rho_a \, V_{na} \, dA. \tag{4}$$

From the previous discussion it is obvious that the energy equilibrium maintained in both the polar and tropical regions is due to the meridional transport of sensible heat by the oceans and the transport of both sensible and latent heat by the atmosphere. However, the relative importance of the sea and air as mechanisms of energy transport has been a point of contention for many years and has only recently been satisfactorily resolved.

The debate over whether the atmosphere or the oceans are the dominant mechanisms of heat transport according to Jung (1956) began over a century ago when M. F. Maury (1856), in discussing the roles of each in maintaining the energy balance of the earth, expressed his belief that the oceans maintained the predominant role in heat transfer. Ferrel (1890) pointed out that although the volume exchange of air is greater than that of the sea, the mass exchange of the sea is greater between the tropics and poles than the air mass exchange. Ferrel further stated that the velocity of the air would need to be 2000 times that of the sea to allow the atmosphere to equal the heat transport of the sea.

Over the next thirty years with the advances in the theory of fluid motion together with improved instrumental and observational techniques, ideas about the relative importance of sea and air in transporting heat began to reverse. In 1925 Angstrom investigated Defant's "austausch" coefficients for the atmosphere and estimated that the oceans transported only as much heat poleward as the atmosphere. V. Bjerknes et al. (1933) felt that the contribution of the oceans was small compared to the energy transported by the air and therefore could be neglected. Sverdrup et al. (1942) stated that although the question had not been adequately studied, it was generally assumed that heat transport by ocean currents is negligible when dealing with averages for the entire earth, but in some regions it could be of considerable importance. In 1952 Jung hypothesized that the ocean's contribution might be greater than previously considered. This was followed by his detailed description of heat transport in the North Atlantic Ocean (Jung, 1955) which indicated that while the oceanic transport of sensible heat is less than the sensible and latent heat transported by the atmosphere, it is not negligible. This fact was reiterated by Neumann et al. (1966) when they stated that although the atmosphere is the principal mode of heat transport much of that heat transported is latent heat acquired from the oceans. Neumann further pointed out that if 4×10^{14} cal/sec of latent heat at 40^{o}N were added to the sensible heat transported by the oceans the total would equal half of the total value required by radiation theory.

B. THE LEVEL OF NO MOTION

In utilizing the dynamical method of preparation of oceanographic data, we are faced with the problem of determining a reference level along

which the velocity is zero. This is necessary so that absolute current velocities may be found when the relative current velocities are referred to this level of no motion. Defant (1961) pointed out "The essential data needed to decide the position of the 'zero level' is largely lacking." We have seen a variety of indirect approaches developed which have tried to relate this level of no motion to some physical or chemical characteristic.

One of the earliest methods utilized was to place the reference level at a sufficiently great depth. This was based on the assumption that the deep waters of the oceans are uniform or nearly so and that in deep water the isopycnal and isobaric surfaces are nearly horizontal. Therefore the absolute current velocities could be found if the level of no motion were placed at a constant great depth.

A second school of oceanographers of which Jacobsen (1916) was the first, believed that the oxygen minimum in the oceans identified the level of minimum horizontal motion. The theory is based on the premise that the consumption of oxygen due to oxidation of organic matter by biological processes takes place at all levels; therefore the level of minimum oxygen content is found where the replenishment of oxygen by horizontal currents is a minimum. Rossby (1936) and Iselin (1936) pointed out that this approach would lead to odd results. This was aptly demonstrated by Dietrich (1936) who computed the magnitude of the Gulf Stream by the dynamic method, assuming the zero-level to be the oxygen minimum layer. His results indicated that the northward flow of the current was limited to the upper layers, while the counter current extended to the bottom with a transport of 78 Sverdrups (sv), twice that of the Gulf Stream.

Aside from these unreasonable results, the assumptions that the vertical distribution of organic matter is uniform and that oxygen consumption is

independent of the oxygen content in the water are incorrect. Therefore the level of no motion corresponding to the oxygen minimum appears unrealistic.

Parr (1938) developed a method for the determination of the layer of no motion in the oceans from the distortion of the thickness of isopycnal layers. This layer of constant density bounded by two isopycnal surfaces is called a pycnomere. According to Parr, the thickness of the pycnomere cannot remain constant in the presence of any current. Therefore, if the pycnomere is undistorted or if the distortion is minimal we must assume there is a complete lack of, or at least minimal water motion within the layer.

Fomin (1964) in analyzing Parr's method points out that the variation of current velocity in the vertical is a function not only of the slope of the isopycnal surfaces, but also, and more importantly, depends on the vertical water density gradient. He states that in areas of strong vertical density gradients the slope of isopycnal surfaces and the distortion of pycnomeres may be insignificant while current velocities vary greatly in the vertical. The converse also holds true. In areas of large slopes of isopycnal surfaces and considerable distortion of pycnomeres and weak density gradients, current velocity usually varies only slightly in the vertical. Therefore since Parr's method ignores the vertical density gradient, it is possible to pick as one's layer of no motion an undistorted pycnomere that is really a region of strong current velocity.

Hidaka developed two methods for the determination of the depth of the layer of no motion. The first method was based on determining the level from the salinity distribution. Hidaka (1949) proposed that the velocity field of the ocean current is constantly interacting with the

fields of the chemical and physical properties of sea water, resulting in a mutual adjustment if one field undergoes perturbation.

The differential equation of salinity distribution, s, in the oceans is:

$$\frac{ds}{dt} = k_1 \frac{\partial^2 s}{\partial x^2} + k_2 \frac{\partial^2 s}{\partial y^2} + k_3 \frac{\partial^2 s}{\partial z^2}$$

where t is time and k_1, k_2, k_3 are the turbulent diffusion coefficients in the x, y, z directions respectively. Hidaka now assumes $\frac{ds}{dt} = 0$ within the layer of no motion, and that $k_1 = k_2$ since the coefficient of horizontal diffusion does not depend on direction.

Depending on whether vertical or horizontal diffusion is dominant, and eliminating the small term(s), Hidaka reduces his equation to two equations which are used to determine the layer of no motion:

$$\frac{\partial^2 s}{\partial x^2} + \frac{\partial^2 s}{\partial y^2} = 0; \quad \frac{\partial^2 s}{\partial z^2} = 0$$

The first equation would be used in areas where horizontal salt diffusion is important, and the second in areas of vertical diffusion.

Fomin (1964) points out that recent evidence indicates that the coefficients of turbulent diffusion in the layer of no motion do not remain finite, as Hidaka asserts. Therefore the equations:

$$k_1 \frac{\partial^2 s}{\partial x^2} + k_1 \frac{\partial^2 s}{\partial y^2} = 0 \quad \text{and} \quad \frac{\partial^2 s}{\partial x^2} + \frac{\partial^2 s}{\partial y^2} = 0$$

do not follow one from the other. Thus, the solution to Hidaka's equations indicates the layer in which salinity is constant or varies linearly, or the depth of the boundaries of the intermediate salinity maximum. But these salinity characteristics have no definite relation to the current velocity field.

Hidaka's second method of determining the level of no motion utilizes the continuity equations and the computation of the vertical distribution of current velocity by the dynamic method. Hidaka's method utilizes a tetrahedral prism extending from the sea surface to the bottom. The apexes of the tetrahedron are oceanographic stations which have observed vertical temperature and salinity profiles. It is assumed that the exchange of salt and water volume takes place only through the lateral faces, and no exchange takes place through the ocean floor and sea surface. It is further assumed that the sum of the volume transport and salt mass transport across the lateral faces must equal zero.

In his method current velocities between stations relative to the current velocity C_i at the i^{th} level (such as the surface) are computed by the dynamic method. By this method, the magnitude of the absolute velocity V(z) at depth z is:

$$V(z) = U(z) + C$$

where C is the current velocity at the sea surface and U(z) is the current computed by the dynamic method relative to the sea surface. Substituting these values into his continuity equations he developed a deterministic set of six equations. Solving the system of equations he determined the surface gradient current velocity between the stations, which is used to determine the vertical distribution of the current velocity components normal to the prism faces.

Fomin (1964) points out that Hidaka's method cannot be used for practical computations since his simplification of the continuity equations is not theoretically correct and also because it leads to a set of equations that cannot be solved with the existing accuracy of measurements at sea.

Defant's (1941) method for the determination of the "zero" level is based on the analysis of differences in the dynamic depths of isobaric surfaces. By examining the dynamic height differences of isobaric surfaces of pairs of neighboring oceanographic stations in the Atlantic, Defant recognized a relatively thick layer whose depth varies uniformly in the horizontal direction while the change in the differences of the dynamic depths of isobaric surfaces was extremely small, amounting to only several dynamic millimeters (Fomin, 1964). Defant points out that the constancy of the differences in the dynamic depths indicates that the gradient component of the current velocity is constant in the vertical within the layer. Therefore, he assumes that this layer is motionless or nearly so and he considers it to be the layer directly adjoining the zero surface (Fomin, 1964).

The constancy in the differences of the dynamic depths of isobaric surfaces means that:

$$\Delta D_A = \Delta D_B$$

or

$$\left[\int_{P_n}^{P_{n+1}} \alpha dp\right]_A = \left[\int_{P_n}^{P_{n+1}} \alpha dp\right]_B ;$$

the differences in the depths between two levels, P_n and P_{n+1}, are equal at two adjacent oceanographic stations, A and B. In these equations ΔD_A and ΔD_B are increments of dynamic depth, and α is the specific volume of sea water.

To the present, Defant's method seems to be one of the most reasonable. However, when this method is used it must be understood that the current velocity is computed with low accuracy due to the accumulation of errors involved in the dynamic method. Therefore, in areas of low current

velocities this method may prove unusable since the computed D values will be comparable to the accumulated computational error.

The next method, and probably the most satisfactory, is that of Sverdrup et al. (1942). This method is based on the equation of continuity. The level of no motion is determined by comparing water mass transport computed by the dynamic method utilizing a horizontal reference surface. This reference surface will be the level of no motion when the net mass transport, in the oceanographic section of interest, above the reference surface is equal and opposite in direction to the net mass transport below this surface. This method has not been widely used because it requires that the data span an entire vertical cross section of the ocean.

Stommel (1956) developed a method for determining the level of no meridional motion based on Ekman's concept of the ocean consisting of a wind driven surface layer of frictional influence, and a deeper frictionless geostrophic layer. Basically the method states that at any position in the ocean the wind stress at the surface produces a net convergence or divergence of water. This water can escape or be introduced only through the bottom of the layer of frictional influence. Therefore the geostrophic layer will begin to stretch or shrink, and any water elements in this layer will stretch or shrink as they move poleward. This stretching and shrinking between the ocean bottom and the bottom of the frictional layer creates a vertical component of velocity which must, by mass conservation, equal the vertical velocity induced at the bottom of the frictional layer by the wind. This matching occurs only for a unique reference level, the level of no meridional motion.

Recently Stommel and Schott (1977) have indicated a new method based on the beta-spiral and the determination of the absolute velocity field from density data. This theory states that since the horizontal component

of velocity rotates with depth in the sea, absolute velocities can be obtained from observations of the density field alone. Assuming geostrophic flow, no flow across density surfaces, and a linear vorticity balance on a beta-plane, then:

$$w = uh_x + vh_y \; ; \; u_z = -\gamma h_{yz} \; ; \; v_z = h_{xz} \; ; \; \gamma = g/f \; ; \; fw_z = \beta v$$

where h is the height of a given density surface, the subscripts x, y, z, indicate derivatives, f is the coriolis parameter, and β is the derivative of f with respect to y. If we differentiate the first equation with respect to the vertical (z), and substitute from the remaining equations we have

$$uh_{xy} + v(h_y - \beta\, z/f)_z = 0.$$

Now, when the coefficient of u or v, h_{xy} or $(h_y - \beta\, z/f)_z$, vanishes at some depth without the other vanishing, that component of the absolute velocity also vanishes; and thereby establishes the "depth of no motion" for that component. Using the beta-spiral of the North Atlantic Ocean's subtropical gyre as a test of this technique, h_{xy} was found to vanish at approximately 900 meters, suggesting that v vanishes near that depth.

In this investigation the method proposed by Sverdrup et al. (1942) is used to determine the level of no motion, due to the comprehensive nature of the data involved and the belief that this method is the most reasonable so far proposed. However, as Jung (1955) emphasized "this problem of determining a level of no motion is still an open one which should be investigated in detail."

III. STATEMENT OF THE PROBLEM

To determine the heat energy transported by the North Atlantic Ocean we must possess comprehensive data concerning the thermal and salinity structure of the ocean, as well as a detailed understanding of the nature of the ocean circulation pattern.

We know that the energy transfer is accomplished by several processes: large-scale advection, smaller scale eddy diffusion, and molecular diffusion, as was pointed out by Sverdrup et al. (1942). Large-scale advection is the dominant mode of transfer, with the contributions of eddy diffusion and molecular diffusion being several orders of magnitude smaller. Therefore eddy and molecular diffusion of energy have not been included in this study.

As shown earlier, the energy flux or transport across any latitude barrier in the ocean is expressed as:

$$T_o^* = \int_o \rho_s \, C_{ps} \, T_s \, V_{ns} \, dO \, , \qquad (2)$$

where the internal energy term or heat transport term, $C_{ps} \, T_s$ determines the total energy flux across a vertical cross section of area dO within the ocean; we will assume that the specific heat at constant pressure of sea water, C_{ps}, has the value of unity. This introduces an insignificant error for the range of depths used in this study (Sverdrup et al. 1942, p. 62).

Velocities were computed utilizing the formula derived by Helland-Hansen and Sandstrom (1903) (Equation 5) and the procedure from Sverdrup et al. (1942) pp. 408-411; 447-448. Implicit in this procedure is the

assumption of geostrophic equilibrium within the oceans. This assumption of geostrophic balance, as was pointed out by Jung (1955), seems to be valid for large-scale motion outside the equatorial region, and is therefore applicable to this study.

Dynamic heights were determined and then were used to compute the geostrophic velocity differences between depths 1 and 2 in an area between adjacent pairs of oceanographic stations. The Helland-Hansen equation was used:

$$V_1 - V_2 = \frac{10C}{L} (D_A - D_B) , \tag{5}$$

where $C = 1/2\ \Omega \sin \theta$, Ω is the earth's angular velocity, θ is the latitude, L is the horizontal distance between stations A and B, and D_A and D_B are the dynamic heights (or depths) of the two stations.

Prior to using this method the reference level or level of no motion must be established. The two criteria that must be met to determine this depth are zero net transport of both water mass and salt across the entire latitude sections of ocean, $\int_o dO$:

$$\int_o \rho_s V_{ns}\, dO = 0 \tag{6}$$

$$\int_o \rho_s SV_{ns}\, dO = 0 \tag{7}$$

where in these equations S is salinity in parts per thousand.

In this study the mass balance was considered the primary criterion in determining the level of no motion (See Section V.B for explanation). Once the level of no motion was satisfactorily determined, a value for the heat flux across each latitude section was determined. A plot of integrated

mass transport for each pair of stations in three layers of water (Upper, Intermediate, and Deep and Bottom Water) also was made to determine the general circulation pattern for the three layers, with these circulation patterns directly responsible for the ocean heat transfer.

IV. PROCEDURE

A. DATA SOURCES

To undertake this study, extensive information on the temperature and salinity structure of the North Atlantic Ocean was needed as inputs for the dynamic method. The Atlantic Ocean Atlas (Fuglister, 1960) for the International Geophysical Year (1957-1958) was found to provide the most synoptic and comprehensive compendium of data for the North Atlantic Ocean made to this time. Seven of the eight east-west sections provided were utilized in this study.(The eighth section extended along the equator, a latitude at which the geostrophic assumption fails since the coriolis parameter goes to zero.) Table I provides information on these latitude cross-sections.

It is to be noted that all but the western-most stations of the $32^{o}N$ section (North America-Bermuda), the $27^{o}N$ section (Florida-Bahama Islands), and the entire $36^{o}N$ latitude section occur between April and December of 1957. This fact is used as justification for the assumption that all data used are simultaneous. However it must be pointed out that this assumption is least justified in the western-most area of the ocean between the $32^{o}N$ and $36^{o}N$ sections where more than five years separate some of the observations.

Although these latitude sections provide considerable temperature and salinity data, there are areas in each section for which no data were obtained. These are the peripheral areas between the western-most stations and the American continent, between the eastern-most stations and Africa, Europe, or England, and the bottom area between the deepest observations of temperature and salinity and the ocean floor.

TABLE I

OCEANOGRAPHIC DATA: SHIPS, STATION NUMBERS, AND DATES

Latitude	Research Vessel	Station Numbers	Dates
8°N	Crawford	154-184	May 6-21, 1957
16°N	Crawford	275-310	Nov 13-29, 1957
24°N	Discovery II	3587-3624	Oct 6-28, 1957
27°N	Atlantis	5343-5335	Jun 27-28, 1955
32°N	Atlantis	5203-5210	Nov 11-16, 1954
32°N	Atlantis	5292-5312	Jun 9-14, 1955
32°N	Atlantis	5564	Apr 22, 1957
32°N	Discovery II	3625-3650	Nov 24-Dec 7, 1957
36°N	Chain	17-77	Apr 19-May 12, 1959
40°N	Crawford	218-255	Oct 2-22, 1957
48°N	Discovery II	3509-3548	Apr 16-27, 1957

To evaluate the significance of those areas not covered by data, results from the Cummings (1977) study of $8^{o}N$, $16^{o}N$, $24^{o}N$ & $27^{o}N$, $32^{o}N$, $36^{o}N$, and $40^{o}N$ were combined with information for $48^{o}N$. The results indicate that the nearshore holiday* areas amounted to less than one percent of the total area of interest (Table II). To see if the exclusion of these areas would seriously prejudice the results of this work, a study was made to estimate the transport of mass, salt, and heat in these peripheral areas. Temperature and salinity values were obtained from the U.S. Navy Fleet Numerical Weather Central's "Hydroclimatological Data Retrieval Program." These values combined with average monthly current values supplied by the appropriate "Pilot Chart of the North Atlantic Ocean" and an estimated average density value of 1.02395 gm/cm^{3} obtained from the work of Greeson (1974), were used to compute the transport values. The results of this analysis (Appendix B) indicate that the transports were in fact low and would not greatly affect the overall net transport values since their inclusion would cause only minor variations in the level of no motion as was aptly demonstrated in Greeson's (1974) study of transports across $40^{o}N$ latitude. These transport values for the peripheral areas were not, however, included in this study since the data involved varied by as much as twenty years from the period of interest.

---

*A holiday area is an area for which no data were available.

TABLE II

PERIPHERAL AREAS

	AREAS IN KM^2 SIDES					AREA PERCENTAGES			
LATITUDE	WEST	EAST	AREA COVERED BY DATA	BOTTOM	TOTAL	$\frac{DATA}{DATA}$	$\frac{DATA}{DATA+SIDES}$	$\frac{DATA}{DATA+BOTTOM}$	$\frac{DATA}{DATA+SIDES+BOTTOM}$
8^oN	2	5	17,630	2,319	19,956	100%	99.9%	88.4%	88.4%
16^oN	0	2	17,384	3,207	20,593	100%	99.9%	84.4%	84.4%
24^oN+27^oN	5	6	27,312	2,806	30,125	100%	99.9%	90.7%	90.7%
32^oN	6	3	23,591	2,830	26,430	100%	99.9%	89.3%	89.3%
36^oN	6	1	23,071	1,902	24,980	100%	99.9%	92.4%	92.4%
40^oN	33	7	18,917	2,137	21,094	100%	99.8%	89.9%	89.7%
48^oN	23.5	12.5	10,485	978	11,463	100%	99.7%	91.5%	91.2%

Values for 8^oN, 16^oN, 24^oN+27^oN, 32^oN, 36^oN, 40^oN According to Cummings, 1977.

B. COMPUTATION OF VELOCITIES, TRANSPORT OF MASS, SALT CONTENT, AND HEAT

To date, actual synoptic velocity measurements have been made in only limited areas of the North Atlantic Ocean. Although this information is invaluable for limited area studies, it is not adequate for a study of this magnitude. However, with the assumption of geostrophic equilibrium, the I.G.Y. temperature and salinity data may be used with the procedure outlined by Sverdrup et al. (1942) (pp 408-411; 447-448) to determine dynamic height and synoptic velocity values for the areas of interest. To facilitate the numerous calculations involved, all computations were performed on an IBM-360/67 computer utilizing a program developed by Greeson (1974), which involves the following actual computational procedures.

The temperature and salinity data taken at various depths are first interpolated to standard depths. After the interpolated values are obtained, sigma-t, the specific volume anomaly, and the specific volume are calculated for each standard depth. Then an average specific volume anomaly for each pair of standard depths for each station is computed by the following equation:

$$\bar{\delta} = \frac{\delta_z + \delta_{(z + \Delta z)}}{2} \tag{8}$$

where $\bar{\delta}$ is the average specific volume anomaly, and δ_z and $\delta_{(z + \Delta z)}$ are the specific volume anomalies at the standard depths of z and $z + \Delta z$.

The next step is to compute the dynamic heights, D, for each station. First, the dynamic height difference, ΔD, between the standard depths is computed by:

$$\Delta D = \bar{\delta} [z - (z + \Delta z)] \tag{9}$$

Then a summation of the dynamic height differences is made:

$$\sum_{0}^{z} \Delta D = D \ , \tag{10}$$

yielding the dynamic height of each oceanographic station. The distance between stations, L, which varies as a function of latitude and longitude, is then computed. Once L is known the relative velocity between pairs of stations for each standard depth is computed using the Helland-Hansen formula (5). From the relative velocities absolute geostrophic velocities can be derived by determining a level of no motion at which the absolute geostrophic velocity is zero.

Density is then computed for each observed salinity, temperature, and pressure by the equation:

$$\rho_{stp} = \frac{1}{\alpha_{stp}} \tag{11}$$

where α_{stp} is the specific volume for a particular salinity, temperature and pressure.

We now have available four values of temperature, salinity, velocity, and density corresponding to the four corners of a rectangle bounded by the two adjacent stations and by a pair of standard depths. These four values of each property then are averaged, yielding a single value for each rectangular area. The area of the rectangle is then determined by multiplying the station spacing, L, with the increment of depth, Δz.

By multiplying the area, the average density, and the average velocity it is possible to determine the mass transport for each rectangular area. This value in turn is multiplied by the average salinity and average absolute temperature to determine the salt flux and heat flux for each rectangular area.

These values then are summed vertically, yielding the net flux of mass, salt, and heat for that pair of stations. These values also are summed horizontally yielding the net flux for each pair of standard depths across the entire latitude section. These net horizontal values then are summed vertically giving the total net flux of mass, salt, and heat computed for the entire latitude section, minus the peripheral areas. This process is depicted in Figure 1.

The computer program utilized calculates the values of transport in the vertical only to the deepest standard depth common for a pair of stations. Therefore the transport value for the area between this deepest common depth and the ocean floor is not included in the net transport figures for each pair of stations. These areas are depicted in Figures 2 through 8 as the area between the bottom and the solid line.

To compute the transport values for these areas the bathymetric profile for each latitude section was first obtained. The oceanographic stations and the deepest common depths then were plotted, and the area between the ocean floor and the deepest common depth for each pair of stations was determined (the "bottom area" between the station pair). In these areas a linear decrease in velocity was assumed to exist between the absolute geostrophic velocity at the deepest common level and zero velocity at the ocean floor; therefore a value of one half the deepest calculated absolute velocity was used as the average velocity value for each area. This average velocity value was multiplied then by the deepest calculated density and by the bottom area to determine the mass transport across the bottom area for each pair of stations. This value in turn was multiplied by the deepest salinity and temperature values to determine the corresponding salt and heat transports. These transport estimates of mass, salt, and heat across the bottom area for each pair of stations then were summed

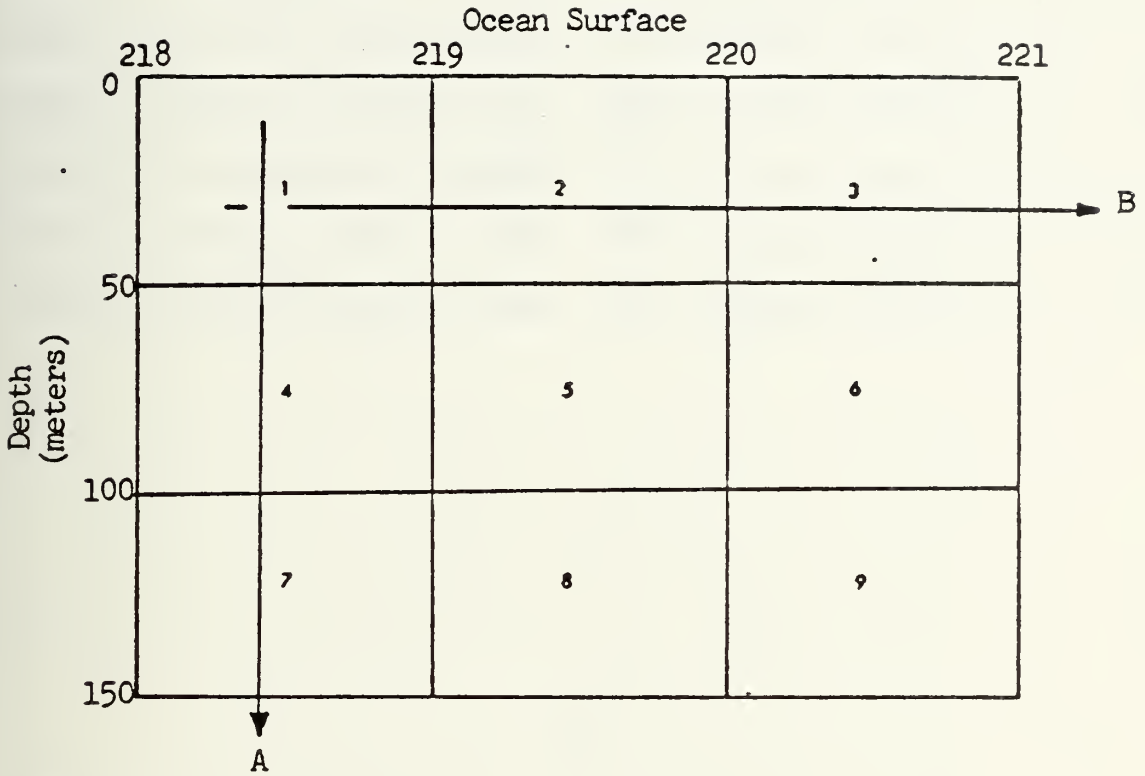

Figure 1. Illustration of the summation process performed in the computer program for a sample cross section of ocean. A represents integrated transport for a pair of stations 218-219. B represents the net transport for the layer 0 to 50m. According to Greeson (1974).

FIGURES 2-8

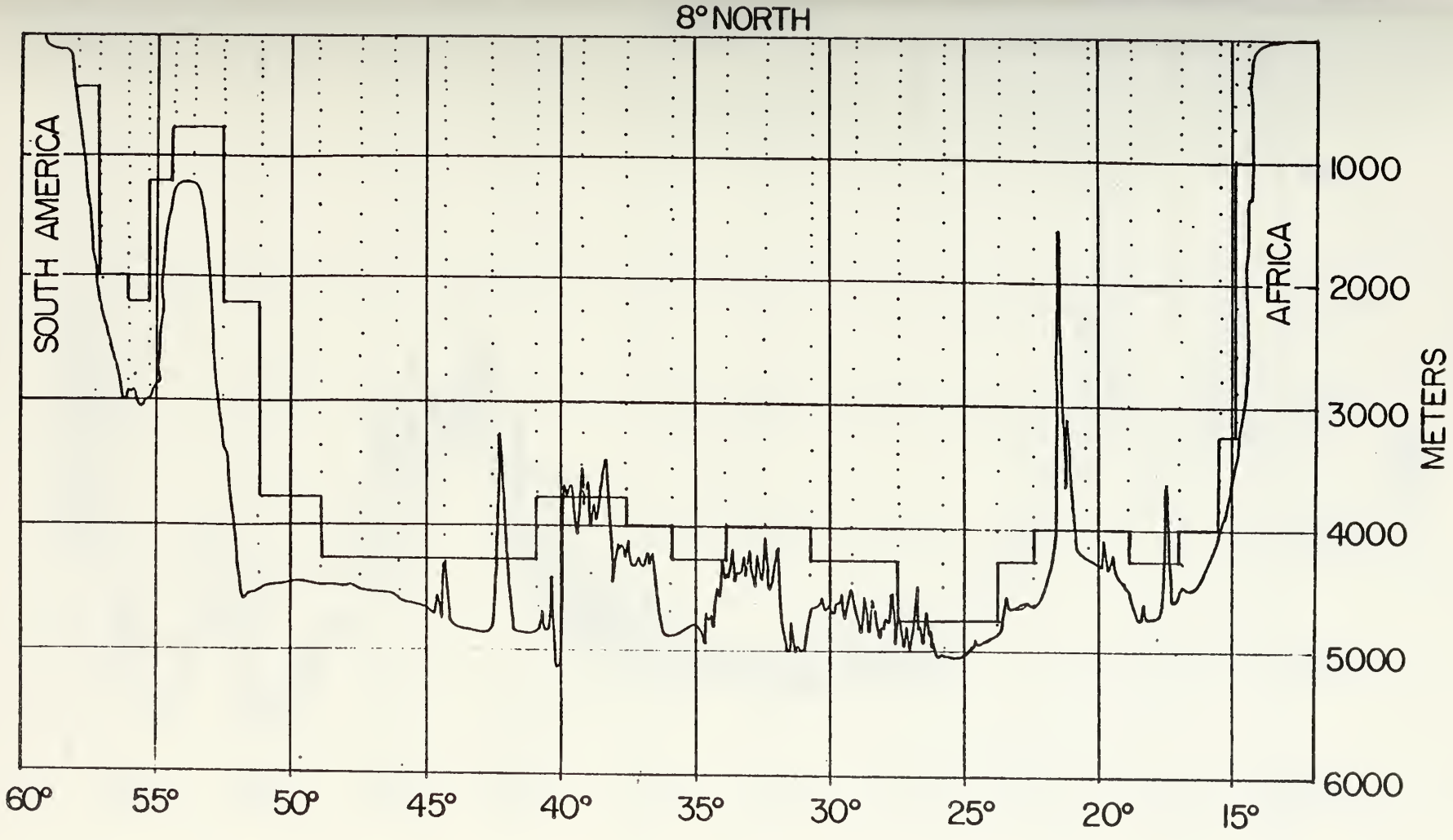
8° NORTH
SOUTH AMERICA
AFRICA
1000
2000
3000
4000
5000
6000
METERS
60°
55°
50°
45°
40°
35°
30°
25°
20°
15°

Figure 2

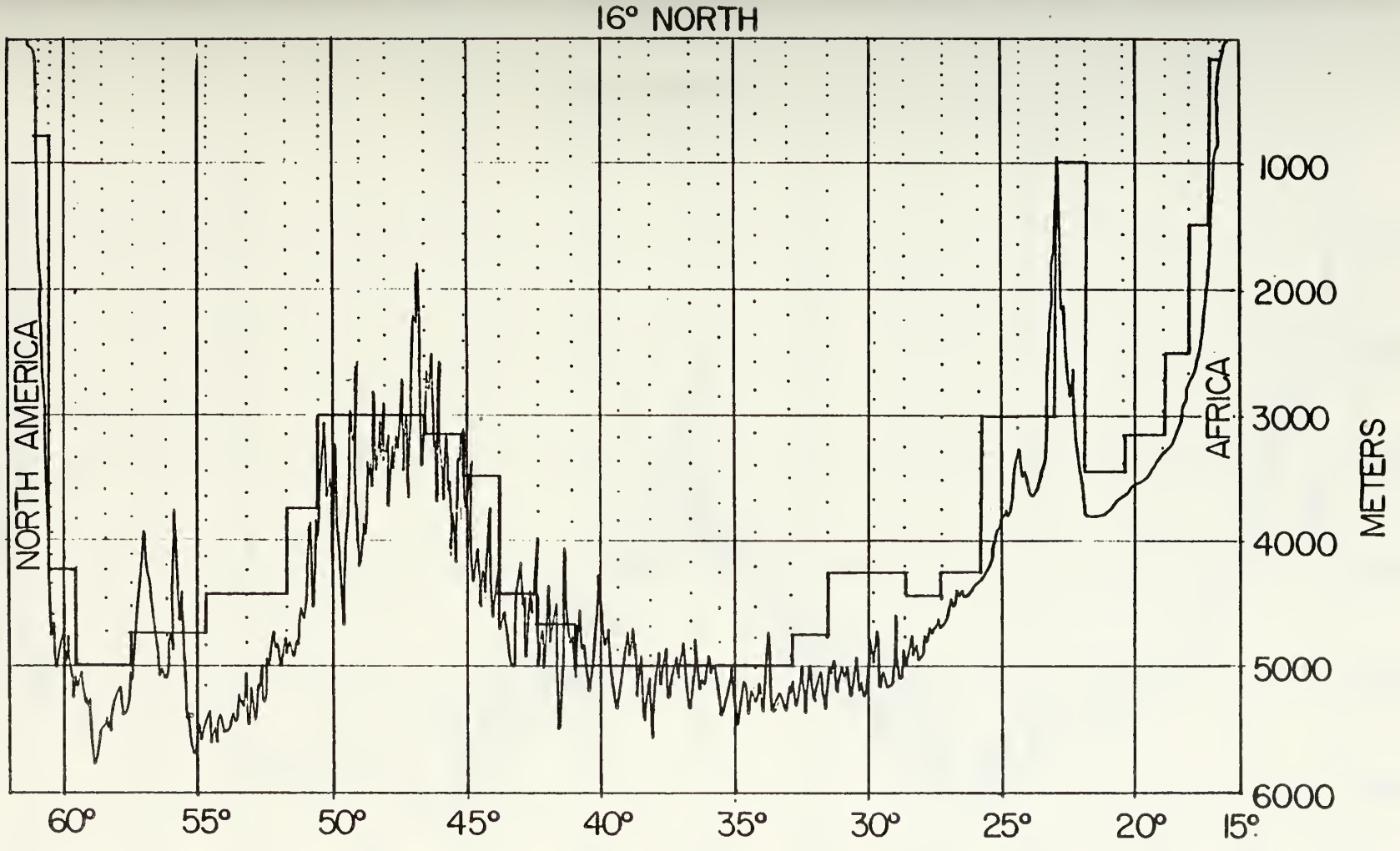
16° NORTH
NORTH AMERICA
AFRICA
1000
2000
3000
4000
5000
6000
METERS
60°
55°
50°
45°
40°
35°
30°
25°
20°
15°

Figure 3

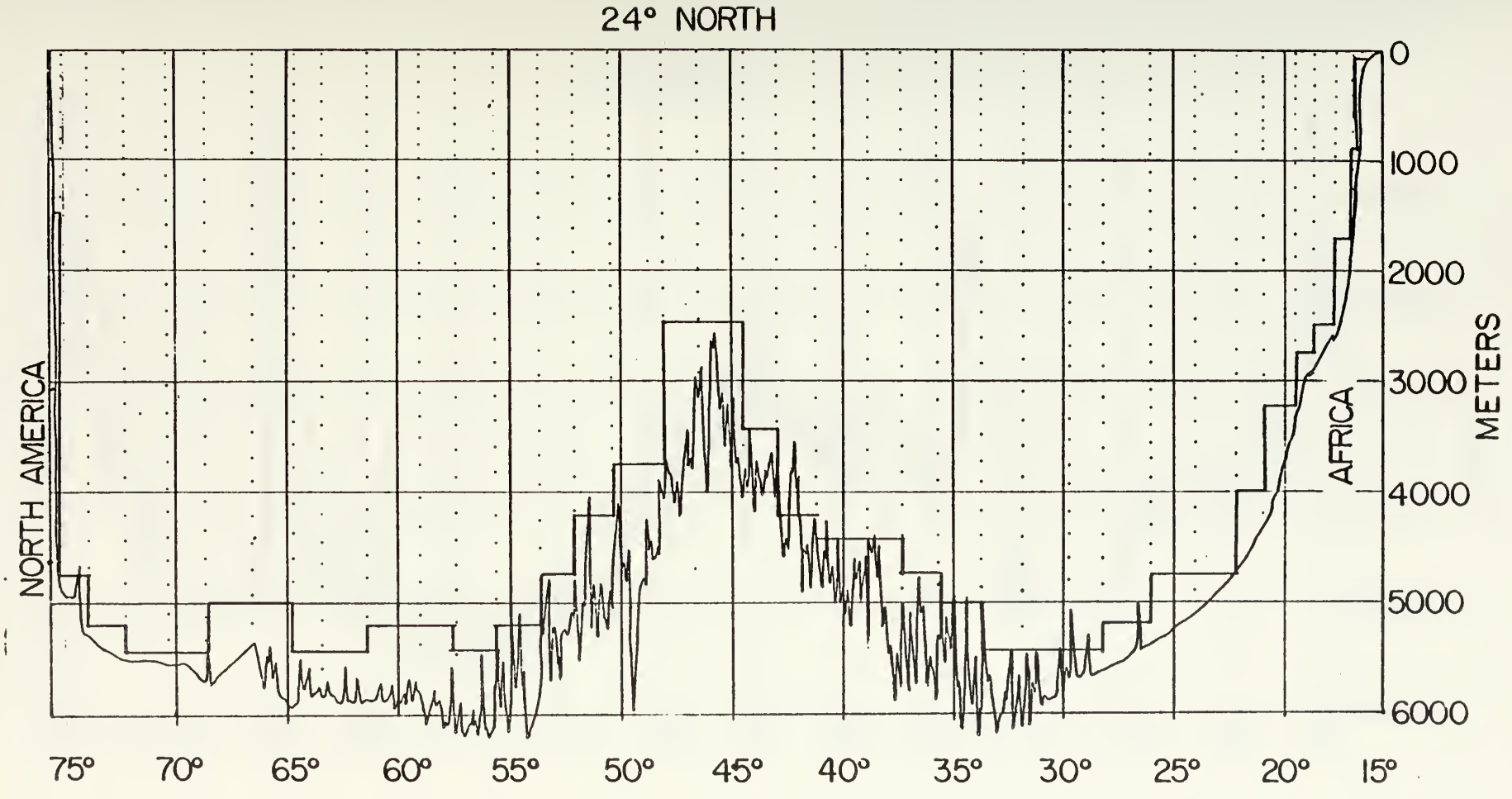
24° NORTH
NORTH AMERICA
AFRICA
METERS
0
1000
2000
3000
4000
5000
6000
75°
70°
65°
60°
55°
50°
45°
40°
35°
30°
25°
20°
15°

Figure 4

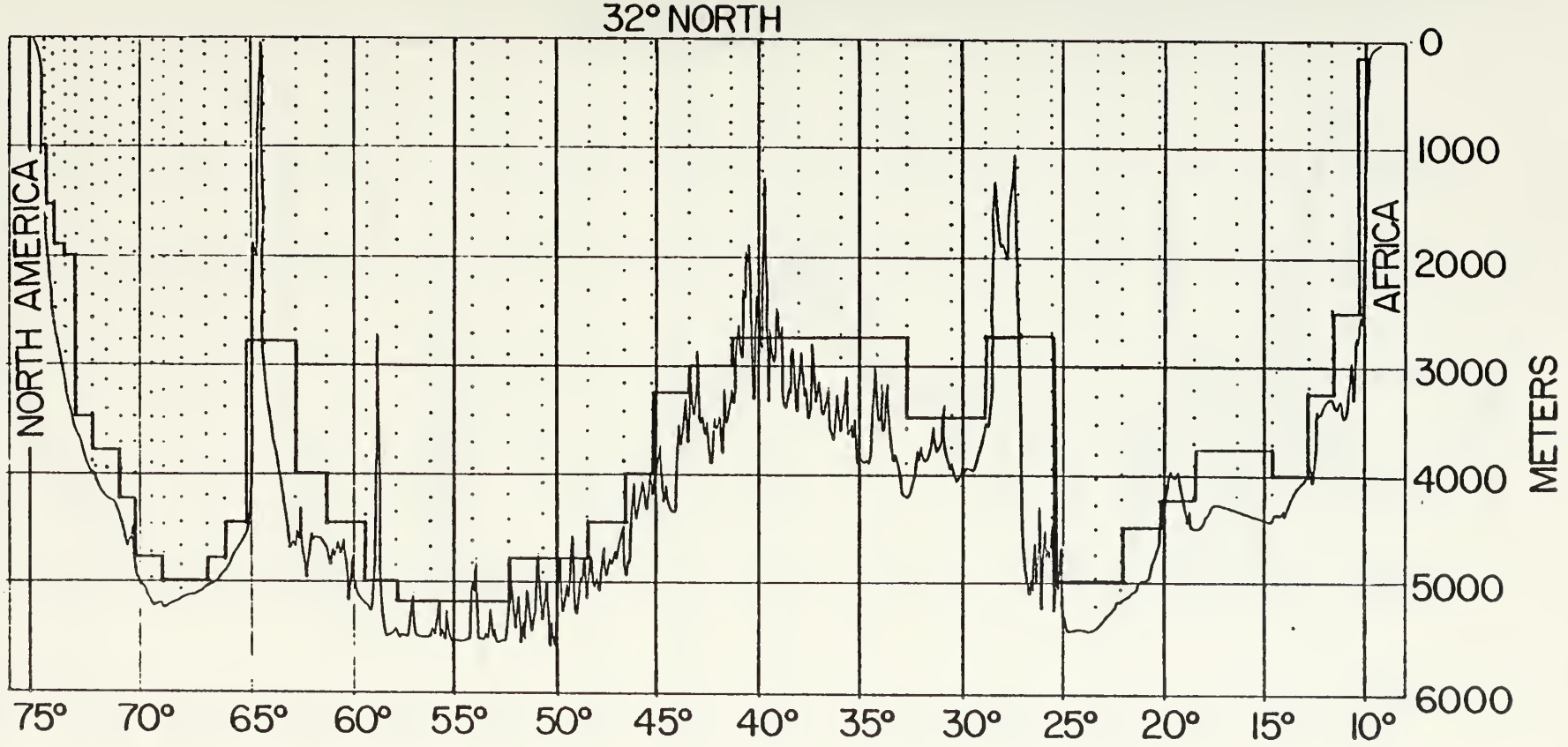
32° NORTH
NORTH AMERICA
AFRICA
0
1000
2000
3000
4000
5000
6000
METERS
75°
70°
65°
60°
55°
50°
45°
40°
35°
30°
25°
20°
15°
10°

Figure 5

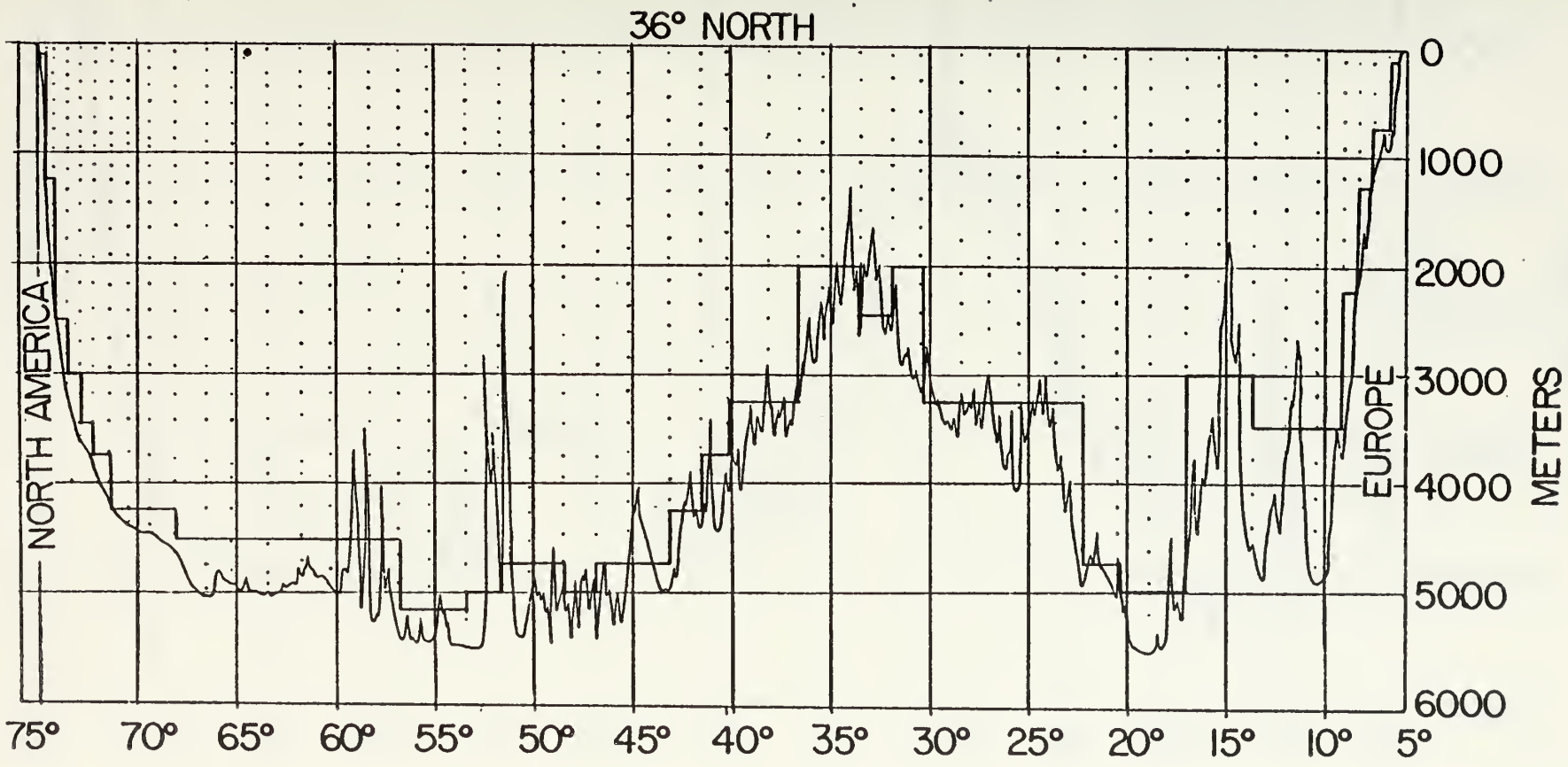
36° NORTH
NORTH AMERICA
EUROPE
METERS
0
1000
2000
3000
4000
5000
6000
75°
70°
65°
60°
55°
50°
45°
40°
35°
30°
25°
20°
15°
10°
5°

Figure 6

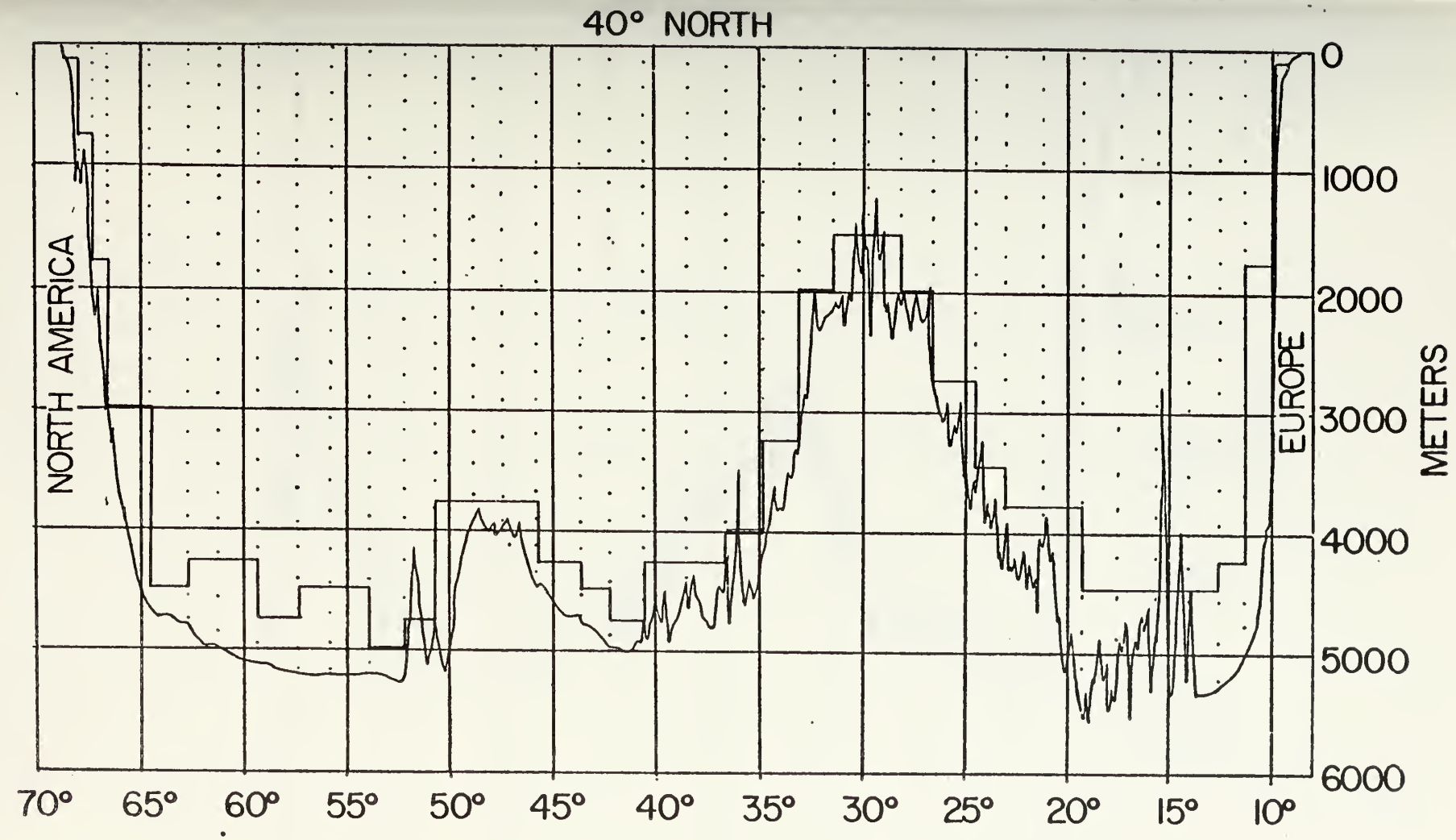
40° NORTH
NORTH AMERICA
EUROPE
METERS
0
1000
2000
3000
4000
5000
6000
70°
65°
60°
55°
50°
45°
40°
35°
30°
25°
20°
15°
10°

Figure 7

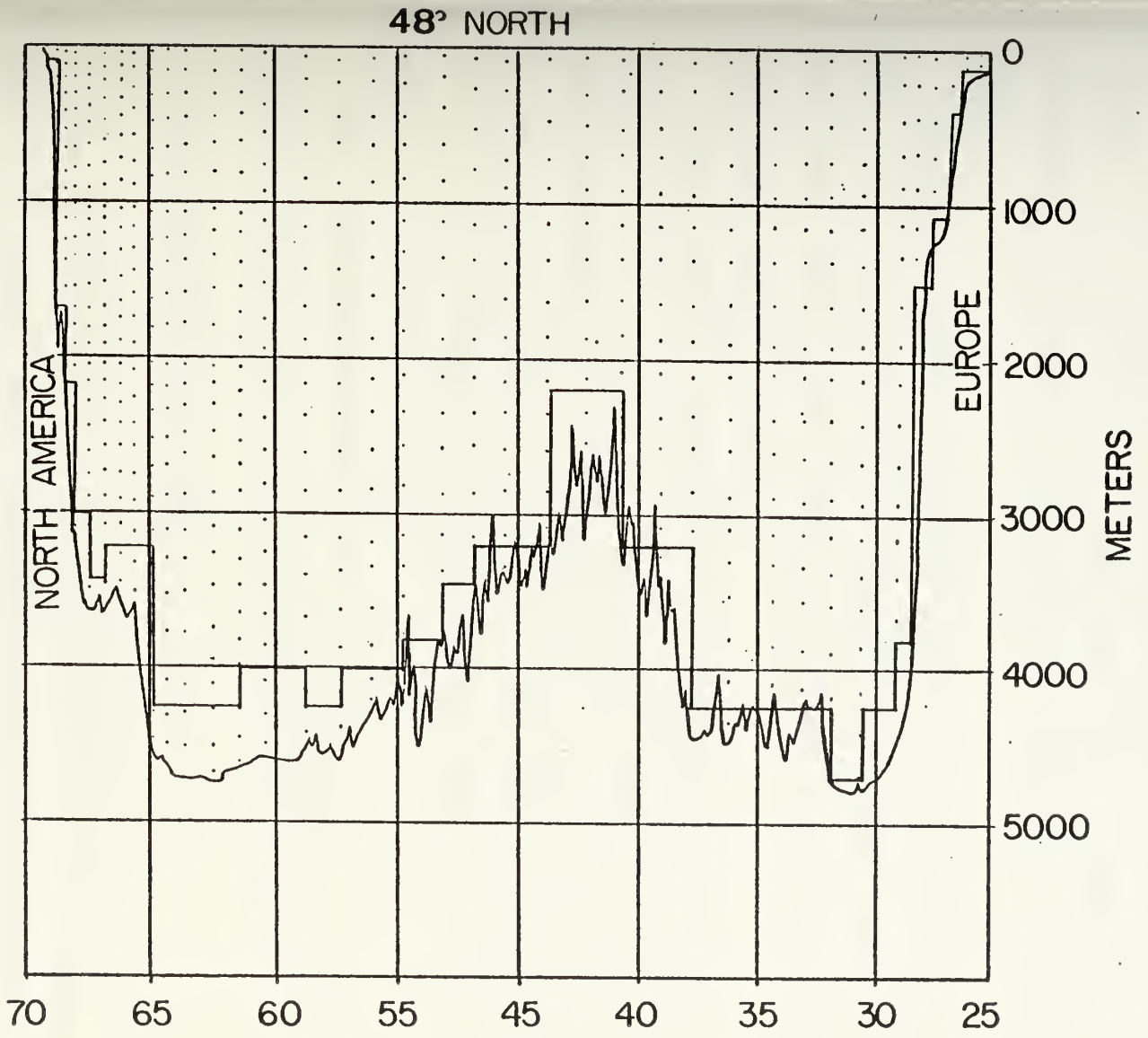
48° NORTH
NORTH AMERICA
EUROPE
METERS
0
1000
2000
3000
4000
5000
70
65
60
55
45
40
35
30
25

Figure 8

to give estimates of the net transport of these three quantities across the bottom area of the entire latitude section.

The values thus determined were added to those previously computed from the surface to the deepest common depth of each station pair to yield the total net transport of mass, salt, and heat for the latitude section.

Each time the level of no motion input is varied, the net transports vary. The level of no motion was considered established when the net flux of mass and salt across the entire latitude section was as close to zero as was considered feasible.

It was essentially impossible to attain exact zero net fluxes of both salt and mass simultaneously*, and it was necessary to establish which flux balance was to be the governing criterion. For this study zero mass flux was considered the primary requirement for balance, with zero salt flux a secondary requirement; however, both flux values were required to approach zero closely.

Once a satisfactory balance of mass and salt transport was achieved, the heat transport value for the latitude section was recorded.

C. IDENTIFICATION OF WATER MASSES

Prior to determining a general circulation pattern for the Upper, Intermediate, and Deep and Bottom Waters of the North Atlantic Ocean, it was necessary to identify the water masses in each of the seven latitude sections. The identification process consisted of matching known

---

*This appears to result from the data spacing, data interpolation and extrapolation techniques, and computer procedures.

temperature and salinity parameters for specific water masses to the interpolated values of temperature and salinity with depth provided for each pair of stations in each latitude section.

Defant (1961), Sverdrup et al. (1942), Williams et al. (1968), and Wright and Worthington (1970) were consulted with each providing specific temperature and salinity parameters for the water masses of the North Atlantic Ocean. However, no one author's criteria fit the data adequately. Therefore, the parameters finally utilized to identify the water masses were selected from the four authors, with the parameters for the transitional waters supplied by this author. Table 3 provides the listing of limits for the temperature and salinity criteria utilized in this study.

In addition to Table 3, some qualifying remarks must be made concerning the identification of the water masses. It will be noted that no parameters are given for surface waters. For this study, North Atlantic Surface Water is considered to be that layer of water exhibiting temperature and salinity variation overlying the central water mass. If no temperature or salinity variation was noted and North Atlantic Central Water parameters were present to the surface, surface water was depicted as extending to the bottom of the mixed layer as determined from temperature and salinity data. Also, in the cases where central water characteristics extended too deep to be reasonable, i.e. deeper than 1000 meters, a minimum salinity value was used as a lower limit. This method was chosen since the minimum salinity value is characteristic of intermediate waters.

Figures 9 through 15 depict the various water masses and transitional waters present. The dark horizontal line indicates the location of the level of no motion for each latitude section.

TABLE III

Temperature and Salinity Criteria for Water Mass Identification in the North Atlantic Ocean

I. Specific Water Masses	Temperature	Salinity	Author
Antarctic Bottom Water	-.4°C	34.66‰	Defant
North Atlantic Deep Water	1.8° to 4.0°C	34.89‰-35.00‰	Wright & Worthington
Antarctic Intermediate Water	3° to 5°C	34.1‰-34.6‰	Defant
Arctic Intermediate Water	3.5°C	34.88‰	Sverdrup
North Atlantic Intermediate Water	3.2° to 6.5°C	34.73‰-34.88‰	Several
Mediterranean Intermediate Water	6° to 10°C	35.3‰-36.4‰	Defant
North Atlantic Central Water	8° to 18°C	35.1‰-36.2‰	Sverdrup
South Atlantic Central Water	6° to 18°C	34.65‰-36.0‰	Williams

II. Transitional Water Masses	Temperature	Salinity
Mediterranean Influence Water	3.8° to 5.84°C	34.88‰-35.3‰
Antarctic Influence Water	4.5° to 6.56°C	34.61‰-34.88‰

FIGURES 9-15

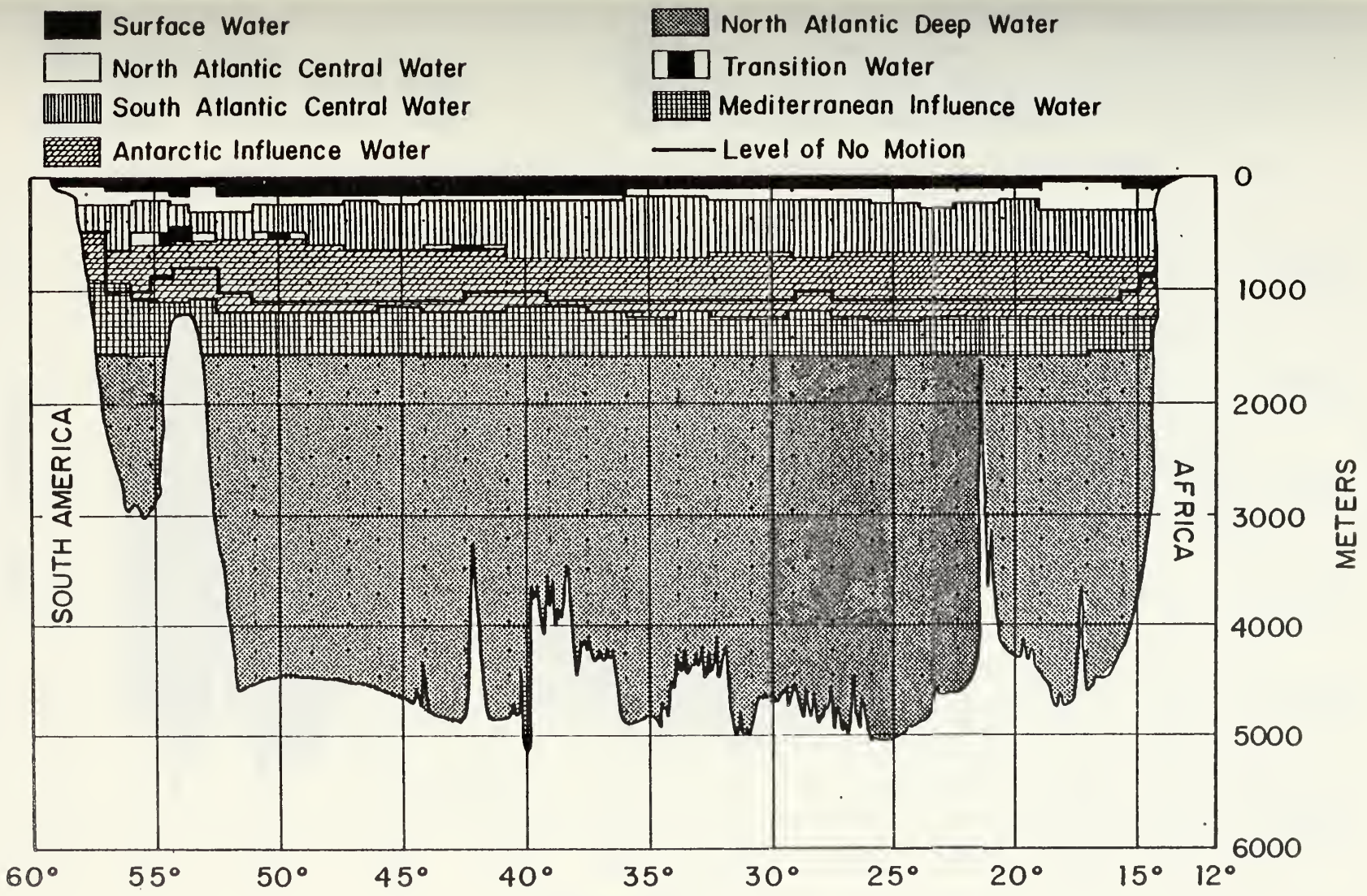
Surface Water
North Atlantic Central Water
South Atlantic Central Water
Antarctic Influence Water
North Atlantic Deep Water
Transition Water
Mediterranean Influence Water
Level of No Motion
SOUTH AMERICA
AFRICA
0
1000
2000
3000
4000
5000
6000
METERS
60°
55°
50°
45°
40°
35°
30°
25°
20°
15°
12°
8° North

Figure 9

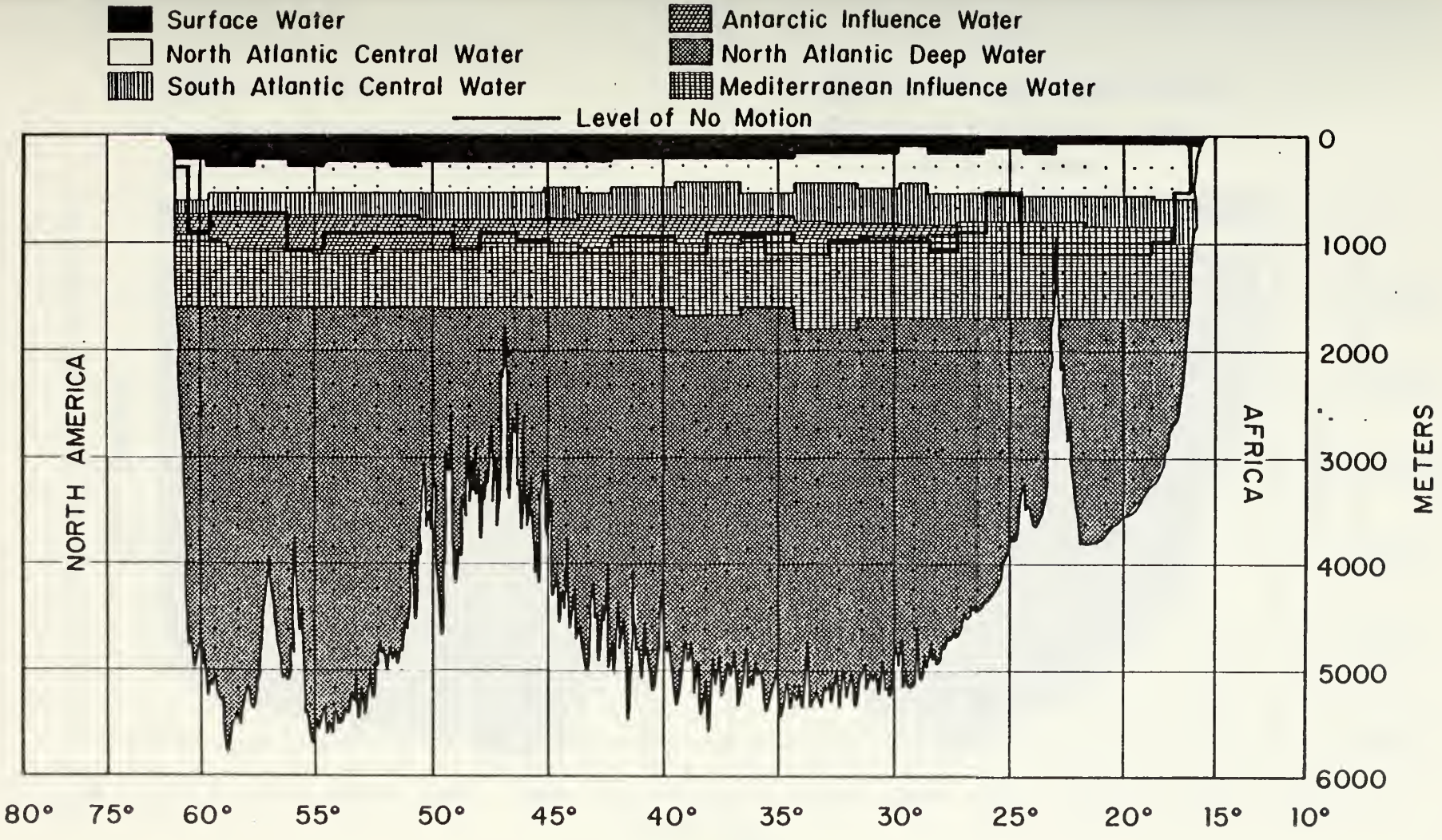

16° North

Figure 10

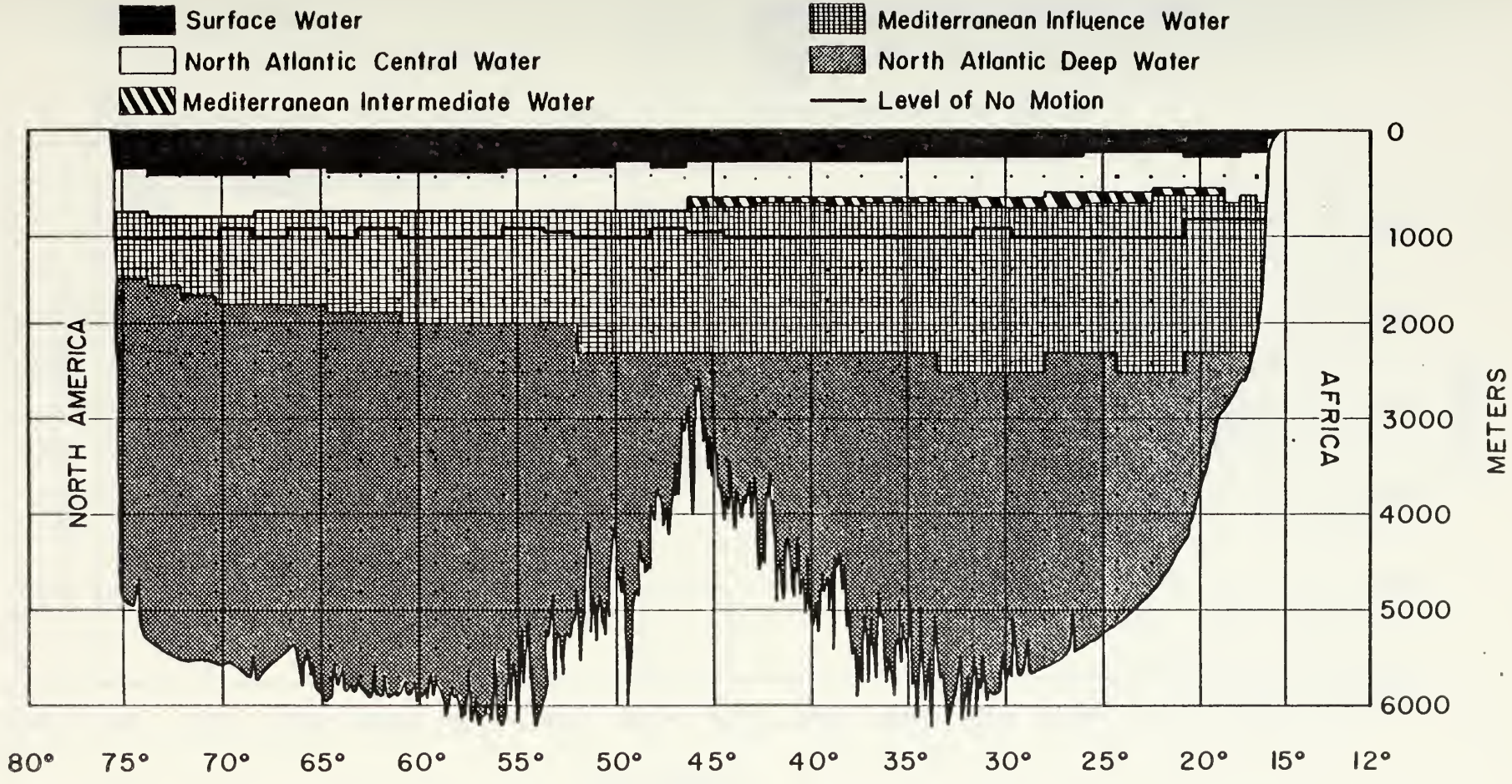
Surface Water
North Atlantic Central Water
Mediterranean Intermediate Water
Mediterranean Influence Water
North Atlantic Deep Water
Level of No Motion
NORTH AMERICA
AFRICA
0
1000
2000
3000
4000
5000
6000
METERS
80°
75°
70°
65°
60°
55°
50°
45°
40°
35°
30°
25°
20°
15°
12°
24° North

Figure 11

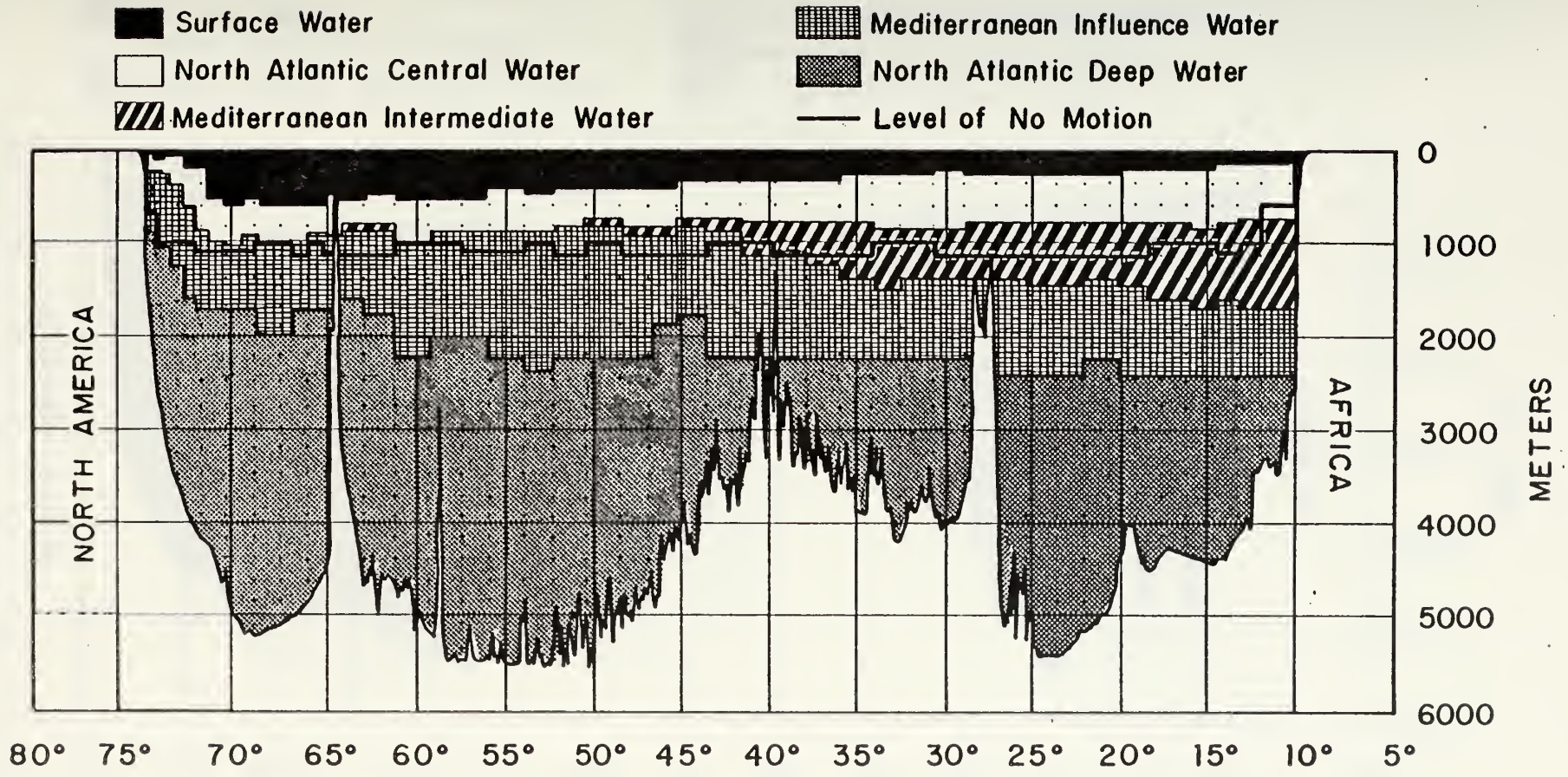

32° North

Figure 12

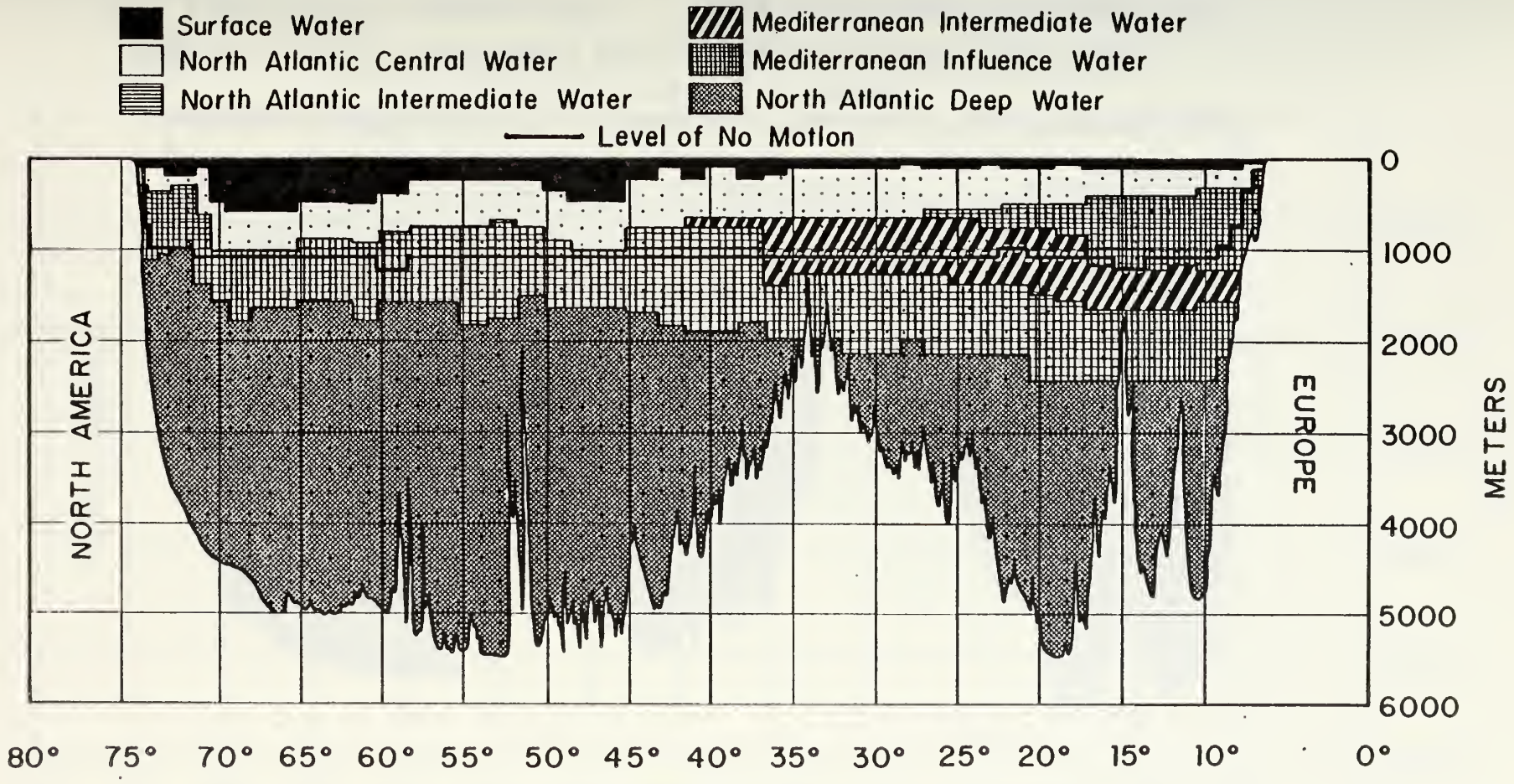
Surface Water
North Atlantic Central Water
North Atlantic Intermediate Water
Mediterranean Intermediate Water
Mediterranean Influence Water
North Atlantic Deep Water
Level of No Motion
NORTH AMERICA
EUROPE
METERS
0
1000
2000
3000
4000
5000
6000
80° 75° 70° 65° 60° 55° 50° 45° 40° 35° 30° 25° 20° 15° 10° 0°
36° North

Figure 13

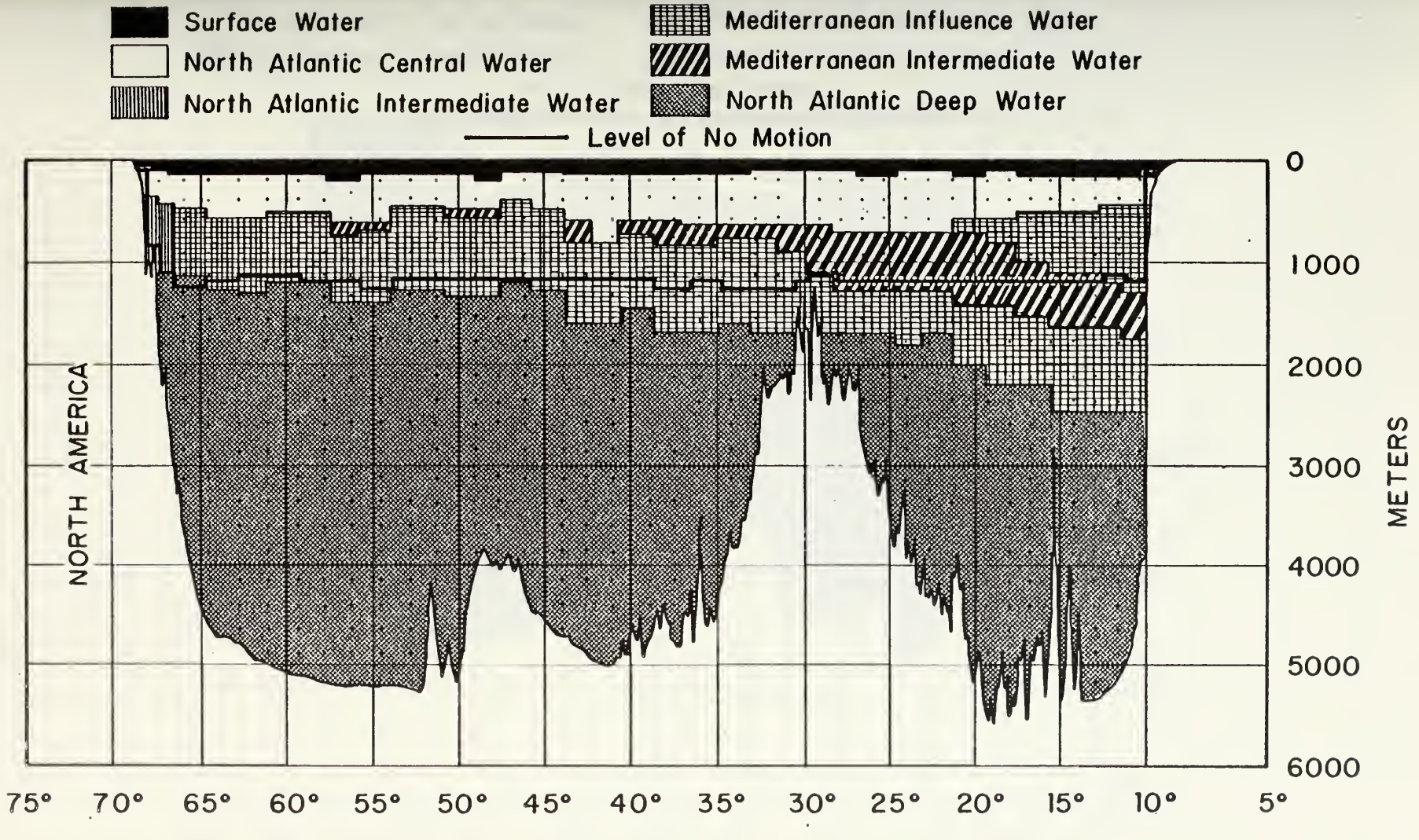
Surface Water
North Atlantic Central Water
North Atlantic Intermediate Water
Mediterranean Influence Water
Mediterranean Intermediate Water
North Atlantic Deep Water
Level of No Motion
NORTH AMERICA
0
1000
2000
3000
4000
5000
6000
METERS
75° 70° 65° 60° 55° 50° 45° 40° 35° 30° 25° 20° 15° 10° 5°
40° North

Figure 14

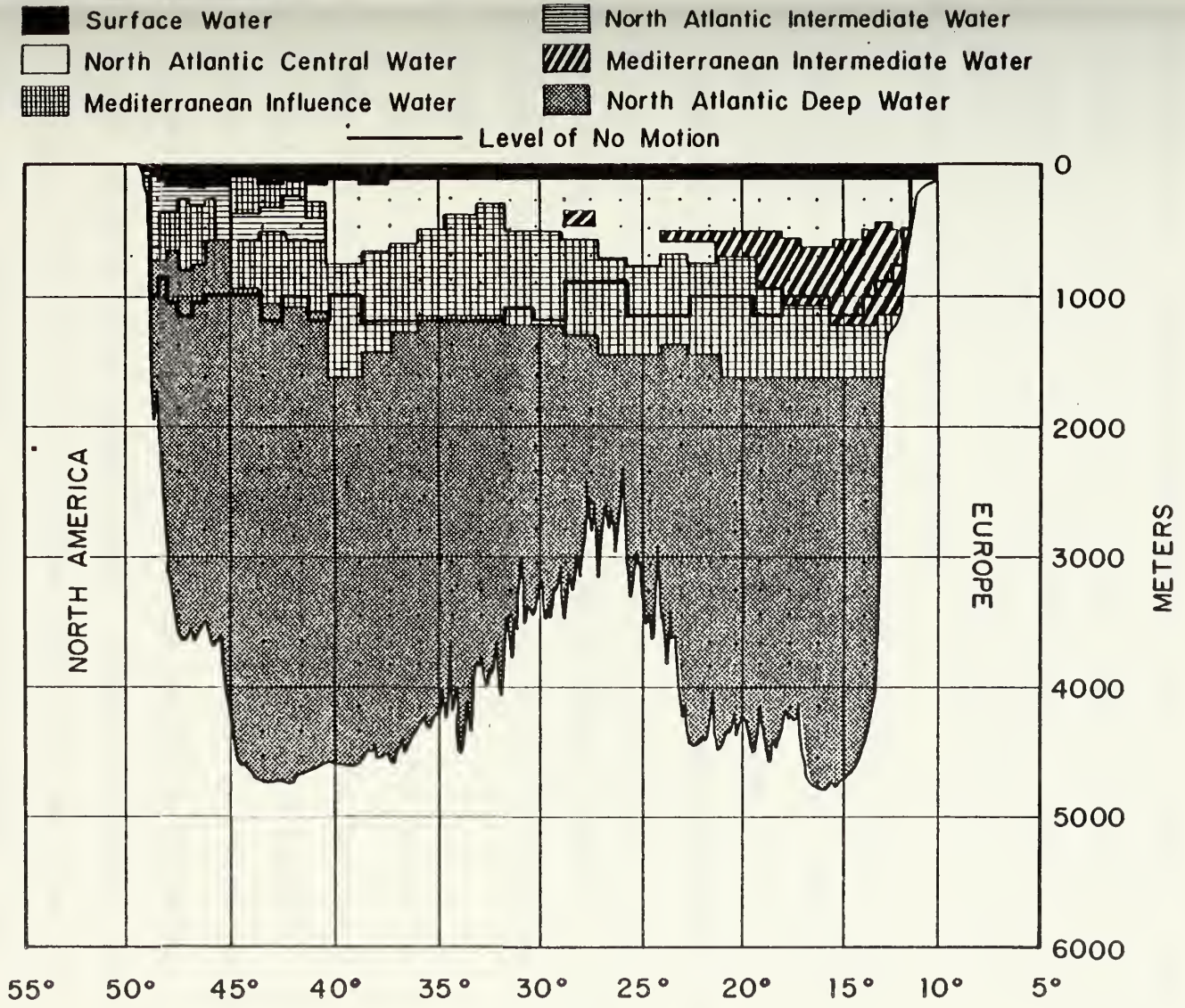
Surface Water
North Atlantic Central Water
Mediterranean Influence Water
North Atlantic Intermediate Water
Mediterranean Intermediate Water
North Atlantic Deep Water
Level of No Motion
NORTH AMERICA
EUROPE
METERS
0
1000
2000
3000
4000
5000
6000
55°
50°
45°
40°
35°
30°
25°
20°
15°
10°
5°
48° North

Figure 15

D. DETERMINATION OF THE GENERAL CIRCULATION PATTERN FOR UPPER, INTERMEDIATE, AND DEEP AND BOTTOM WATER

After the individual water masses for all seven latitude sections had been identified, the water column between pairs of stations in each of the seven sections was divided into three layers: Upper Water, consisting of surface and central waters; Intermediate Water, composed of all intermediate and transitional waters; and Deep and Bottom Water, which consists entirely of North Atlantic Deep Water.

Next, the absolute mass transport for the three layers of water for each pair of stations was computed. This consisted of adding, for all station pairs, the mass transport values between sequential pairs of standard depths for each layer; this yielded an integrated vector quantity of mass transport for each layer (for this study positive values indicate northward transport, and negative values southward transport). Appendix A contains the tabulated results in detail for each of the seven latitude sections.

The mass transport vectors for all station pairs in each of the three layers then were plotted. These vectors were summed for each layer across the entire latitude section yielding a net layer mass transport value. The sum of the net layer mass transports for the three layers in each latitude section was required to match the previously determined mass balance figure to three decimal places. Figures 16 through 18 depict the computed integrated mass transport vectors for the three layers of water. The values depicted in these figures are rounded to the first or second decimal places; Appendix A shows the detailed values to greater accuracy.

The next task was the determination of the general circulation pattern for the Upper, Intermediate, and Deep and Bottom Waters based upon the net mass transport values across each of the latitude circles (see Figures 20 through 22).

To determine a reasonable circulation pattern along each of the latitude sections a pattern of cyclonic and anticyclonic eddies was constructed. The idea of using this extensive pattern of eddies may raise doubts in the minds of some oceanographers, but Robinson (1976) states "eddies are found almost everywhere they are looked for," and the report of the ARIES expedition pointed out "mid-ocean eddies extended from the sea surface to the bottom" (Robinson, 1976).

The pattern of circulation between the seven sections was then constructed. It will be noted that no eddies are shown in the intervening areas between the latitude sections, due to the fact that no direct synoptic measurements were available for these regions. However, it is the author's opinion that the hypothetical mass circulation depicted in these areas is the net result of mass distribution due to undefined mesoscale ocean eddies.

One additional point of clarification must be made. It will be noted that symbols for the loss and gain of water occur throughout the circulation diagrams. Although these symbols appear as specific point sources and sinks, that is not the author's intention. The symbols merely indicate amounts of water that must upwell or sink in these general areas in order to maintain continuity of mass between latitude sections and between the three layers of water.

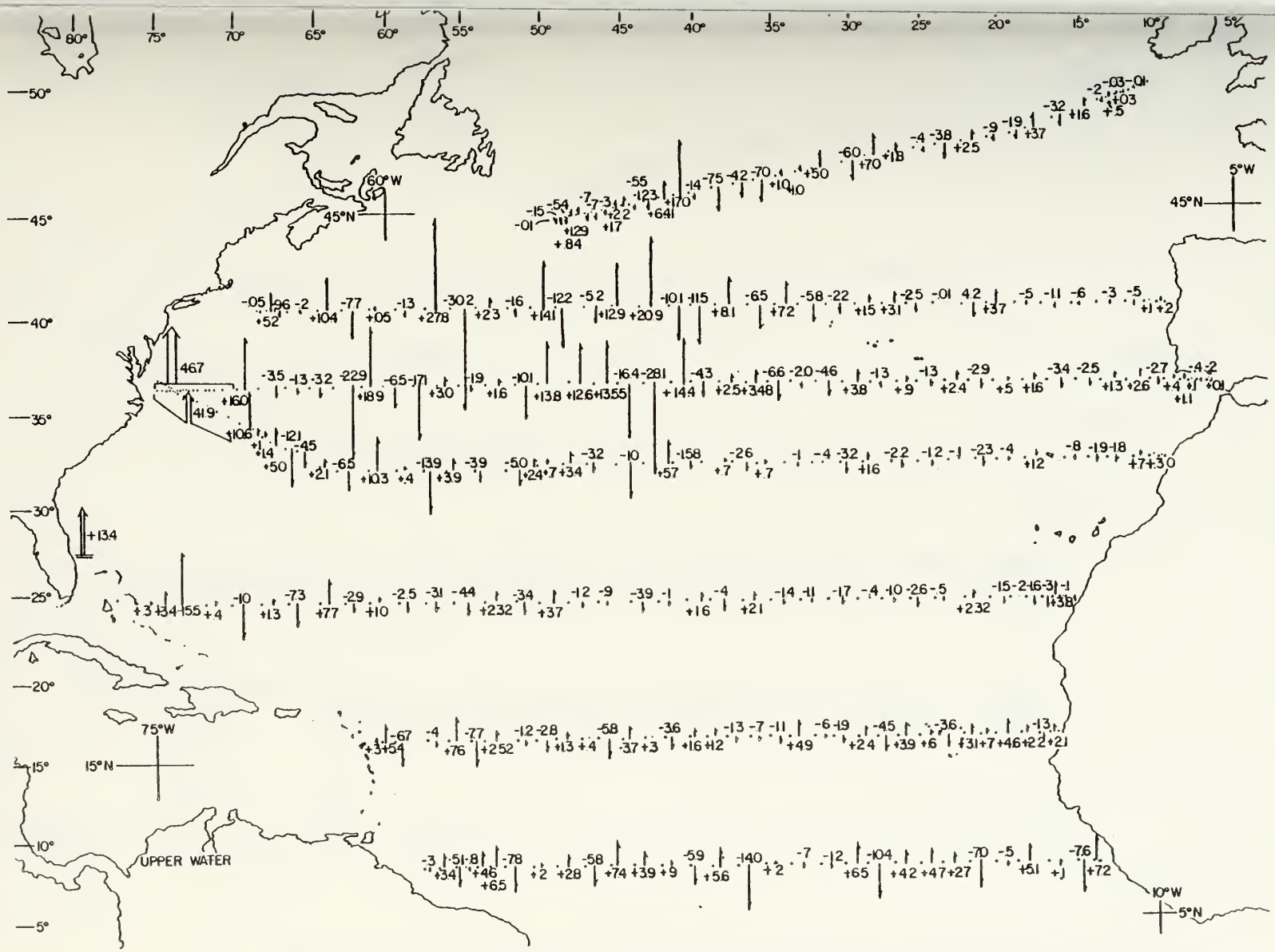

Figure 16. Integrated Mass Transport Vectors - Upper Water

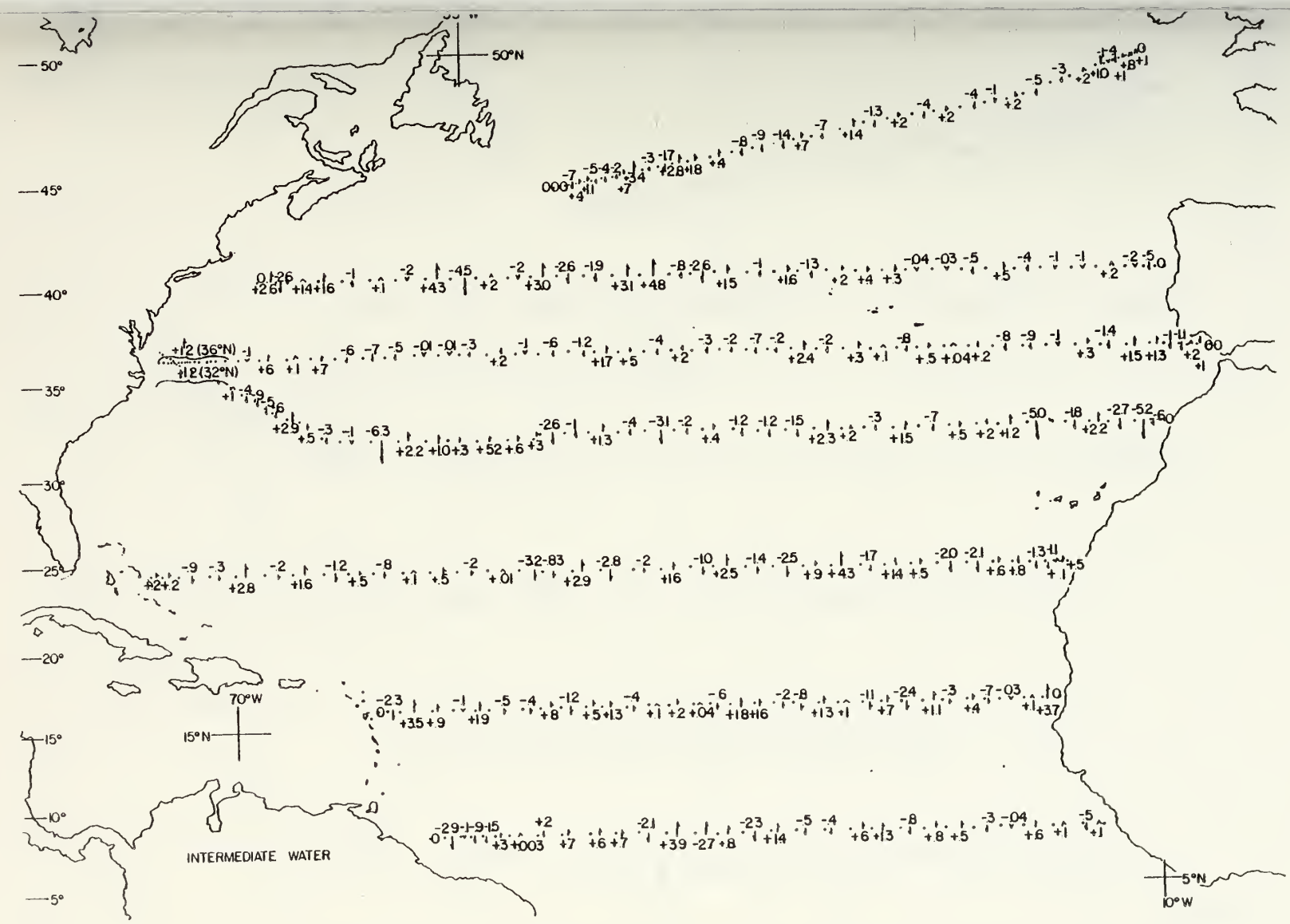

Figure 17. Integrated Mass Transport Vectors - Intermediate Water

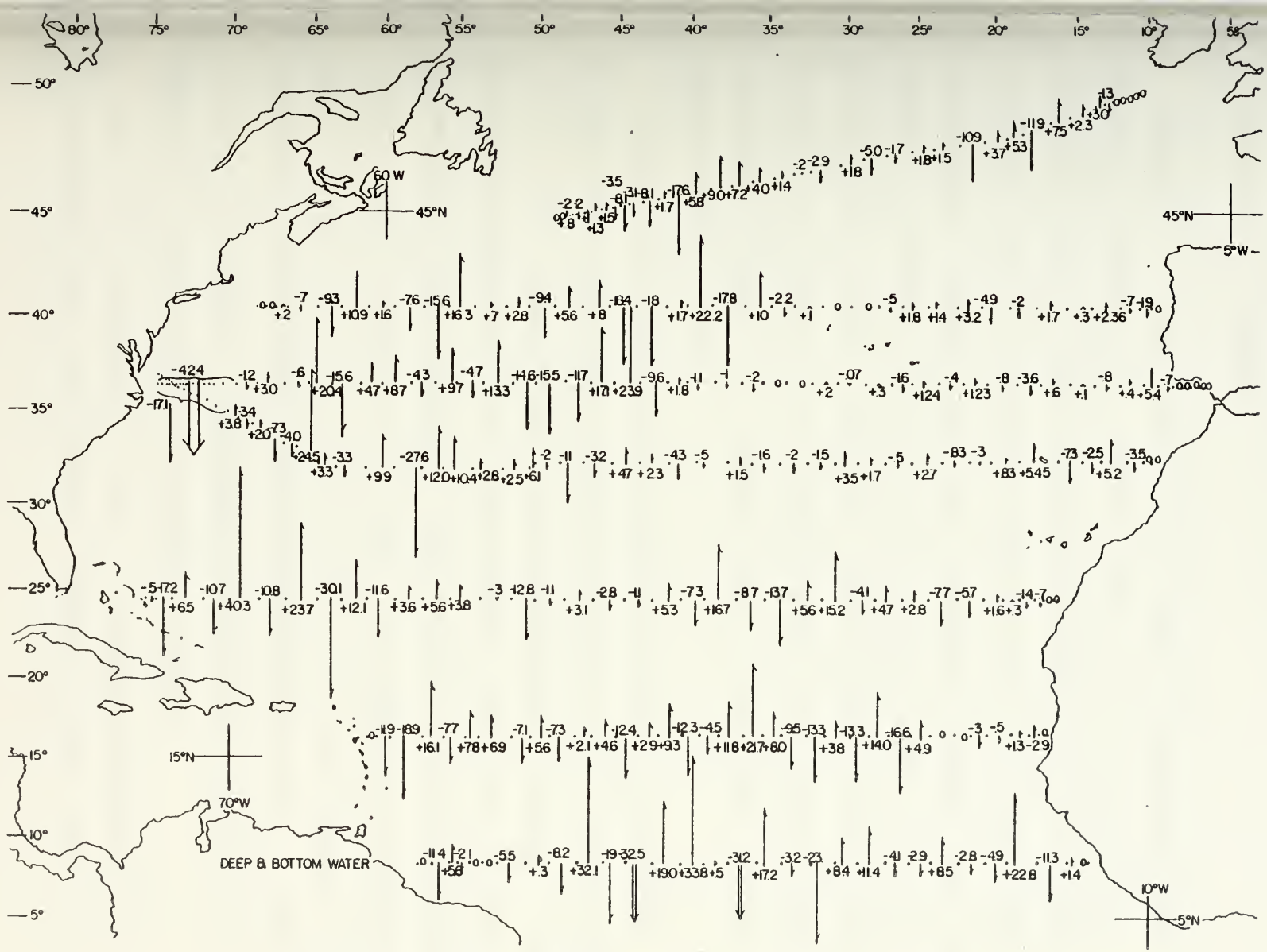

Figure 18. Integrated Mass Transport Vectors - Deep and Bottom Water

V. DISCUSSION OF RESULTS

A. THE LEVEL OF NO MOTION

The method utilized to determine the level of no motion was that proposed by Sverdrup et al. (1942). According to this method, the horizontal reference surface chosen for the ensemble of station pairs in a latitude section is considered to form the level of no motion when the net transport of mass and salt above the reference surface is equal and opposite in direction to that below the reference surface across the entire latitude section. The depths of the reference surfaces comprising the level of no motion for all latitude sections are listed in Table IV, and the distribution of the reference levels has been shown for each section in Figures 9-15.

A comparison of the level of no motion for each of the latitude sections used in this study with those of previous works, notably those of Riley (1951), Neumann (1954), and Jung (1955), was also made. Reasonable correlation was found with Jung's results, which were also based on the procedure of Sverdrup et al. (1942), and with a portion of Neumann's results, based on Defant's (1941) method. The agreement with Neumann's results exists with only his 20^{o}N and 30^{o}N sections and failed at both low and high latitudes where his "zero level" either shoals or deepens in response to changes in the planetary vorticity with latitude. The comparison of these results is contained in Table V.

Jung (1955) stated that his level of no motion coincided with the 7^{o} isothermal surface, which was also Sverdrup's assumed level for the

TABLE IV

Breakdown of the Level of No Motion for all Latitude Sections

I. 8^{o} North Section (30 Pairs of Stations)

LONM	No. of Times Used/Section	% of Total
1100 meters	18	60%
1000 meters	7	23.3%
900 meters	2	6.7%
800 meters	2	6.7%
500 meters	1	3.3%
	30	100.0%

II. 16^{o} North Section (33 Pairs of Stations)

LONM	No. of Times Used/Section	% of Total
1100 meters	13	39.4%
1000 meters	5	15.1%
900 meters	10	30.3%
750 meters	2	6.1%
500 meters	2	6.1%
50 meters	1	3.0%
	33	100.0%

III. 24^{o} North Section (37 Pairs of Stations)

LONM	No. of Times Used/Section	% of Total
1100 meters	25	67.6%
1050 meters	1	2.7%
1000 meters	5	13.5%
900 meters	5	13.5%
50 meters	1	2.7%
	37	100.0%

IV. 32^{o} North Section (53 Pairs of Stations)

LONM	No. of Times Used/Section	% of Total
1100 meters	29	54.7%
1000 meters	18	33.9%
900 meters	1	1.9%
700 meters	1	1.9%
500 meters	2	3.8%
100 meters	1	1.9%
50 meters	1	1.9%
	53	100.0%

TABLE IV (Cont'd)

V. 36^{o} North Section (59 Pairs of Stations)

LONM	No. of Times Used/Section	% of Total
1250 meters	1	1.7%
1200 meters	3	5.1%
1150 meters	1	1.7%
1100 meters	39	66.1%
1000 meters	8	13.6%
700 meters	2	3.4%
500 meters	1	1.7%
400 meters	1	1.7%
150 meters	1	1.7%
100 meters	1	1.7%
50 meters	1	1.7%
	59	100.0%

VI. 40^{o} North Section (37 Pairs of Stations)

LONM	No. of Times Used/Section	% of Total
1300 meters	2	5.4%
1250 meters	9	24.3%
1200 meters	18	48.6%
1150 meters	4	10.8%
1100 meters	1	2.7%
850 meters	1	2.7%
150 meters	1	2.7%
50 meters	1	2.7%
	37	100.0%

VII. 48^{o} North Section (39 Pairs of Stations)

LONM	No. of Times Used/Section	% of Total
1200 meters	12	30.8%
1100 meters	2	5.1%
1000 meters	14	35.9%
900 meters	4	10.3%
800 meters	1	2.6%
500 meters	1	2.6%
300 meters	1	2.6%
150 meters	1	2.6%
100 meters	2	5.1%
50 meters	1	2.6%
	39	100.0%

TABLE V

A COMPARISON OF THE LEVEL OF NO MOTION FOR THE NORTH ATLANTIC OCEAN

LAT.	BAKER*	LAT.	JUNG (1955)+	LAT.	NEUMANN (1954)+	LAT.	RILEY (1951)+
		0°	900m			0°	900m
8°	900-1100m	9°	55 -30 W long 25 20 15 100m 75m 50m 40m			9°	34.95 isohaline and 2000-2500; 3000-3500
				10°	500m		
16°	750-1100m	18°	85 -80 60 -20 1000m 900m			18°	" "
				20°	880m		
24°	900-1100m	27°	75 -45 40 -15 1000m 900m			27°	" "
				30°	1200m		
32°	700-1100m						
36°	750-1250m	36°	70 -40 35 30 -20 15 -10 1000m 900m 800m 700m			36°	" 3000m
40°	850-1300m	45°	45 -25 20 -5 1000m 800m			45°	" "
48°	800-1200m			50°	1900m		
		54°	50 -35 30 -15 1000m 800m			54°	2500m
		63°	60 -55 40 -0 ; 0 -5 E 700m 500m				

* Baker's results excluding shallow-water, near-shore station values

\+ Results as read from Jung (1955), Table II

southeastern North Atlantic Ocean. On comparing the levels of no motion used in this study with the isothermal and isohaline diagrams contained in the Atlantic Ocean Atlas (Fuglister, 1960), no correlation was found to exist with any isohaline surface; only the 24°N section level of no motion exhibited any correlation with an isothermal surface, coinciding with the 6°C isothermal surface for a sizable portion of the latitude section.

Finally, an examination of the variability in depth of the level of no motion over the area of interest in this study was made and is shown in Table IV. The level was found to remain rather consistent in depth with 85% of all station pairs found to have their segment of the level of no motion residing between 900 meters and 1200 meters. If all near-shore shallow water stations are ignored, leaving only the deepwater stations, 93% of the level of no motion segments lie between 900 meters and 1200 meters.

B. MASS AND SALT TRANSPORT

Prior to determining a value for the heat transport across each of the latitude sections, the best possible balance of water mass and salt was required. The requirement of zero net transport of mass was considered the primary criterion for continuity with the salt balance a secondary criterion. This procedure was adopted after it was found impossible in several sections to arrive at a condition where both a zero net flux of mass and salt existed and the level of no motion remained consistent in depth over the entire latitude section. However, with the adopted procedure, it was possible to obtain excellent mass balance results and satisfactory salt balance results for all latitude sections.

Table VI summarizes the computed net mass and salt transport values for the seven latitude sections of interest; this is an indication of the degree to which the intended mass and salt continuity was attained.

It is interesting to note in Jung's (1955) paper using Meteor Atlas data that he also was unable to achieve a zero net flux of salt across his latitude sections. On comparing his results with those obtained in this work, a remarkable similarity is found. His largest net flux of salt occurs at 45°N whereas in this study it occurs at 40°N, while in both works the most satisfactory salt balance occurs at 36°N latitude. Table VII contains the net salt transports from Jung's (1955) paper.

C. HEAT TRANSPORT

The net meridional transport of heat across a latitude section of the ocean can be represented by the expression

$$C_{ps} (T_n - T_s) \rho_s V_{ns} ;$$

or, if we assume the specific heat at constant pressure of seawater, C_{ps}, to be unity, by

$$(T_n - T_s) \rho_s V_{ns} , \qquad (8)$$

where $\rho_s V_{ns}$ is the meridional mass transport, and the north-south water temperatures are designated T_n and T_s. For a mass balance to exist across a latitude section, as is required by mass continuity, the mass transports $\rho_s V_{ns}$ (north) and $\rho_s V_{ns}$ (south) must cancel. However, the heat transport value does not necessarily vanish since the temperatures of the waters transported in opposing directions may differ resulting in a net meridional flux of heat.

TABLE VI

NET MASS AND SALT TRANSPORT VALUES

Latitude	48°N	40°N	36°N	32°N	24°N	16°N	8°N
Net Mass* Transport	.00491	-.01933	-.31651	.04297	-.02362	.13161	.06502
Net Salt+ Transport	3.12456	9.45634	-.00718	.15148	.10100	-6.23340	-5.23500

* All mass units x 10^{12} gm/sec

+ All salt units x 10^{12} °/oo/sec

TABLE VII

NET SALT TRANSPORT FOR THE NORTH ATLANTIC OCEAN
FROM JUNG (1955) TABLE V

Latitude	63^{o}	54^{o}	45^{o}	36^{o}	27^{o}	18^{o}	9^{o}
Net Salt* Transport	1.096	5.992	36.559	-.003	8.095	6.019	1.812

* All salt units x 10^{12} (^{o}/oo - 30)/sec

This method of computation is not the only procedure available for measuring meridional heat transport in the ocean. Other methods have been proposed such as those of Sverdrup (1955) and Vander Haar and Oort (1973). However, since this method is based on computations from direct measurements of salinity and temperature it was selected as the most suitable approach.

Table VIII contains the net heat transport values determined by this work. Figure 19 gives a comparison of these values with those obtained by Jung (1955); Sverdrup (1956); Sellers (1965); Vander Haar and Oort (1973); and a study conducted by Jung in 1974 through 1976 using this study's data, but neglecting the peripheral areas.

D. OCEANIC EDDY CIRCULATION

The pattern of cyclonic and anticyclonic eddies used in the general circulation pattern of the present investigation was a natural outgrowth of the pattern of mass transport vectors computed for the North Atlantic Ocean. Figures 16 through 18, which depict the integrated mass transport vectors for the three layers of water, show a remarkably consistent pattern of opposing flow for adjacent pairs or larger combinations of oceanographic stations. To accommodate the net transport of mass across each latitude section, an eddy circulation pattern was drawn.

This concept of eddy circulation existing in the North Atlantic Ocean is consistent with past observations. Historically, observations of eddy circulation as found in the Gulf Stream rings has been reported by Iselin (1936 , 1940), Fuglister (1947), Iselin and Fuglister (1948), Fuglister and Worthington (1951), Fuglister (1963), Barrett (1963), Fuglister (1971), Richardson (1976) and Parker (1971). The results of

TABLE VIII

NET HEAT TRANSPORT VALUES

Latitude	$48^{o}N$	$40^{o}N$	$36^{o}N$	$32^{o}N$	$24^{o}N$	$16^{o}N$	$8^{o}N$
Net Heat* Transport	95.20546	135.06939	140.84598	122.60636	76.69357	9.29520	-81.47400

* All heat values x 10^{12} cal/sec

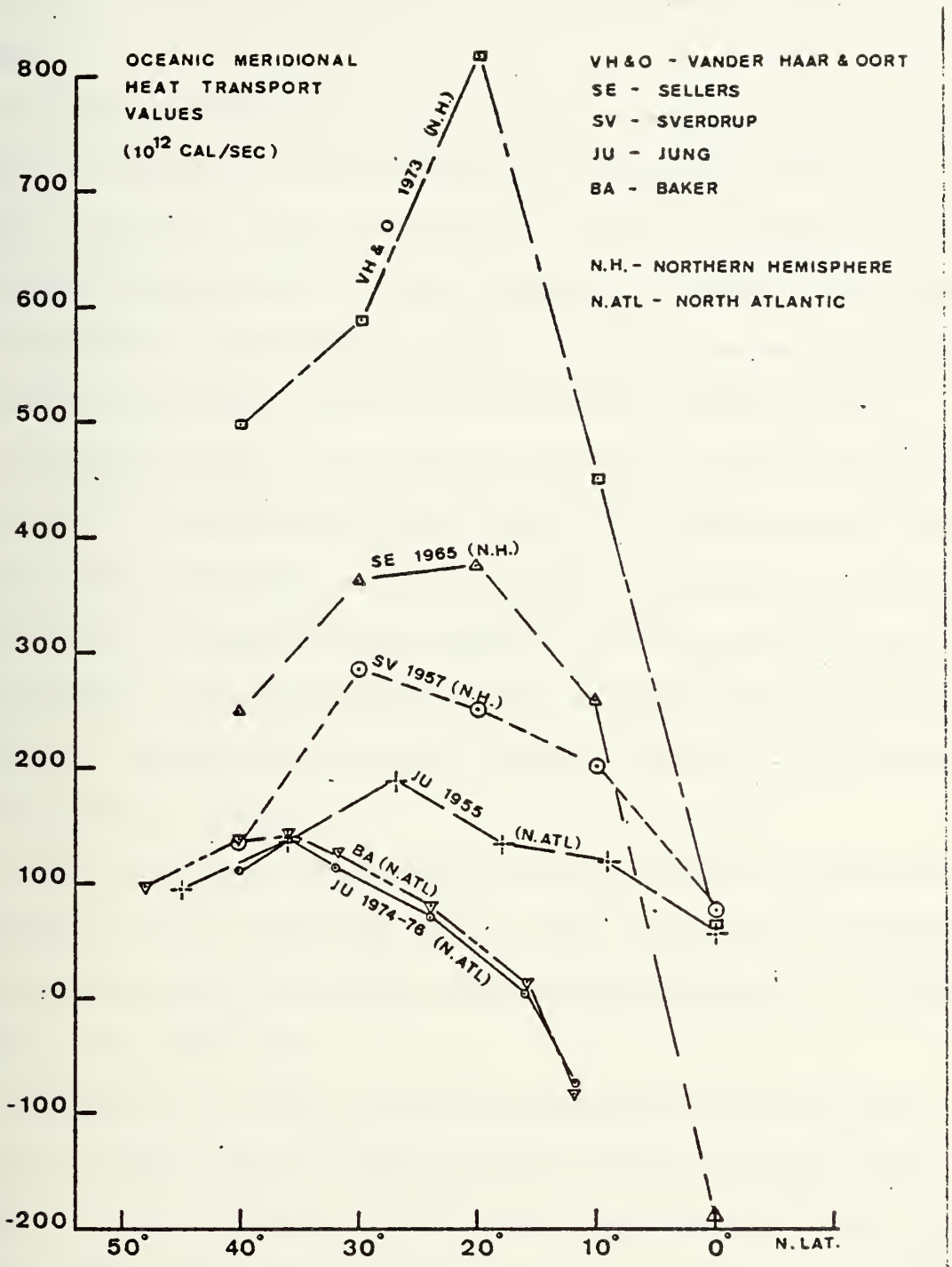

Figure 19. Comparison of Heat Transport Values for the North Atlantic Ocean and the Northern Hemisphere

these studies and of others began the investigation to identify this eddy phenomenon and to see its association with the general circulation of the oceans.

The eddy phenomenon, technically named low frequency mesocale variability, is composed of slow fluctuations on the order of 100 to 200 kilometers in diameter. These fluctuations or areas of variability usually take one of three recognized forms: meanders in the Gulf Stream, cyclonic and anticyclonic rings formed by meanders that have become separated from the Gulf Stream proper, and the mid-ocean eddies (Robinson, 1976).

The mid-ocean eddy, as an entity in itself, was first introduced in the results of the ARIES Expedition (1959-1960). The expedition's observations indicated that not only did mid-ocean eddies exist, but they are several orders of magnitude more energetic than the average circulation. Their results also indicated that the eddy structure extends from the surface to the ocean floor and has a typical radius of 100 to 200 kilometers (Robinson, 1976).

Today the existence of the eddy field and its general characteristics definitely has been established by the results of the Mode-1 experiment which produced the first synoptic map of mid-ocean eddies for a sizable portion of the deep ocean.

In examining the eddy circulation proposed along each latitude section for these layers of water, it will be noted that some eddies exhibit cyclonic circulation at the surface, becoming anticyclonic at depth. The opposite case also holds true. This reverse in circulation with depth has been observed by McCartney, Worthington, and Schmitz (1978). In their study of large cyclonic Gulf Stream rings in the Northern Sargasso Sea, moored current meter data indicated a strong cyclonic circulation

($45 \times 10^6 m^3/s$) overlying a much weaker anticyclonic circulation ($4 \times 10^6 m^3/s$), with the reversal occurring at approximately 200m. These results were then assumed to hold true for the case of anticyclonic circulation overlying cyclonic circulation.

Lastly, although many questions remain to be answered concerning the source(s) of mid-ocean eddies and how they are related to the general circulation of the North Atlantic Ocean, given their strength, long life, and ubiquitous nature, it can be assumed that they contribute significantly to the transfer of mass, salt, and heat in the North Atlantic Ocean.

E. THE GENERAL CIRCULATION PATTERN AND ITS COMPARISON WITH PREVIOUS WORKS

The following discussion of the general circulation of the Upper, Intermediate, and Deep and Bottom Waters as determined in this study has placed special emphasis on the comparison of these results with those of Sverdrup et al. (1942), Jung (1955), and Worthington (1976). However, other authors were referenced for more limited comparisons. The work of Defant (1941) was found extremely useful for his descriptive coverage of the current system of the North Atlantic, yet comparisons were limited to those authors whose descriptions included actual volume transport figures.

In making this comparison with Worthington's work, some difficulty was encountered. Worthington has divided the North Atlantic into five layers based on temperature criteria. Table IX lists these five layers of North Atlantic Water.

In relating these two works it was found that Worthington's Warm Water, Upper and Mid-Thermocline layers correspond to this study's Upper Water in the absence of Mediterranean Intermediate Water. In the presence

TABLE IX

THE FIVE LAYERS OF NORTH ATLANTIC WATER*

	Layer	Temperature Range
1.	Warm Water	Warmer than $17^{o}C$
2.	Upper Thermocline	$12^{o}C$ - $17^{o}C$
3.	Mid-Thermocline	$7^{o}C$ - $12^{o}C$
4.	Lower Thermocline	$4^{o}C$ - $7^{o}C$
5.	Deep	Colder than $4^{o}C$

* According to Worthington, 1976.

of Mediterranean Intermediate Water the correlation ends at the Mid-Thermocline layer's $10^{o}C$ isotherm. The Intermediate Water of this study in turn corresponds to the Lower Thermocline layer, or the Lower Thermocline plus that portion of the Mid-Thermocline layer colder than $10^{o}C$, depending upon the absence or presence of Mediterranean Intermediate Water. In all cases, the Deep and Bottom Water corresponds to Worthington's Deep layer.

In making the comparison of transport values, it was noted that although Jung's paper considered mass transport, those of Sverdrup and Worthington utilized volume transport in terms of Sverdrups (10^{6} m^{3}/sec). To determine the significance of the error involved in such a comparison, the results of a study conducted by Cummings (1977) were used. Cummings compared a large sampling of mass transport values expressed in units of 10^{12} gm/sec and volume transport values in Sverdrups for the North Atlantic. His results indicated the values were consistent to within 2.7%. This error is considered well within acceptable limits.

1. <u>The Circulation Pattern of the Upper Water</u>*

The North Equatorial Current as depicted in Figure 20 is a broad east to west flowing current extending from $16^{o}N$ to $24^{o}N$ latitude. The primary flow is zonal in nature resulting from the influence of the Northern Hemisphere trade winds. The net transport across the $16^{o}N$ and $24^{o}N$ latitude sections results in a net convergence of 19.5 mass units in this region. Mass continuity is maintained by an outflow of 13.4 units into the Caribbean and a loss of 6.1 units by sinking from the upper levels to the Deep and Bottom Water off the coast of Africa.

---

*All mass units are in terms of 10^{12} gm/sec.

The value of the flow into the Caribbean is quite low when compared to the 30sv and 26sv as determined by Worthington and Sverdrup. The 6.1 units lost by sinking finds some support from Worthington's study which indicates 5sv sink from the warm water in this area. However, the sinking is limited in depth to the Upper Thermocline layer.

The outflow from the Caribbean through the straits of Florida again is the extremely low value of 13.4 units, less than 50% of Worthington's 30sv, Jung's 27.5 units, and slightly greater than half of Sverdrup's 26sv. No obvious reason for this anomalously low value is evident. Yet, this is the maximum transport possible as determined by the 27^{o}N latitude section which spans the Florida Current. Some support for this value was found in Wertheim's (1954) study of flow rates and transport in the straits of Florida which indicated a transport of 14sv in December 1952, and 16-18sv in November and December 1953 (Cummings, 1977). The data for the 16^{o} and 24^{o} sections also are autumn data (October-November, 1957) as were the Wertheim data; the 27^{o} data were, however, early summer data from June 1955.

At approximately 30^{o}N the Florida Current is joined by the Antilles Current flowing along the north and east sides of the West Indies. The transport associated with the Antilles current is 19.2 units resulting in a total net northward transport of 32.6 units for this portion of the Gulf Stream. The transport value of 19.2 units associated with the Antilles Current is much higher than the value of 5sv indicated by Worthington, and compensates the Gulf Stream somewhat for the small transport of the Florida Current. Support for this high transport value is found with Sverdrup who indicates that although the Antilles Current usually is considered to be nearer 12sv, it may reach a maximum of 15 to 20sv.

North of the junction of the Antilles Current and the Florida Current, we see the Gulf Stream supplemented by 6.3 units upwelled from the Intermediate Water and 7.8 units from the Sargasso Sea. These additions are supported by Sverdrup et al. (1942) p. 676, who note that the downstream intensification, after combining the Antilles Current and the Florida Current, is due to the addition of Sargasso Sea water and upwelled deep water.

We now have the maximum net northward transport of 46.7 units for the Gulf Stream found at 36°N latitude. This value is 61% of Worthington's value of 76.9sv as determined for 38°N latitude, but is much more comparable to Sverdrup's 55sv, and to Jung's 57.8 units determined for 36°N.

North of 36°N the flow again becomes zonal in nature. As the current proceeds easterly, it divides into two flows, one turning south to create the large return gyre of the North Atlantic Current. The return flow carries with it the majority of the transport, 32 units, leaving 15 units for the formation of the North Atlantic Current. Once again these values are low compared to Worthington, Sverdrup, and Jung, but the relative magnitudes of the currents are correct.

The North Atlantic Current then undergoes a division sending 4.2 units to join the Azores Current which travels southeasterly to join the Portugal Current. The northern element of the current flows northeasterly and is joined off the coast of England by 1 unit flowing north along the western coast of Europe.

The union of the Portugal Current and the Azores Current occurs northwest of the Straits of Gibraltar. The combined flow of 2.6 units proceeds southeasterly forming the Canary Current. Near 32°N this flow is augmented by 0.7 units upwelled from the Intermediate Water. The current then flows southwesterly along the west coast of Africa; as it

approaches 24°N the effects of the trade winds become evident with the eventual combining of the Canary Current with the North Equatorial Current.

At the Straits of Gibraltar, an exchange of 1.0 units with the Mediterranean occurs. This outflow of highly saline Mediterranean Water flows northwesterly towards Cape St. Vincent where it entrains 0.5 units of North Atlantic water and sinks to the Intermediate Water. This value for the exchange with the Mediterranean is low compared to the 2sv proposed by Sverdrup; however, it equals Worthington's 1sv.

After the division of the Gulf Stream, the southern component which forms the North Atlantic Gyre is found to divide again, forming two components: a more intense southward flow of 19.3 units extending east to 45°W longitude, and a very broad diffuse southward flow of 10.3 units extending from 41°W to 21°W. The transport value of the more westward portion of the gyre, acting as the principal mechanism of return flow for the Gulf Stream system, is found to be very similar to the 15-20sv proposed by Sverdrup, and the 19.4 units of Jung; but again it is found to be extremely low compared to the 60sv flow of Worthington's gyre.

It will be noted that within the gyre, several areas of upwelling occur. These locations and the quantities of water indicated, although not directly supported by the other studies, are required to maintain mass continuity between the latitude sections and the different layers involved.

In the region between 8°N and 16°N we find the Equatorial Countercurrent flowing to the southeast, transporting 4.6 units. The current is found to extend from approximately 16°N, 57°W to 8°N, 25°W. These values are very comparable to limits established by Defant (1941), Table 147, in their longitudinal extent, but are found to extend far

beyond the 10°N northern latitude limit. This situation possibly could result from an anomalous migration of the Northern Hemisphere trade winds belt during 1957, thereby allowing the Equatorial Countercurrent to extend farther north than expected. Another explanation arises from the fact that the oceanographic stations of the 8°N section were occupied during May 1957, while those of the 16°N section were occupied in November 1957, each occurring during different phases of the annual north-south migration of the trade wind belt.

The influx of water from the South Equatorial Current amounts to 5.3 units. This value compares most favorably with all authors; however, the location of this addition is much further to the east than previously reported.

One last feature of this circulation pattern is the jet of northward flowing water forming an eastern boundary current off the coast of Africa and Europe. This flow begins at 8°N as a narrow high transport jet of 7.2 units, that continues northward with decreasing magnitude, throughout the entire area of interest. This feature has not been reported before in the general circulation of the upper waters of the Atlantic, although Lacombe and Tchernia (1960), Lacombe (1961), and Madelain (1967) have demonstrated that a current consisting of Mediterranean Water travels north along the Portuguese continental slope at a depth of about 1000 meters. However, this is much too deep to account for this current (Ivers, 1975).

2. The Circulation Pattern of the Intermediate Water

In making the comparison of this general circulation pattern (Figure 21) with previous studies, a paucity of quantitative transport

information was found to exist for the intermediate waters. It is only with Jung's (1955) study that a comprehensive quantitative analysis was found. Worthington's (1976) work, although more recent, is much more limited in its scope, dealing principally with the two major anticyclonic gyres of the North Atlantic. The coverage of the intermediate circulation by Sverdrup et al. (1942) is limited to a brief descriptive discussion. Therefore the following discussion will, of necessity, be more qualitative in nature with quantitative comparisons made whenever possible.

The region between 8°N and 16°N is found to be dominated by the northward flow of 6.9 units of Antarctic Influence Water which is more than three times that proposed by Jung (1955). Sverdrup's model depicting Antarctic Intermediate Water flowing north along the coast of South America and eventually joining the Gulf Stream contrasts to the computed southward flow of 2.3 units with no Antarctic Influence Water penetrating the 16°N section in this locale.

A possible explanation for this rather abrupt termination is the strong zone of convergence found between 16°N and 24°N latitude. This convergence results in 10.7 units, predominantly Antarctic influence Water, sinking to the Deep and Bottom Water. This area of loss is supported by Jung (1955) who indicates losses of 1.45 units to the Deep and Bottom Water and 1.97 units to the North Atlantic Central Water.

North of 24°N the circulation pattern becomes rather obscure. After careful examination, however, it is found to consist of three large and complex anticyclonic gyres and a very weak northward flow associated with the Gulf Stream.

As the Antilles Current crosses 24°N, 0.8 units are lost to southward flow, with another 0.5 units entrained in an area of active upwelling. The remaining 1.3 units continues north, eventually becoming

the intermediate level Gulf Stream. This value is found to be in sharp contrast to the 17 units and 21sv proposed by Jung (1955) and Worthington (1976). As the Gulf Stream passes 36°N, the flow divides forming zonal and northeasterly components. The zonal component extends east to 55°W longitude at which point it alters to a southerly flow. Although this appears to be forming a return mechanism from the Gulf Stream, the return flow is never completed. The southward flowing water enters an area of convergence and upwelling where it rises to join the Upper Water. The northeasterly component continues until joining the northern anticyclonic gyre along the 48°N section.

The first of the three aforementioned gyres is a small closed anticyclone located in the western-most portion of the 40°N latitude section. Although its transport, 0.6 units, is less than the 3sv indicated for Worthington's gyre, its physical size and location are nearly identical.

The second of the anticyclonic gyres incorporates the majority of the flow across the 48°N latitude section. The flow involves 4.1 units, little more than half of Worthington's value, of which 2.7 units are supplied by the Gulf Stream and Mediterranean Waters. Although the northern extent of this gyre cannot be determined for further comparison, the southern limit matches reasonably well with Worthington's northern gyre.

The last and most extensive of the Intermediate Water gyres is that associated with the circulation of the Mediterranean Waters. In contrast to the simple flow pattern proposed by Sverdrup et al. (1942), Figure 188, a complex anticyclonic gyre composed of many smaller eddies was found extending from the Iberian coast to 55°W and from 40°N to 30°N. Upon sinking the Mediterranean Water is distributed to the west, north, and south by this extensive system of eddies accounting for the presence of

Mediterranean Intermediate Water and/or Mediterranean Influence Water over a large percentage of the North Atlantic Ocean (see Figures 9 through 15). The distribution pattern resulting from this type of circulation is well supported by Worthington (1976), Figure 23, depicting salinity along the $6^{o}C$ isothermal surface in the North Atlantic.

Again, it must be made clear that the numerous areas of sinking and upwelling have been determined principally by the need to maintain mass continuity.

3. The Circulation Pattern of the Deep and Bottom Water

In conducting an investigation of the deep circulation of the oceans, one finds a myriad of contrasting, and in many cases conflicting, interpretations of circulation patterns and transport values. The pattern proposed in this study attempts to provide a reasonable and geostrophically-consistent solution based on the given data.

The dominant feature of the circulation pattern proposed for the Deep and Bottom Water (Figure 22) is the intense southward transport along the western boundary of the ocean. Appearing as the converse of the surface and intermediate Gulf Stream, the flow is formed by the union of a south-westerly flow of 20.5 units from the Labrador Sea, and a zonal component of 21.9 units. On passing south of $36^{o}N$ the flow is greatly reduced losing 11.6 units to a return gyre, and 13.6 units to an area of turbulent flow and upwelling. The flow continues south along the South American coast, eventually transporting 13.2 units south of $8^{o}N$ latitude.

This pattern is in direct contradiction to that depicted by Worthington (1976), Figure 11, who has proposed a large anticyclonic gyre extending from $32^{o}N$ to $40^{o}N$ and from $75^{o}W$ to $45^{o}W$ transporting 62sv to the north, with a

weaker countercurrent of 6sv inshore of the gyre. Schmitz (1977), in commenting on this circulation scheme, points out that Worthington's pattern is somewhat doubtful due to its violation of geostrophic balance. Schmitz also indicates that moored instrument data have revealed that a northeastward flow is in fact present but located 100-200 km south of the position indicated by Worthington, with a deep strong countercurrent under the axis of the Gulf Stream. Schmitz thus supports the results of this study which indicates a northeastward flow exists seaward of the Gulf Stream from 24°N to 40°N.

The strongest support for this study's flow pattern from 65°W to the western boundary is found in Figure 23 from Tucholke, Wright, and Hollister (1973). This figure is a summary of actual current measurements and photographic evidence of bottom currents. Close comparison of this figure with the circulation pattern of Deep and Bottom Water proposed in this study shows a remarkable degree of correlation.

As we continue eastward, we see the remainder of the Deep and Bottom Water circulation pattern appears as an extensive system of cyclonic and anticyclonic eddies with little or no large-scale coherent current pattern. However, two additional features are present that find support, or at least mention, in previous works. The first, found in the Central North Atlantic in the region of 48°N, 45°W, is a southward flow of North Atlantic Deep Water penetrating south of 24°N. This flow is found to be nearly identical to Defant's (1941) "Middle Branch" of deep water that flows along the eastern slope of the Mid-Atlantic Ridge. The second feature is the large anticyclonic gyre located between 24°N and 32°N, and extending from 70°W to 45°W. Although not directly supported, Schmitz (1977) indicates that moored data from 60°W hints at the existence of a weak deep easterly flow or a closed gyre in this location.

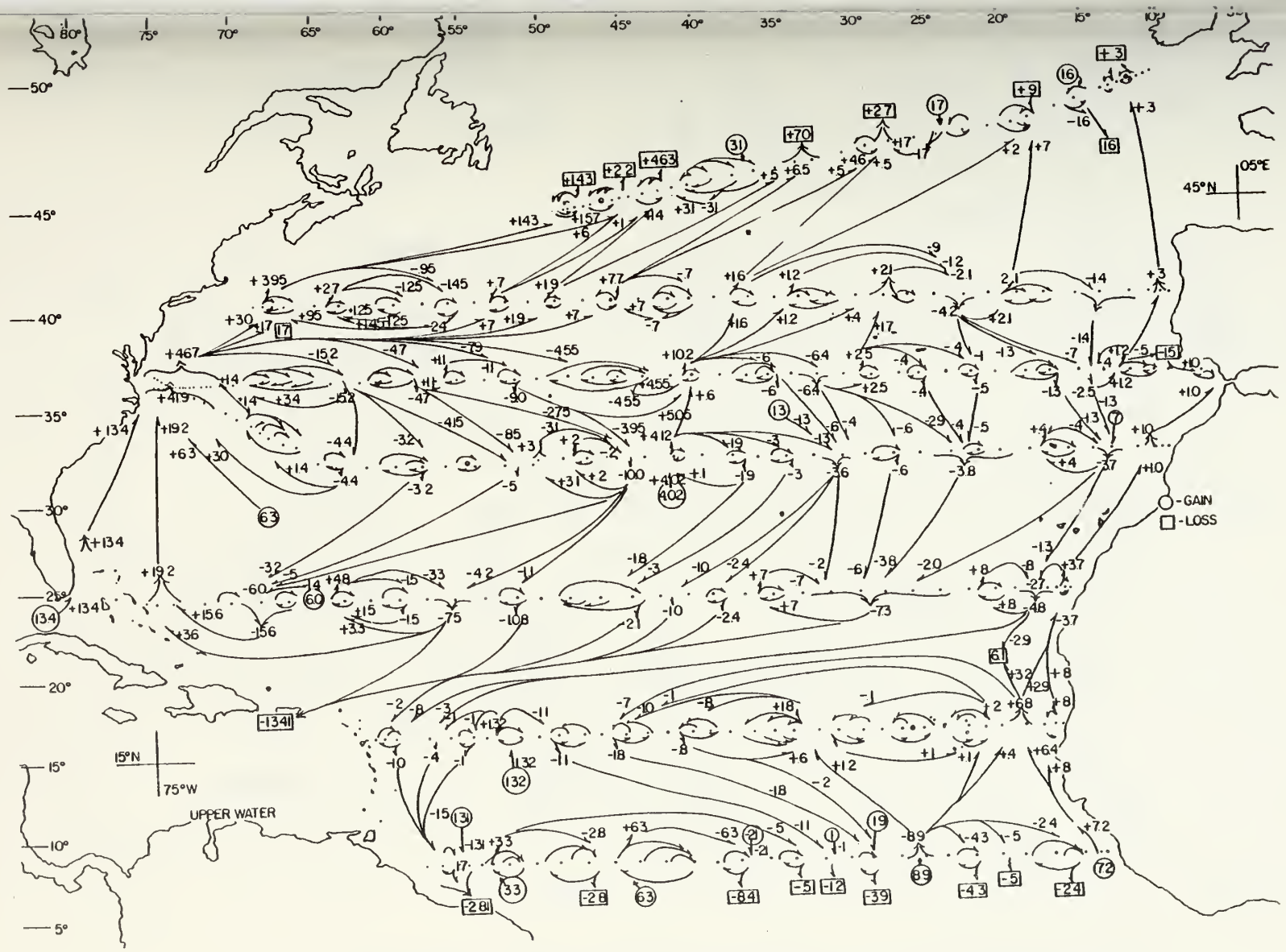

Figure 20. General Circulation Pattern - Upper Water

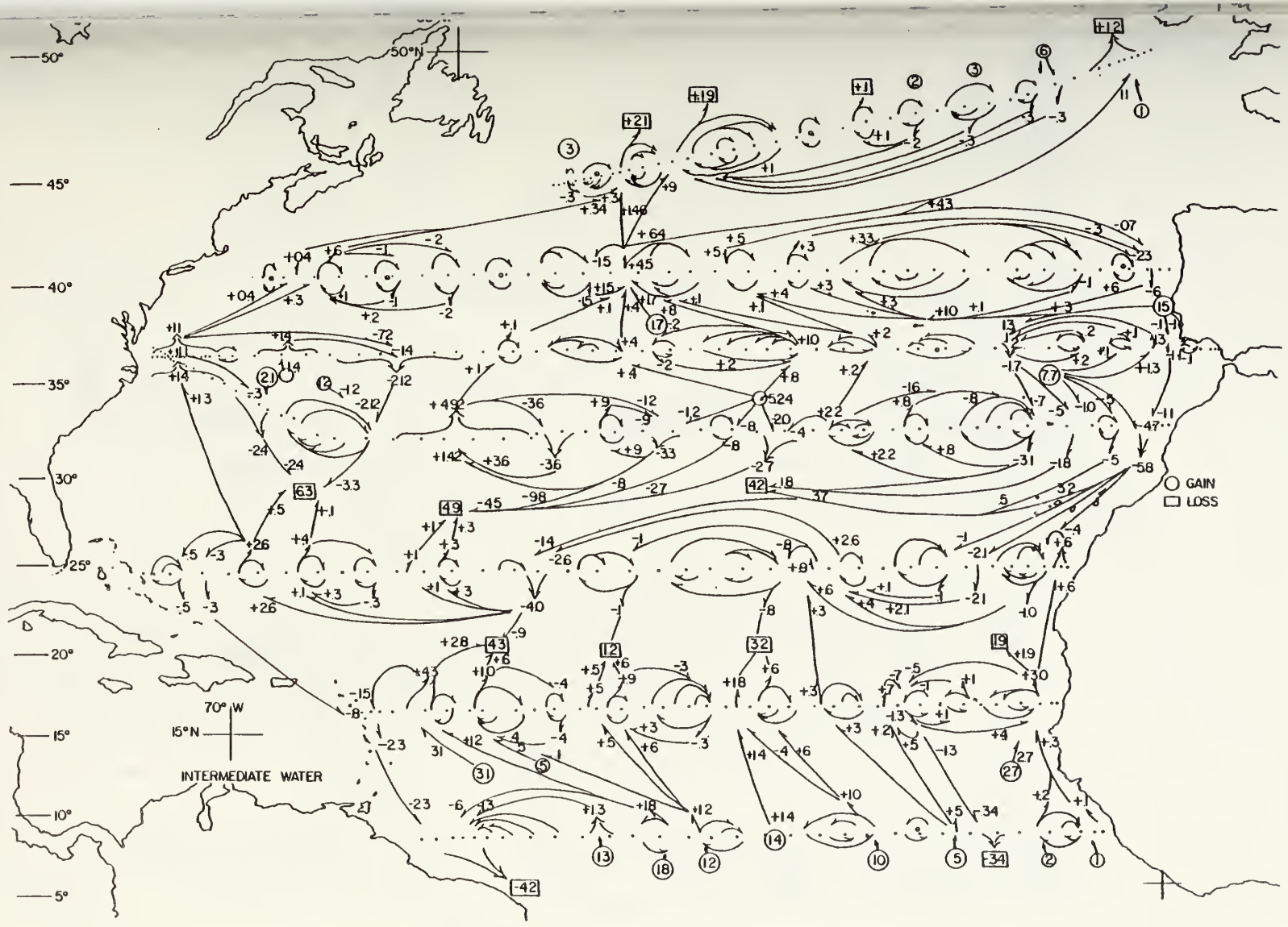

Figure 21. General Circulation Pattern - Intermediate Water

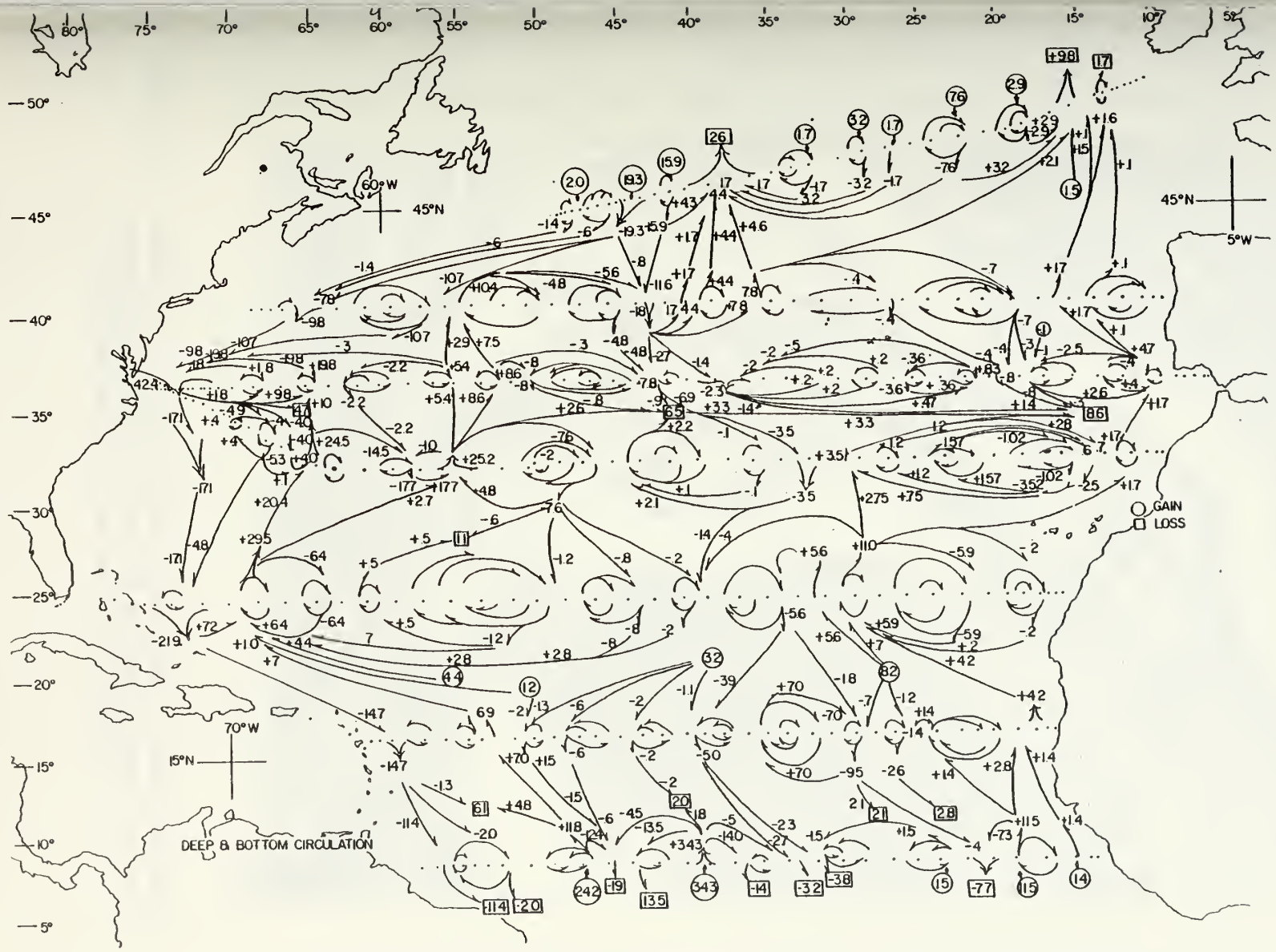

Figure 22. General Circulation Pattern - Deep and Bottom Water

Figure 23. Summary of direct current measurements (white arrows) and photographic evidence of bottom currents according to Tucholke, Wright, and Hollister (1973).

4. A Comparison of Geostrophic and Directly Measured Currents

The circulation patterns presented in the previous sections were predicated upon mass transport values resulting from calculated geostrophic currents. To gain some insight into the degree of correlation that exists between these computed values and directly measured values, the results of a study conducted by Cummings (1977) are introduced.

Cummings, using these same I.G.Y. data, conducted probably the most extensive comparison to date of geostrophic and directly measured currents. Using 110 direct current values extending from 16°N to 40°N, Cummings found extremely encouraging results: 54% showed agreement in both magnitude and direction; 21% showed agreement in direction but not magnitude; and 25% showed no agreement in either category. As an addendum, Cummings stated that of these 110 values, only 25 occurred during the period of this study, 1955-1959; of these, 19 (76%) agreed in both magnitude and direction; 4 (16%) agreed in direction only; and 2 (8%) showed no agreement.

To determine the degree of correlation between the geostrophic velocities of Cummings' study and those of this study, a comparison of the mass transport values of the two works was made. The results of this comparison, contained in Table X, shows that a 90% overall correlation exists between the two works. It should be pointed out, however, that a higher degree of correlation most likely exists since Cummings' work computed mass transport values for only two layers, that above and below the level of no motion. Therefore, in relating those two layers to the three layers of this study, the comparison could be done only for the two most representative layers, namely the Upper, and Deep and Bottom Water, thereby eliminating the mass transport values of the Intermediate Water.

The high degree of correlation that exists between Cummings' work and the present study allows the assumption to be made that the geostrophic calculations and the resulting circulation pattern of this study are well supported by actual current observations.

TABLE X

COMPARISON OF MASS TRANSPORT VALUES OF THIS STUDY WITH THOSE COMPUTED BY CUMMINGS (1977)*

LAT.	NO. OF STATION PAIRS	WATER LAYER	AGREEMENT IN MAGNITUDE AND DIRECTION	%	AGREEMENT IN DIRECTION BUT NOT MAGNITUDE	%	NO AGREEMENT**	%
40°N	37	Upper	27	73%	10	27%	0	0%
	37	D+B+	36	97%	1	3%	0	0%
36°N	59	Upper	58	98%	1	2%	0	0%
	59	D+B	57	97%	1	2%	1	2%
32°N	53	Upper	52	98%	1	2%	0	0%
	53	D+B	47	89%	6	11%	0	0%
27°N	9	Upper	9	100%	0	0%	0	0%
24°N	37	Upper	35	95%	1	2.5%	1	2.5%
	37	D+B	29	78%	7	19%	1	3%
16°N	35	Upper	33	94%	0	0%	2	6%
	35	D+B	26	74%	9	26%	0	0%
TOTAL	451		409	91%	37	8%	5	1%

* Positive agreement criterion was established as $\pm$ 2 x 10^{12} gm/sec with no change in direction.

** No agreement was considered to exist if no directional correlation existed.

\+ D+B = Deep and Bottom Water

VI. CONCLUSIONS

This study represents the culmination of a series of three papers dealing with the I.G.Y. data for the North Atlantic Ocean. Using procedures pioneered by Jung (1955), this work attempted to determine: (1) a level of no meridional motion based on the principles of mass and salt conservation; (2) the effect of the bottom peripheral areas on the net heat transport of the North Atlantic; and (3) a circulation pattern for the three layers of water from computed mass transport values that are consistent with the geostrophic assumption and the continuity of mass.

A level of no motion was determined that lies near 1100m throughout the North Atlantic based on the procedures of Sverdrup et al. (1942). It was also established that there is no definite correlation between this level and any specific isothermal or isohaline surfaces.

In the comparisons of the net meridional heat transports with those of other studies (Figure 19), it was seen that the inclusion of the heat transported in the bottom peripheral areas did not affect the overall net heat flux to any appreciable degree. It can be stated, however, that the meridional heat transport during the I.G.Y. was anomalously low.

The general circulation patterns from this study, as previously stated, do not hope to reflect all aspects of the unique circulation of the North Atlantic Ocean; but they do portray a detailed and quasi-synoptic representation of the geostrophic currents within the ocean which are responsible for the net flux of heat during the given data period.

APPENDIX A

GEOSTROPHIC DATA

The following pages contain the net mass transport values for the Upper, Intermediate, and Deep and Bottom Waters of each pair of stations contained in the seven latitude sections of this study. All mass transport values are in terms of 10^{12} gm/sec.

The following abbreviations are used throughout:

Upper Water:

SFC = Surface Water
NAC = North Atlantic Central Water
SAC = South Atlantic Central Water

Intermediate Water:

AIW = Antarctic Influence Water
NAI = North Atlantic Intermediate Water
MIW = Mediterranean Influence Water
MED = Mediterranean Intermediate Water

Deep and Bottom Water:

NAD= North Atlantic Deep Water

8°N UPPER WATER

STAT NO.	STAT TOTAL	SFC	NAC	SAC
184-183	-.32480	.3497	-.3651	-.30939
183-182	3.37836	2.04544	-.02816	1.36108
182-181	-5.32287	-6.08849	-.66904	1.43466
181-180	-.80834	2.61926	-.84838	-2.57922
180-179	4.64607	6.11178	.20446	-1.67017
179-178	6.51088	5.13219	.81995	.55874
178-177	-7.82134	-6.66287	-1.41203	.25356
177-176	.20621	-1.91179	.36204	1.75596
176-175	2.76941	.96563	.26285	1.54093
175-174	-5.81477	-.49343	-.44971	-4.87163
174-173	7.43579	1.18149	1.55769	4.69661
173-172	3.92033	2.49905	.08053	1.34075
172-171	.85964	.69029	.15914	.01021
171-170	-5.91738	-3.52636	-.30088	-2.09014
170-169	5.62026	2.58847	.50285	2.52894
169-168	-13.90499	-11.38228	-1.04002	-1.56269
168-167	.20855	-1.61772	-.1576	1.98387
167-166	-.65905	2.12051	.47576	-3.25532
166-165	-1.1508	-.03255	-.61903	-.49922
165-164	6.53048	.3224	1.54919	4.65889
164-163	-10.42494	-2.6136	-1.40572	-6.40562
163-162	4.1658	2.57738	.31313	1.27529
162-161	4.76626	-.02663	2.57404	2.21885
161-160	2.71238	.58522	.81299	1.31417
160-159	-6.99697	-1.42063	-2.03828	-3.53806
159-158	-.51109	.74823	.22592	-1.48524
158-157	5.09587	-.35991	2.19068	3.2651
157-156	.11789	1.60385	-.12904	-1.35692
156-155	-7.55937	-3.40879	-2.77043	-1.38015
155-154	7.16964	.64678	3.53911	2.98375
TOTAL	-1.18289			

8°N INTERMEDIATE WATER

STAT NO.	STAT TOTAL	AIW	MIW
184-183	0.0	0.0	0.0
183-182	-2.8661	1.13552	-4.00162
182-181	-.0826	-1.91447	1.83187
181-180	-.89814	-.89814	0.0
180-179	-1.51636	-1.51636	0.0
179-178	.26819	.26819	0.0
178-177	.00349	.34643	-.34294
177-176	.15296	1.16702	-1.01406
176-175	.69371	1.56759	-.87388
175-174	.5974	-2.23964	2.83704
174-173	.66038	1.92734	-1.26696
173-172	-2.06395	1.27584	-3.33979
172-171	3.85953	.11845	3.74108
171-170	2.73922	-.15509	2.89431
170-169	.78764	.88727	-.09963
169-168	-2.27535	.30148	-2.57683
168-167	1.42611	.25223	1.17388
167-166	-.46517	-.77316	.30799
166-165	-.43354	.50328	-.93682
165-164	.63247	.50525	.12722
164-163	1.27165	-.35059	1.62224
163-162	-.75824	.64709	-1.40533
162-161	.77515	.71649	.05866
161-160	.48097	-.02054	.50153
160-159	-.31092	-.67352	.3626
159-158	-.04039	-.31075	.27063
158-157	.57567	.82100	-.24533
157-156	.08379	-.27526	.35905
156-155	-.49528	-.23910	-.25618
155-154	.05175	.05175	0.0
TOTAL	2.85404		

8°N DEEP AND BOTTOM WATER

STAT NO.	STAT TOTAL (ALL WATER IS NAD)
184-183	0.0
183-182	-11.40281
182-181	5.62678
181-180	-2.06200
180-179	0.0
179-178	0.0
178-177	-5.50047
177-176	.30760
176-175	-8.15742
175-174	32.07795
174-173	-18.97981
173-172	-32.45529
172-171	18.98081
171-170	33.81475
170-169	.46318
169-168	-31.22556
168-167	17.21635
167-166	-3.17139
166-165	-23.51369
165-164	8.36104
164-163	11.37969
163-162	-4.08616
162-161	-2.87780
161-160	8.46067
160-159	-2.80924
159-158	-4.90601
158-157	22.83172
157-156	-11.33475
156-155	1.35568
155-154	0.0
TOTAL	-1.60618

16°N UPPER WATER

STAT NO.	STAT TOTAL	SFC	NAC	SAC
310-309	.34770	.33627	.01143	0.0
309-308	5.39426	.87842	3.76160	.75424
308-306	-6.66477	-3.14138	-2.74021	-.78318
306-305	-.39526	-.79918	.38139	.02253
305-304	7.56191	4.77028	2.14307	.64826
304-303	-7.68819	-5.59720	-1.87273	-.18826
303-302	2.52293	1.81804	.65114	.05375
302-301	-1.19017	-1.34605	-.04053	.19641
301-300	-2.76900	-1.97636	-.56650	-.22614
300-299	1.33217	.60332	.30332	.42553
299-298	.41919	.62829	-.08969	-.11945
298-297	-5.76798	-3.62647	-1.43627	-.70524
297-296	3.69650	1.71249	.91145	1.07256
296-295	.27368	.05929	.14799	.06650
295-294	-3.62508	-2.25465	-.94982	-.42061
294-293	1.59223	.20334	.90577	.48312
293-292	1.23317	.54485	.26988	.41844
292-291	-1.32984	-.53624	-.44680	-.34680
291-290	-.70958	.30017	-.53531	-.47444
290-289	-1.11386	-1.78895	.23602	.43907
289-288	4.89943	1.21808	1.91041	1.77094
288-287	-.59201	-.32724	.05470	-.31947
287-286	-1.94739	-.69728	-.96580	-.28431
286-285	2.36345	-.19083	1.25522	1.29906
285-284	-4.45934	-.20978	-3.03588	-1.21368
284-283	3.85413	.93891	2.41673	.49849
283-282	.62648	.33240	.30148	-.00740
282-281	-3.62958	-1.30361	-1.49996	-.82601
281-280	3.10476	.37764	1.67809	1.04903
280-279	.68370	.09192	.36544	.22634
279-278	4.56607	1.29906	2.28174	.32679
278-277	2.16292	.63056	1.32637	.20599
277-276	-1.39817	-1.41590	-.65135	.66908
276-275	.07940	.07940	0.0	0.0
TOTAL	5.49752*			

* This total contains 2.047 mass units contributed by the bottom peripheral area of stations 276-275 not included in the above summary.

16°N INTERMEDIATE WATER

STAT NO.	STAT TOTAL	AIW	MIW
310-309	0.0	0.0	0.0
309-308	-2.36433	.37714	-2.74147
308-306	3.53219	.93816	2.59403
306-305	.87399	.21631	.65768
305-304	-.04480	.47676	-.52156
304-303	1.90134	.15423	1.74711
303-302	-.47244	.02610	-.49854
302-301	-.39710	.01203	-.40913
301-300	.76216	.01013	.75203
300-299	-1.18890	.13291	-1.32181
299-298	.50350	-.00529	.50879
298-297	1.31333	-.26468	1.57801
297-296	-.40753	.40016	-.80769
296-295	.08828	.11370	-.02542
295-294	.21514	-.19236	.40753
294-293	.03596	.10138	-.06542
293-292	-.58777	.25037	-.83814
292-291	1.77032	-.03379	1.80411
291-290	1.57450	-.12105	1.69555
290-289	-.15103	.19912	-.35015
289-288	-.78472	.44019	-1.22491
288-287	1.29972	-.04423	1.34395
287-286	.07502	-.01656	.09158
286-285	-1.06783	.07146	-1.13929
285-284	.64787	-.10105	.74892
284-283	-2.36351	0.0	-2.36351
283-282	1.10722	0.0	1.10722
282-281	-.25309	0.0	-.25309
281-280	.39727	0.0	.39727
280-279	-.72795	0.0	-.72795
279-278	-.03207	0.0	-.03207
278-277	.13633	0.0	.13633
277-276	3.73846	0.0	3.73846
276-275	0.0	0.0	0.0
TOTAL	9.11645		

16°N DEEP AND BOTTOM WATER

STAT NO.	STAT TOTAL (ALL WATER IS NAD)
310-309	0.0
309-308	-11.86731
308-306	-18.87209
306-305	16.06306
305-304	-7.72756
304-303	7.84082
303-302	6.85646
302-301	-7.03319
301-300	5.57014
300-299	-7.29519
299-298	2.11222
298-297	4.64007
297-296	-12.39570
296-295	2.86841
295-294	9.27541
294-293	-12.24428
293-292	-4.48943
292-291	11.78491
291-290	21.68922
290-289	7.97124
289-288	-9.46687
288-287	-13.26967
287-286	3.78026
286-285	-13.31789
285-284	13.96027
284-283	-16.57470
283-282	4.93409
282-281	0.0
281-280	0.0
280-279	-2.97441
279-278	-.48774
278-277	1.27340
277-276	2.91500
276-275	0.0
TOTAL	-14.48235

24°N UPPER WATER

STAT NO.	STAT TOTAL	SFC	NAC
3624-3623	.29845	-.86167	1.16012
3623-3622	3.38121	3.24083	.14038
3622-3621	15.50684	10.45671	5.05013
3621-3620	.39388	-.09491	.48879
3620-3619	-9.95086	-7.06233	-2.88853
3619-3618	1.27708	.79817	.47891
3618-3617	-7.27175	-5.61016	-1.66159
3617-3616	7.71168	5.34272	2.36896
3616-3615	-2.88011	-2.22091	-.65920
3615-3614	1.04967	.57133	.47834
3614-3613	-2.50160	-1.79955	-.70205
3613-3612	-3.04990	-2.46167	-.58823
3612-3611	-4.43060	-2.95456	-1.47604
3611-3610	2.32944	1.70473	.62471
3610-3609	-3.36373	-2.73383	-.62990
3609-3608	3.66237	2.69897	.96340
3608-3607	-1.17248	-1.21386	.04133
3607-3606	-.85913	-.58475	-.27438
3606-3605	-3.93210	-2.90018	-1.03192
3605-3604	-1.03951	-.32555	-.71396
3604-3603	1.58159	.47600	1.10559
3603-3602	-3.95641	-2.19684	-1.75957
3602-3601	2.11601	1.07806	1.03795
3601-3600	-1.41678	-1.03215	-.38463
3600-3599	-1.12176	-.44489	-.67687
3599-3598	-1.65708	-1.15832	-.49876
3598-3597	-.31895	-.10022	-.21873
3597-3596	-1.00327	-.80739	-.19588
3596-3595	-2.67481	-1.53620	-1.13861
3595-3594	-.46873	-.34400	-.12473
3594-3593	2.32844	.84761	1.48083
3593-3592	-1.49438	-.90897	-.58541
3592-3591	-.15900	-.16654	.00754
3591-3590	-1.49210	-.97980	-.51230
3590-3589	-2.93181	-1.39728	-1.53453
3589-3588	3.79237	1.48959	2.30278
3588-3587	-.03892	-.03892	0.0
TOTAL	-14.11674		

24°N INTERMEDIATE WATER

STAT NO.	STAT TOTAL	MIW	MED
3624-3623	.18976	.18976	0.0
3623-3622	.20823	.20823	0.0
3622-3621	-.93935	-.93935	0.0.
3621-3620	-.26321	-.26321	0.0
3620-3619	2.83645	2.83645	0.0
3619-3618	-.23515	-.23515	0.0
3618-3617	1.55946	1.55946	0.0
3617-3616	-1.21845	-1.21845	0.0
3616-3615	.48669	.48669	0.0
3615-3614	-.82912	-.82912	0.0
3614-3613	.05045	.05045	0.0
3613-3612	.50000	.50000	0.0
3612-3611	-.17095	-.17095	0.0
3611-3610	.01347	.01347	0.0
3610-3609	-3.23184	-3.23184	0.0
3609-3608	-.82703	-.82703	0.0
3608-3607	2.89328	2.89328	0.0
3607-3606	-2.84478	-2.84015	-.00463
3606-3605	-.17866	-.05211	-.12655
3605-3604	1.57195	1.67757	-.10562
3604-3603	-.93753	-1.08242	.14489
3603-3602	2.63124	2.95798	-.32674
3602-3601	-1.34929	-1.45094	.10165
3601-3600	-2.48478	-2.54483	.06005
3600-3599	.88008	.94669	-.06661
3599-3598	4.29027	4.39826	-.10799
3598-3597	-1.64690	-1.66892	.02202
3597-3596	1.37962	1.42530	-.04568
3596-3595	.50733	.59981	-.09248
3595-3594	-1.98821	-2.08747	.09926
3594-3593	-2.06235	-2.17584	.11349
3593-3592	.56153	.60203	-.04050
3592-3591	.76311	.77637	-.01326
3591-3590	-1.28938	-1.28938	0.0
3590-3589	-1.14159	-1.14159	0.0
3589-3588	.04502	.04502	0.0
3588-3587	.55429	.55429	0.0
TOTAL	-1.71634		

24°N DEEP AND BOTTOM WATER

STAT NO.	STAT TOTAL (ALL WATER IS NAD)
3624-3623	-.51525
3623-3622	-17.19300
3622-3621	6.48019
3621-3620	-10.69333
3620-3619	40.28519
3619-3618	-10.80161
3618-3617	23.72204
3617-3616	-30.10491
3616-3615	12.09790
3615-3614	-11.56423
3614-3613	3.54576
3613-3612	5.55202
3612-3611	3.83257
3611-3610	-.32115
3610-3609	-12.81473
3609-3608	-1.13451
3608-3607	3.09145
3607-3606	-2.79427
3606-3605	-1.13130
3605-3604	5.28338
3604-3603	-7.32353
3603-3602	16.71581
3602-3601	-8.66357
3601-3600	-13.68396
3600-3599	5.60559
3599-3598	15.14507
3598-3597	-4.07922
3597-3596	4.66236
3596-3595	2.80469
3595-3594	-7.69124
3594-3593	-5.64486
3593-3592	1.56596
3592-3591	.26493
3591-3590	-1.35405
3590-3589	-.69033
3589-3588	0.0
3588-3587	0.0
TOTAL	2.45586

27°N UPPER WATER

STAT NO.	STAT TOTAL	SFC	NAC
5343-5342	.13942	.13942	0.0
5342-5341	.50616	.46458	.04159
5341-5340	.93047	.74721	.18326
5340-5339	2.15102	1.82379	.32723
5339-5338	2.73575	2.17764	.55811
5338-5337	5.22364	3.74867	1.47497
5337-5336	.64035	-.30703	.94738
5336-5335	.93804	.85477	.08327
5335-5334	.08872	.08872	0.0
TOTAL	13.35357		

32°N UPPER WATER

STAT NO.	STAT TOTAL	SFC	NAC
5293-5294	.02976	.02976	0.0
5294-5295	-.20966	-.20966	0.0
5295-5296	.63670	.44328	.19342
5296-5297	1.89598	1.24678	.64920
5297-5298	4.75840	1.95149	2.80691
5298-5299	22.31201	10.09817	12.21384
5299-5301	22.18105	5.86380	16.31725
5301-5302	4.40468	2.98447	1.42021
5302-5303	2.94194	2.27507	.66687
5303-5304	-1.06250	-.32296	-.73954
5304-5305	-7.57239	-6.24843	-1.32396
5305-5306	-5.00832	-3.89252	-1.11580
5306-5307	-3.41771	-2.36590	-1.05181
5307-5308	10.62174	7.90705	2.71468
5308-5309	.95512	.74170	.21342
5309-5310	1.44368	1.12902	.31466
5310-5311	4.98524	4.09717	.88807
5311-5312	-12.13440	-9.74656	-2.38784
5312-5564	-4.53284	-3.04284	-1.49000
5564-5203	2.09002	1.92367	.16635
5203-5204	-6.52051	-4.97519	-1.54532
5204-5205	10.32867	7.34940	2.97927
5205-5206	.40475	.76413	-.35938
5206-5207	-13.90942	-10.47902	-3.43040
5207-5208	3.92797	2.95398	.97399
5208-5209	-3.86884	-2.38756	-1.48128
5209-5210	-5.01550	-3.43319	-1.58231
5210-3625	2.38197	1.49869	.88328
3625-3626	.72253	.06318	.65935
3626-3627	3.36381	1.80013	1.56368
3627-3628	-3.17552	-1.37158	-1.80394
3628-3629	-9.97327	-6.04966	-3.92361
3629-3630	5.67104	3.33868	2.33236
3630-3631	-1.58173	-1.20971	-.37202
3631-3632	.71572	.93615	-.22043
3632-3633	-2.59478	-2.38538	-.20940
3633-3634	.69865	.50516	.19349
3634-3635	-.95131	-.81745	-.13386
3635-3636	-.44661	-.23597	-.21064
3636-3637	-3.22584	-1.25925	-1.96659
3637-3638	1.56640	.93808	.62832
3638-3639	-2.26965	-1.33136	-.93829
3639-3640	-1.15142	-.56128	-.59014
3640-3641	.12471	-.10411	.22882
3641-3642	-2.27938	-1.13049	-1.14889
3642-3643	-.43450	-.27069	-.16381
3643-3644	1.23166	.49549	.73617
3644-3645	-.78854	-.56856	-.21998
3645-3646	-1.93153	-.36000	-1.57153
3646-3647	-1.77553	-.74527	-1.03026
3647-3648	.66468	.42725	.23743
3648-3649	.27891	.18725	.09166
3649-3650	0.0	0.0	0.0
TOTAL	15.50609		

32°N INTERMEDIATE WATER

STAT NO.	STAT TOTAL	MIW	MED
5293-5294	0.0	0.0	0.0
5294-5295	.08775	.08775	0.0
5295-5296	.10971	.10971	0.0
5296-5297	.40516	.40516	0.0
5297-5298	.93623	.93623	0.0
5298-5299	1.83973	1.83973	0.0
5299-5301	-.60331	-.60331	0.0
5301-5302	-1.89340	-1.89340	0.0
5302-5303	-.77625	-.77625	0.0
5303-5304	.25336	.25336	0.0
5304-5305	.52083	.52083	0.0
5305-5306	.32049	.32049	0.0
5306-5307	.06405	.06405	0.0
5307-5308	-.42450	-.42450	0.0
5308-5309	-.84165	-.84165	0.0
5309-5310	-.41493	-.41493	0.0
5310-5311	-.55318	-.55318	0.0
5311-5312	2.90975	3.03106	-.12131
5312-5564	.53183	.53183	0.0
5564-5203	-.31041	-.30277	-.00764
5203-5204	-.09471	.03465	-.12936
5204-5205	-6.31716	-6.49939	.18223
5205-5206	2.15106	2.15106	0.0
5206-5207	.99082	.99082	0.0
5207-5208	.27939	.27939	0.0
5208-5209	.51552	.51552	0.0
5209-5210	.60868	.60868	0.0
5210-3625	.30462	.30462	0.0
3625-3626	-2.57434	-2.67826	.10392
3626-3627	-.90421	-1.09767	.19346
3627-3628	1.33164	1.50995	-.17831
3628-3629	-.37857	-.21603	-.16254
3629-3630	-3.12045	-3.42810	.30765
3630-3631	-.17600	-.21114	.03514
3631-3632	.34905	.57149	-.22244
3632-3633	-1.24906	-1.37161	.12255
3633-3634	-1.23445	-1.23270	-.00175
3634-3635	-1.50267	-1.16858	-.33409
3635-3636	2.32751	1.96618	.36133
3636-3637	.16193	.31455	-.15262
3637-3638	-.31336	-.39505	.08169
3638-3639	1.52485	1.54960	-.02475
3639-3640	-.69881	-.51739	-.18142
3640-3641	.50535	.38677	.11858
3641-3642	.19878	.29488	-.09610
3642-3643	1.21633	1.19386	.02247
3643-3644	-4.96106	-3.29546	-1.66560
3644-3645	-1.80010	-1.15766	-.64244
3645-3646	2.20254	2.04158	.16096
3646-3647	-2.70624	-1.87863	-.82761
3647-3648	-5.17714	-2.20369	-2.97345
3648-3649	-.05630	0.0	-.05630
3649-3650	0.0	0.0	0.0
TOTAL	-16.98194*		

*Total contains -.54664 mass units from bottom area of stations 3648-3649 not included in the above summary.

32°N DEEP AND BOTTOM WATER

STAT NO.	STAT TOTAL (ALL WATER IS NAD)
5293-5294	0.0
5294-5295	-.14073
5295-5296	-.35281
5296-5297	-.00427
5297-5298	-1.00934
5298-5299	-3.07328
5299-5301	-6.65255
5301-5302	-9.93086
5302-5303	-3.50470
5303-5304	-.27033
5304-5305	7.56952
5305-5306	.28872
5306-5307	3.84289
5307-5308	-3.37894
5308-5309	1.96654
5309-5310	-7.29261
5310-5311	-3.95432
5311-5312	24.53632
5312-5564	3.30069
5564-5203	-3.38433
5203-5204	9.92456
5204-5205	-27.62533
5205-5206	11.99174
5206-5207	10.38506
5207-5208	2.77542
5208-5209	2.52036
5209-5210	6.13964
5210-3625	-1.97510
3625-3626	-10.96918
3626-3627	-3.20511
3627-3628	4.73687
3628-3629	2.27673
3629-3630	-4.31168
3630-3631	-.50523
3631-3632	1.50072
3632-3633	-1.58014
3633-3634	-1.92638
3634-3635	-1.55010
3635-3636	3.45122
3636-3637	1.72430
3637-3638	-.43513
3638-3639	2.73125
3639-3640	-.82500
3640-3641	-.32340
3641-3642	.82914
3642-3643	5.45383
3643-3644	-7.32136
3644-3645	-2.46785
3645-3646	5.15309
3646-3647	-2.54292
3647-3648	-1.06637
3648-3649	0.0
3649-3650	0.0
TOTAL	1.51926

36°N UPPER WATER

STAT NO.	STAT TOTAL	SFC	NAC
18-19	-.03601	-.03601	0.0
19-20	.14504	.07040	.07464
20-21	-.92198	-.36333	-.55864
21-22	1.14382	.80194	.34188
22-23	-.99780	-.52709	-.47071
23-24	-.28286	-.16570	-.11716
24-25	-.47079	-.42929	-.04150
25-26	.40873	.40522	.00351
26-27	.42862	.24804	.18054
27-28	1.79916	1.16361	.63555
28-29	4.81280	2.31438	2.49842
29-30	19.82719	6.23256	13.59463
30-31	13.79654	9.25528	4.54126
31-32	-14.81871	-10.44710	-4.37161
32-33	21.91861	13.09026	8.82835
33-34	15.96383	12.71794	3.24589
34-35	-3.45635	-3.45123	-.00512
35-36	-1.30261	-.74899	-.55362
36-37	-3.23962	-2.22475	-1.01487
37-38	-22.89120	-15.73201	-7.15919
38-39	18.93819	12.28772	6.65047
39-40	-6.54181	-4.55049	-1.99132
40-41	-17.06665	-10.46823	-6.59842
41-42	2.96643	1.37034	1.59609
42-43	-1.91020	-1.04900	-.86120
43-44	1.63104	.97921	.65183
44-45	-10.59629	-5.39943	-5.19686
45-46	13.83881	6.74651	7.09230
46-47	12.61871	7.63479	4.98392
47-48	13.55607	9.85415	3.70192
48-49	-16.37634	-11.38845	-4.98789
49-50	-28.08490	-11.89505	-16.18985
50-51	14.41843	4.08020	10.33823
51-52	-4.27903	-2.78979	-1.48925
52-53	2.50956	1.23884	1.27072
53-54	3.48090	1.56127	1.91963
54-55	-6.62879	-3.00458	-3.62421
55-56	-.45492	-.10089	-.35403
56-57	-1.54988	-.58363	-.96625
57-58	-4.68197	-1.32142	-3.36055
58-59	3.79552	1.28066	2.51486
59-60	-1.33435	-.24944	-1.08491
60-61	.89861	-.07368	.97229
61-62	-1.31813	-.40736	-.91077
62-63	2.43387	.53557	1.89830
63-64	-2.93210	-.67272	-2.25938
64-65	.53373	.14296	.39077

36°N UPPER WATER- CONTINUED

STAT NO.	STAT TOTAL	SFC	NAC
65-66	1.62668	.40517	1.22151
66-67	-3.42892	-1.16763	-2.26129
67-68	-2.47979	-.57672	-1.90307
68-69	1.30545	.30962	.99583
69-70	2.55489	.67487	1.88002
70-71	-2.67502	-.73291	-1.94211
71-72	.38389	.09011	.29378
72-73	1.03943	.48487	.55456
73-74	.10156	.04385	.05771
74-75	-.39723	-.21658	-.18065
75-76	-.20210	-.20210	0.0
76-77	.00605	.00605	0.0
TOTAL	17.52581		

36°N INTERMEDIATE WATER

STAT NO.	STAT TOTAL	MIW	MED
18-19	0.0	0.0	0.0
19-20	.12119	.12119	0.0
20-21	-.33338	-.33338	0.0
21-22	.32365	.32365	0.0
22-23	-.72691	-.72691	0.0
23-24	-.25768	-.25768	0.0
24-25	.08429	.08429	0.0
25-26	-.13803	-.13803	0.0
26-27	-.09363	-.09363	0.0
27-28	.65239	.65239	0.0
28-29	.83370	.83370	0.0
29-30	1.22073	1.22073	0.0
30-31	.62257	.62257	0.0
31-32	-.39442	-.39442	0.0
32-33	.53909	.53909	0.0
33-34	-1.29913	-1.29913	0.0
34-35	-.10286	-.10286	0.0
35-36	.58265	.58265	0.0
36-37	.08138	.08138	0.0
37-38	.66444	.66444	0.0
38-39	-.61185	-.61185	0.0
39-40	-.68731	-.68731	0.0
40-41	-.49844	-.49844	0.0
41-42	-.00487	-.00487	0.0
42-43	-.00678	-.00678	0.0
43-44	-.25321	-.25321	0.0
44-45	.16978	.16978	0.0
45-46	-.07968	-.07968	0.0
46-47	-.57701	-.57701	0.0
47-48	-1.19516	-1.19516	0.0
48-49	1.66396	1.66396	0.0
49-50	.47279	.47279	0.0
50-51	-.42126	-.42126	0.0
51-52	.19264	.20835	-.01571
52-53	-.26007	-.27223	.01226
53-54	-.18331	-.26018	.07687
54-55	-.68592	-.56605	-.11987
55-56	-.17781	-.11570	-.06211
56-57	2.43134	2.31977	.11157
57-58	-.24287	.33683	-.57970
58-59	.27212	-.09360	.36572
59-60	.07708	.27154	-.19446
60-61	-.80131	-1.20673	.40542
61-62	.44901	.56273	-.11372
62-63	.03679	-.09849	.13528
63-64	.19234	.21261	-.02027
64-65	-.78934	-.69665	-.09269

36°N INTERMEDIATE WATER- CONTINUED

STAT NO.	STAT TOTAL	NIW	MED
65-66	-.89863	-.72384	-.17479
66-67	-.06741	-.23259	.16518
67-68	.31001	.32971	-.01970
68-69	-1.35608	-1.04260	-.31348
69-70	1.45651	1.09457	.36194
70-71	1.30968	.80373	.50595
71-72	-1.05063	-.69287	-.35776
72-73	-.50471	-.50471	0.0
73-74	.09813	.09813	0.0
74-75	.75777	.75777	0.0
75-76	0.0	0.0	0.0
76-77	0.0	0.0	0.0
TOTAL	.62068*		

* This total contains -.29564 mass units contributed by the bottom peripheral areas of the following stations: -.58417 units from station pair 72-73 ; .12257 units from station pair 73-74; and .16596 units from station pair 74-75.

36°N DEEP AND BOTTOM WATER

STAT NO.	STAT TOTAL (ALL WATER IS NAD)
18-19	0.0
19-20	.15680
20-21	.53057
21-22	-.07403
22-23	1.54217
23-24	-.40487
24-25	-.80570
25-26	.45022
26-27	-.36578
27-28	-.45610
28-29	-3.65122
29-30	-12.05018
30-31	-5.46189
31-32	5.64814
32-33	-8.86169
33-34	-1[illegible].55914
34-35	-1.20714
35-36	2.96859
36-37	-.69886
37-38	20.38948
38-39	-15.61164
39-40	4.73402
40-41	8.69133
41-42	-4.32715
42-43	9.73861
43-44	-4.68205
44-45	13.24583
45-46	-14.57470
46-47	-15.52757
47-48	-11.69013
48-49	17.12689
49-50	23.94253
50-51	-9.62460
51-52	1.77155
52-53	-1.05768
53-54	-.95446
54-55	-.21808
55-56	0.0
56-57	0.0
57-58	.15434
58-59	-.06792
59-60	.30511
60-61	-1.60163
61-62	1.24348
62-63	-.43909
63-64	1.23135
64-65	-.79077

36°N DEEP AND BOTTOM WATER- CONTINUED

STAT NO.	STAT TOTAL (ALL WATER IS NAD)
65-66	-3.64039
66-67	.60408
67-68	.12472
68-69	-.81671
69-70	.43942
70-71	5.44905
71-72	-.72958
72-73	0.0
73-74	0.0
74-75	0.0
75-76	0.0
76-77	0.0
TOTAL	-18.46247

40° N UPPER WATER

STAT NO.	STAT TOTAL	SFC	NAC
218-219	-.04788	-.03583	-.01205
219-220	5.21774	1.70588	3.51186
220-221	-.96065	.23393	-1.19458
221-222	-.19006	-.18203	-.00803
222-223	10.38285	3.00718	7.37567
223-224	-7.67326	-1.98048	-5.69278
224-225	.04960	.06036	-.01076
225-226	-1.30019	-.51937	-.78082
226-227	27.83837	12.12414	15.71423
227-228	-30.27794	-7.30474	-22.97320
228-229	2.27416	1.19430	1.07986
229-230	-1.61474	-.71312	-.90162
230-231	14.09853	3.58525	10.51328
231-232	-12.23265	-4.72620	-7.50645
232-233	-5.21509	-1.65181	-3.56328
233-234	12.92696	4.48559	8.44137
234-235	20.89605	3.09161	17.80444
235-236	-10.14042	-1.40635	-8.73407
236-237	-11.44643	-2.43838	-9.00805
237-238	8.10690	1.43768	6.66922
238-239	-6.48199	-1.35873	-5.12326
239-240	7.20672	1.21143	5.99529
240-241	-5.81490	-.95434	-4.86056
241-242	-.22323	-.09638	-.12685
242-243	1.50425	.16422	1.34003
243-244	3.06300	.36950	2.69350
244-245	-2.47102	-.48772	-1.98330
245-246	-.00699	-.01844	.01145
246-247	-4.18647	-.57803	-3.60844
247-248	3.67331	.48586	3.18745
248-249	-.47383	-.07633	-.39750
249-250	-1.01936	-.19144	-.82792
250-251	-.55086	-.32397	-.22689
251-252	-.28913	-.00874	-.28039
252-253	-.46120	-.09350	-.36770
253-254	.07594	.05034	.02560
254-255	.03691	.03691	0.0
TOTAL	14.43674*		

* This total contains .16374 mass units contributed by the bottom peripheral area of stations 254-255 not included in the above summary.

40°N INTERMEDIATE WATER

STAT NO.	STAT TOTAL	MIW	MED	NAI
218-219	0.0	0.0	0.0	0.0
219-220	2.62171	1.79335	0.0	.82837
220-221	-2.61501	-.96222	0.0	1.65279
221-222	.04745	.04745	0.0	0.0
222-223	1.57072	1.57072	0.0	0.0
223-224	-.99491	-.99491	0.0	0.0
224-225	.13776	.13776	0.0	0.0
225-226	-.22663	-.22663	0.0	0.0
226-227	4.31605	2.44990	1.86615	0.0
227-228	-4.49205	-2.59960	-1.89245	0.0
228-229	.17960	.17960	0.0	0.0
229-230	-.19700	-.19700	0.0	0.0
230-231	3.00265	2.29768	.70497	0.0
231-232	-2.63093	-2.01226	-.61867	0.0
232-233	-1.94039	-1.94039	0.0	0.0
233-234	3.13593	3.13593	0.0	0.0
234-235	4.81552	1.97984	2.83568	0.0
235-236	-.83146	-.83146	0.0	0.0
236-237	-2.58909	-1.54566	-1.04343	0.0
237-238	1.54188	-.01488	1.55676	0.0
238-239	-1.03440	-.30385	-.73055	0.0
239-240	1.56927	.90190	.66737	0.0
240-241	-1.28488	-.75064	-.53424	0.0
241-242	.27035	.08141	.18894	0.0
242-243	.37627	-.07513	.45140	0.0
243-244	.26629	-.26783	.53412	0.0
244-245	-.04355	.22365	-.26720	0.0
245-246	-.02802	.17271	-.20073	0.0
246-247	-.52602	.18442	-.71044	0.0
247-248	.56730	-.26282	.83012	0.0
248-249	-.43430	-.55174	.11744	0.0
249-250	-.10412	-.14524	.04112	0.0
250-251	-.07136	-.01901	-.05235	0.0
251-252	.19781	.23061	-.03280	0.0
252-253	-.23334	-.37261	.13927	0.0
253-254	-.54460	.34856	-.89316	0.0
254-255	0.0	0.0	0.0	0.0
TOTAL	3.68615*			

* This total contains -.10835 mass units contributed by the bottom peripheral areas of the following stations: -.09110 units from station pair 241-242; and -.01725 units from station pair 242-243.

40°N DEEP AND BOTTOM WATER

STAT NO.	STAT TOTAL (ALL WATER IS NAD)
218-219	0.0
219-220	0.0
220-221	.19147
221-222	-.70677
222-223	-9.27722
223-224	10.94129
224-225	1.58421
225-226	-7.56315
226-227	-15.61833
227-228	16.26318
228-229	.73626
229-230	2.78113
230-231	-9.35389
231-232	5.55042
232-233	8.00027
233-234	-18.40148
234-235	-17.95566
235-236	1.65467
236-237	22.21143
237-238	-17.80792
238-239	9.91281
239-240	-2.22031
240-241	.13494
241-242	0.0
242-243	0.0
243-244	-.50899
244-245	1.82697
245-246	1.47397
246-247	3.19672
247-248	-4.81305
248-249	-2.05300
249-250	1.68681
250-251	.24704
251-252	2.36107
252-253	-.69757
253-254	-1.91959
254-255	0.0
TOTAL	-18.142267

48°N UPPER WATER

STAT NO.	STAT TOTAL	SFC	NAC
3509-3510	-.00981	-.00981	0.0
3510-3511	-.15161	-.15161	0.0
3511-3512	-.53552	-.53552	0.0
3512-3513	.84282	.84282	0.0
3513-3514	1.29535	1.29535	0.0
3514-3515	-.67930	-.67930	0.0
3515-3516	-.71278	-.71278	0.0
3516-3517	-.36541	-.36541	0.0
3517-3518	1.71756	1.71756	0.0
3518-3519	2.21573	2.21573	0.0
3519-3520	-.55629	-.55629	0.0
3520-3521	-1.23456	-1.23456	0.0
3521-3522	6.41815	3.99011	2.42804
3522-3523	17.03908	3.86525	13.17383
3523-3524	-1.47752	-.06010	-1.41742
3524-3525	-7.54162	-1.97081	-5.57081
3525-3526	-4.16548	-1.04673	-3.11875
3526-3527	-6.94611	-2.17632	-4.76979
3527-3528	1.00725	.40910	.59815
3528-3529	1.03338	.41257	.62081
3529-3530	4.89086	1.56058	3.33028
3530-3531	-5.94717	-1.97482	-3.97235
3531-3532	6.98923	2.04339	4.94584
3532-3533	1.81258	.29875	1.51383
3533-3534	-.35963	-.08926	-.27037
3534-3535	-3.78857	-.82127	-2.96730
3535-3536	2.47470	.65940	1.81530
3536-3537	-.90544	-.33530	-.57014
3537-3538	-1.86396	-.56325	-1.30071
3538-3539	3.68074	.88576	2.79498
3539-3540	-3.19582	-.72731	-2.46851
3540-3541	1.56617	.33683	1.22934
3541-3542	-.17904	-.05062	-.12842
3542-3543	.47447	.13179	.34268
3543-3544	.03057	.00643	.02414
3544-3545	-.03639	-.03358	-.00281
3545-3546	-.00770	-.00770	0.0
3546-3547	.00585	.00585	0.0
3547-3548	.00289	.00289	0.0
TOTAL	12.83765		

48°N INTERMEDIATE WATER

STAT NO.	STAT TOTAL	MIW	MED	NAI
3509-3510	0.0	0.0	0.0	0.0
3510-3511	0.0	0.0	0.0	0.0
3511-3512	-.67318	-.05702	0.0	-.61616
3512-3513	.41689	.10413	0.0	.31276
3513-3514	1.10080	.53201	0.0	.56879
3514-3515	-.49992	-.22803	0.0	-.27189
3515-3516	-.44236	-.28556	0.0	-.15680
3516-3517	-.17099	-.10245	0.0	-.06854
3517-3518	.69397	.18753	0.0	.50644
3518-3519	3.42882	2.96343	0.0	.46539
3519-3520	-.20883	-.17198	0.0	-.03685
3520-3521	-1.68176	-1.03406	0.0	-.64770
3521-3522	2.82592	1.76582	0.0	1.06010
3522-3523	1.79552	1.79552	0.0	0.0
3523-3524	.42217	.42217	0.0	0.0
3524-3525	-.83182	-.83182	0.0	0.0
3525-3526	-.97029	-.97029	0.0	0.0
3526-3527	-1.43363	-1.43363	0.0	0.0
3527-3528	.67024	.67024	0.0	0.0
3528-3529	-.67521	-.67521	0.0	0.0
3529-3530	1.37737	1.37737	0.0	0.0
3530-3531	-1.26854	-1.26854	0.0	0.0
3531-3532	.15823	.15823	0.0	0.0
3532-3533	-.44624	-.44624	0.0	0.0
3533-3534	.11933	.11933	0.0	0.0
3534-3535	-.35591	-.35591	0.0	0.0
3535-3536	-.10297	-.31489	.21192	0.0
3536-3537	.19792	.35745	-.15953	0.0
3537-3538	-.45640	.02806	-.48446	0.0
3538-3539	-.31704	-1.01762	.70058	0.0
3539-3540	.18956	.55299	-.36343	0.0
3540-3541	1.09598	-.11268	1.0191	0.0
3541-3542	-.07626	-.06174	-.01452	0.0
3542-3543	-.42285	-.34850	-.07435	0.0
3543-3544	.08868	-.00186	.09054	0.0
3544-3545	.15415	.15415	0.0	0.0
3545-3546	0.0	0.0	0.0	0.0
3546-3547	0.0	0.0	0.0	0.0
3547-3548	0.0	0.0	0.0	0.0
TOTAL	3.80428*			

* This total contains .10294 mass units contributed by the bottom peripheral areas of the following stations: .02537 units from station pair 3543-3544; .05809 units from station pair 3544-3545; and .01948 units from station pair 3545-3546.

48°N DEEP AND BOTTOM WATER

STAT NO.	STAT TOTAL (ALL WATER IS NAD)
3509-3510	0.0
3510-3511	0.0
3511-3512	.85412
3512-3513	-.16718
3513-3514	-2.04567
3514-3515	.11280
3515-3516	1.29288
3516-3517	1.45585
3517-3518	-3.58715
3518-3519	-8.12712
3519-3520	-3.08709
3520-3521	-8.08643
3521-3522	1.70124
3522-3523	-17.55530
3523-3524	5.78760
3524-3525	9.01827
3525-3526	7.22985
3526-3527	3.98344
3527-3528	1.39936
3528-3529	-.19862
3529-3530	-2.90514
3530-3531	1.78800
3531-3532	-4.91310
3532-3533	-1.72700
3533-3534	1.75836
3534-3535	1.44476
3535-3536	-10.93589
3536-3537	3.68454
3537-3538	5.27132
3538-3539	-11.87332
3539-3540	7.57365
3540-3541	2.37592
3541-3542	3.08240
3542-3543	-1.24236
3543-3544	0.0
3544-3545	0.0
3545-3546	0.0
3546-3547	0.0
3547-3548	0.0
TOTAL	-16.63701

APPENDIX B

MASS, SALT, AND HEAT TRANSPORT ESTIMATES FOR PERIPHERAL AREAS

In calculating the estimated values of mass, salt, and heat transport for the peripheral areas the following procedure was followed.

Temperature and salinity information was obtained for the area and month of interest from the Fleet Numerical Weather Central's "HYDAT" program. The program output supplied all available temperature and salinity data for the area and month requested as well as computing temperature statistics. If no data were found to exist for the desired area, the closest station's temperature and salinity data were considered representative of the entire area (this occurred for the 8^{o}N western peripheral area and the 32^{o}N eastern peripheral area).

Next, the monthly average surface current velocity was taken from the "Pilot Chart of the North Atlantic Ocean" for the month of interest. This value was assumed to equal the geostrophic surface current velocity. A linear decrease in velocity was assumed with zero velocity at the bottom. Therefore, a value of one-half the surface current velocity was considered to equal the mean current velocity for the entire area.

The value of average current velocity was then multiplied by the peripheral area (Table II) and the average density value of 1.02395 gm/cm^3 (Greeson, 1974),determining the mass transport. This value was in turn multiplied by the mean temperature and salinity values for the peripheral area,determining the salt and heat transport.

The results of this study are contained on the following pages.

I. $48^{o}N$

A. WEST AREA

$T = -.23^{o}C$
$S = 33.26\ ^{o}/_{oo}$
$AREA = 2.35 \times 10^{11}\ cm^2$
VEL =-10.16cm/sec
$MASS\ T = -2.44 \times 10^{12}$ gm/sec
$SALT\ T = -81.31 \times 10^{12}\ ^{o}/_{oo}$/sec
$HEAT\ T = -667.25 \times 10^{12}$cal/sec

B. EAST AREA

$T = 11.35^{o}C$
$S = 35.56\ ^{o}/_{oo}$
$AREA = 1.25 \times 10^{11} cm^2$
VEL = 10.16cm/sec
$MASS\ T = 1.30 \times 10^{12}$ gm/sec
$SALT\ T = 46.24 \times 10^{12}\ ^{o}/_{oo}$/sec
$HEAT\ T = 369.98 \times 10^{12}$ cal/sec

$TOTAL\ MASS\ TRANS = -1.14 \times 10^{12}$ gm/sec
$TOTAL\ SALT\ TRANS = -35.07 \times 10^{12}\ ^{o}/_{oo}$/sec
$TOTAL\ HEAT\ TRANS = -270.27 \times 10^{12}$ cal/sec

II. $40^{o}N$ (Values taken from Greeson, 1974, Table IV)

A. WEST AREA

$MASS\ T = -6.439 \times 10^{12}$ gm/sec
$SALT\ T = -213.540 \times 10^{12}\ ^{o}/_{oo}$/sec
$HEAT\ T = -1842.942 \times 10^{12}$ cal/sec

B. EAST AREA

$MASS\ T = -.128 \times 10^{12}$ gm/sec
$SALT\ T = -4.589 \times 10^{12}\ ^{o}/_{oo}$/sec
$HEAT\ T = -32.026 \times 10^{12}$ cal/sec

$TOTAL\ MASS\ TRANS = -6.567 \times 10^{12}$ gm/sec
$TOTAL\ SALT\ TRANS = -218.129 \times 10^{12}\ ^{o}/_{oo}$/sec
$TOTAL\ HEAT\ TRANS = -1874.968 \times 10^{12}$ cal/sec

III. $36^{o}N$

A. WEST AREA

$T = 19.82^{o}C$
$S = 36.09\ ^{o}/_{oo}$
$AREA = 6 \times 10^{10}\ cm^2$
VEL =-20.3 cm/sec
$MASS\ T = -1.24 \times 10^{12}$ gm/sec
$SALT\ T = -45.01 \times 10^{12}\ ^{o}/_{oo}$/sec
$HEAT\ T = -365.40 \times 10^{12}$ cal/sec

B. EAST AREA

$T = 13.27^{o}C$
$S = 35.96\ ^{o}/_{oo}$
$AREA = 1 \times 10^{10}\ cm^2$
VEL =-12.7 cm/sec
$MASS\ T = -.13 \times 10^{12}$ gm/sec
$SALT\ T = -4.67 \times 10^{12}\ ^{o}/_{oo}$/sec
$HEAT\ T = -37.25 \times 10^{12}$ cal/sec

$TOTAL\ MASS\ TRANS = -1.37 \times 10^{12}$ gm/sec
$TOTAL\ SALT\ TRANS = -49.68 \times 10^{12}\ ^{o}/_{oo}$/sec
$TOTAL\ HEAT\ TRANS = -402.65 \times 10^{12}$ cal/sec

IV. $32^{o}N$

A. WEST AREA

$T = 17.87^{o}C$
$S = 35.96\ ^{o}/_{oo}$
$AREA = 6x10^{10}\ cm^2$
VEL =-20.3 cm/sec
$MASS\ T = -1.25x10^{12}$ gm/sec
$SALT\ T = -44.85x10^{12}\ ^{o}/_{oo}$/sec
$HEAT\ T = -362.96x10^{12}$ cal/sec

B. EAST AREA

$T = 17.21^{o}C$
$S = 36.38\ ^{o}/_{oo}$
$AREA = 3x10^{10}\ cm^2$
VEL =-12.7 cm/sec
$MASS\ T = -.39x10^{12}$ gm/sec
$SALT\ T = -14.19x10^{12}\ ^{o}/_{oo}$/sec
$HEAT\ T = -113.28x10^{12}$ cal/sec

TOTAL MASS TRANS = $-1.64x10^{12}$ gm/sec
TOTAL SALT TRANS = $-59.04x10^{12}\ ^{o}/_{oo}$/sec
TOTAL HEAT TRANS = $-476.24x\ 10^{12}$ cal/sec

V. $24^{o}N$

A. WEST AREA

$T = 14.39^{o}C$
$S = 35.77\ ^{o}/_{oo}$
$AREA = 5x10^{9}\ cm^2$
VEL = 12.7 cm/sec
$MASS\ T = .065x10^{12}$ gm/sec
$SALT\ T = 2.33x10^{12}\ ^{o}/_{oo}$/sec
$HEAT\ T = 18.69x10^{12}$ cal/sec

B. EAST AREA

$T = 18.62^{o}C$
$S = 36.33\ ^{o}/_{oo}$
$AREA = 6x10^{10}\ cm^2$
VEL = -12.7 cm/sec
$MASS\ T = .78x10^{12}$ gm/sec
$SALT\ T = -28.16x10^{12}\ ^{o}/_{oo}$/sec
$HEAT\ T = -226.13x10^{12}$ cal/sec

TOTAL MASS TRANS = $-.71x10^{12}$ gm/sec
TOTAL SALT TRANS = $-25.83x10^{12}\ ^{o}/_{oo}$/sec
TOTAL HEAT TRANS = $-207.44x10^{12}$ cal/sec

VI. $16^{o}N$

A. WEST AREA

No peripheral area associated with this section.

B. EAST AREA

No net meridional transports in this section. Peripheral area is characterized by opposing currents of equal magnitude.

TOTAL MASS TRANS = 0.0
TOTAL SALT TRANS = 0.0
TOTAL HEAT TRANS = 0.0

VII. $8^{o}N$

A. WEST AREA

$T = 14.79^{o}C$

$S = 34.99\ ^{o}/_{oo}$

$AREA = 2x10^{10}\ cm^{2}$

$VEL = 25.4\ cm/sec$

$MASS\ T = 0.52x10^{12}\ gm/sec$

$SALT\ T = 18.2x10^{12}\ ^{o}/_{oo}/sec$

$HEAT\ T = 149.78x10^{12}\ cal/sec$

$TOTAL\ MASS\ TRANS = 0.52x10^{12}\ gm/sec$

$TOTAL\ SALT\ TRANS = 18.2x10^{12}\ ^{o}/_{oo}/sec$

$TOTAL\ HEAT\ TRANS = 149.78x10^{12}\ cal/sec$

B. EAST AREA

No net meridional transport in this area. Peripheral area is characterized by zonal currents.

BIBLIOGRAPHY

1. Bjerknes, V.F.K., and others, Physicalische Hydrodynamic, Julius Springer, 1933.

2. Bryan, K., "Measurement of Meridional Heat Transport by Ocean Currents," Journal of Geophysical Research, v. 67, no. 9, pp. 3403-2414, 1962.

3. Budyko, M.I., The Heat Balance of the Earth's Surface, U.S. Department of Commerce, 1956.

4. Cummings, W.J., A Description of the General Circulation in the North Atlantic Ocean Based on Mass Transport Values derived from IGY (1957-1958) Temperature and Salinity Data, Master's Thesis, Naval Postgraduate School, Monterey, CA, 1977.

5. Defant, A., Die absolute Topographic des physisikalischen Meeresniveaus und der Druckflachen, sowie die Wasserbewegungen im Atlantischen Ozean. Wiss. Ergebn. D. Deutschen Atlantischen Exped. auf d. Forschungs - u. Vermessungsschiff 'Meteor' - 1925-1927, v. VI (2 Teil., 5 Leif.), Walter De Gruyter and Co., 1941.

6. Defant, A., Physical Oceanography, v. 1, Pergamon Press, 1961

7. Fomin, L. M., The Dynamic Method in Oceanography, pp. 117-148, Elsevier Publishing Co., 1964.

8. Fuglister, F.C., Atlantic Ocean Atlas of Temperature and Salinity Profiles and Data from the International Geophysical Year of 1957-1958, v. 1, Woods Hole Oceanographic Institution, 1960.

9. Greeson, T.D., Mass, Salt, and Heat Transport Across 40^{o}N Latitude in the Atlantic Ocean Based on IGY Data and Dynamic Height Calculations, Master's Thesis, Naval Postgraduate School, Monterey, CA, 1974.

10. Haltiner, G.J. and Martin, F.L., Dynamic and Physical Meteorology, p. 13, McGraw-Hill, 1957.

11. Hidaka, K., "Depth of motionless layer as inferred from the distribution of salinity in the ocean," Trans. Am. Geophys. Union, v. 30, no. 3, 1940.

12. Ivers, W.D., The Deep Circulation in the North Atlantic, with Especial Reference to the Labrador Sea, Ph.D. Thesis, University of California, San Diego, 1975.

13. Jacobsen, J.P., "Contribution to the hydrography of the Atlantic," Medd. Komm. Havundersgelser, Ser. Hydrografi, v. 2, 1916.

14. Jung, G.H., "Note on the Meridional Transport of Energy By The Oceans," Journal of Marine Research, v. XI, no. 2, pp. 139-146, 15 Nov 1952.

15. Jung, G.H., Heat Transport in the North Atlantic Ocean, Ph.D. Thesis, The A.&M. College of Texas, College Station, TX, 1955.

16. Jung, G.H., Energy Transport by Air and Sea, The Dynamic North, Book I, OPNAV P03-8, Chief of Naval Operations, Tech. Asst. for Polar Projects, pp. 1-16, 1956.

17. Metcalf, W.G., Oceanographic Data from Crawford Cruise 16, October - December 1957, from the International Geophysical Year 1957-1958, W.H.O.I. Reference No. 58-31, unpublished manuscript.

18. McCartney, M.S., Worthington, L.V., and Schmitz, W.J., "Large Cyclonic Rings From the Northeast Sargasso Sea," Journal of Geophysical Research, v. 83, no. C2, pp. 901-914, 20 February 1978.

19. Neumann, G. and Pierson, W.J., Jr ., Principles of Physical Oceanography, pp. 244-247, Prentice-Hall, 1966.

20. Parker, C.E., "Gulf Stream rings in the Sargasso Sea," Deep-Sea Research, v. 18, pp. 981-993, 1971.

21. Parr, A., "Analysis of current profiles by a study of pycnomeric distortion and identifying properties," Journal of Marine Research, v. 4, 1938.

22. Richardson, P., "Gulf Stream Rings," Oceanus, v. 19, no. 3, pp. 65-68, 1976.

23. Robinson, A.R., "Eddies and Ocean Circulation," Oceanus, v. 19, no. 3, pp. 2-17, 1976.

24. Schmitz, W.J., "On the deep general circulation in the Western North Atlantic," Journal of Marine Research, v. 35, pp. 21-28, February 1977.

25. Sellers, W.D., Physical Climatology, University of Chicago Press, 1965.

26. Stommel, H., "On the determination of the depth of no meridional motion," Deep-Sea Research, v. 3, pp. 273-278, 1956.

27. Stommel, H. and Schott, F., "The Beta Spiral and the determination of the absolute velocity field from hydrographic station data," Deep-Sea Research, v. 24, pp. 325-329, 1977.

28. Sverdrup, H.U., Johnson, M.W., and Fleming, R.H., The Oceans: Their Physics, Chemistry, and General Biology, Prentice-Hall, 1942.

29. Sverdrup, H.U., Oceanography, Handbuch der Physik, Springer Verlag, 1957.

30. Tucholke, B.E., Wright, W.R., and Hollister, C.D., "Abyssal circulation over the Greater Antilles Outer Ridge," Deep-Sea Research, v. 20, pp. 973-995, November, 1973.

31. Vander Haar, T.H. and Oort, A.H., "New estimates of energy transport by northern hemisphere oceans," Journal of Physical Oceanography, v. 3, no. 2, pp. 169-172, 1973.

32. Wertheim, G.K., "Studies of the electrical potential between Key West, Florida and Havana, Cuba," Trans. Am. Geophys. Union, v. 35, pp. 872-882, 1954.

33. Williams, J., Higginson, J.J., and Rohrbough, J.D., Sea & Air: The Marine Environment, 2d, Ed.,p. 189, Naval Institute Press, 1968.

34. Worthington, L.V., Oceanographic Data From R.R.S. Discovery II From The International Geophysical Year Cruises 1 and 2, 1957, W.H.O.I. Reference No. 58-30, unpublished manuscript .

35. Worthington, L.V., On The North Atlantic Circulation, The Johns Hopkins University Press, 1976.

36. Wright, W.R. and Worthington, L.V., The water masses of the North Atlantic Ocean; a volumetric census of temperature and salinity. Serial Atlas of The Marine Environment, Folio 19, pp. 1-8, American Geographical Society, 1970.

INITIAL DISTRIBUTION LIST

		No. Copies
1.	Department of Oceanography, Code 68 Naval Postgraduate School Monterey, CA 93940	3
2.	Oceanographer of the Navy Code N-45 Hoffman Building No. 2 200 Stovall Street Alexandria, VA 22332	1
3.	Office of Naval Research Code 410 NORDA, NSTL Bay St. Louis, MS 39520	1
4.	Dr. Robert E. Stevenson Scientific Liaison Office, ONR Scripps Institution of Oceanography La Jolla, CA 92037	1
5.	Library, Code 3330 Naval Oceanographic Office Washington, DC 20373	1
6.	SIO Library University of California, San Diego P.O. Box 2367 La Jolla, CA 92037	1
7.	Department of Oceanography Library University of Washington Seattle, WA 98105	1
8.	Department of Oceanography Library Oregon State University Corvallis, OR 97331	1
9.	Commanding Officer Fleet Numerical Weather Central Monterey, CA 93940	1
10.	Commanding Officer Naval Environmental Prediction Research Facility Monterey, CA 93940	1

11. Department of the Navy — 1
Commander Oceanographic System Pacific
Box 1390
Pearl Harbor, HI 96860

12. Defense Documentation Center — 2
Cameron Station
Alexandria, VA 22314

13. Library (Code 0212) — 2
Naval Postgraduate School
Monterey, CA 93940

14. Director — 1
Naval Oceanography and Meteorology
National Space Technology Laboratories
Bay St. Louis, MS 39520

15. NORDA — 1
Bay St. Louis, MS 39520

16. Dr. Glenn H. Jung, Code 68Jg — 2
Department of Oceanography
Naval Postgraduate School
Monterey, CA 93940

17. Dr. J. J. von Schwind, Code 68Vs — 1
Department of Oceanography
Naval Postgraduate School
Monterey, CA 93940

18. LT T. L. Baker, USN — 2
12318 Overcup
Houston, TX 77024

19. Dr. Abraham H. Oort — 1
Geophysical Fluid Dynamics Laboratory/NOAA
Princeton University
P.O. Box 308
Princeton, NJ 08540

20. Director of Defense Research and Engineering — 1
Office of the Secretary of Defense
Washington, DC 20301
ATTN: Office, Assistant Director (Research)

21. Office of Naval Research
Arlington, VA 22217
ATTN: Code 480 — 3
ATTN: Code 460 — 1
ATTN: Code 102-OS — 1

22. Director
Naval Research Laboratory
Washington, DC 20390
ATTN: Library, Code 2029 (ONRL) 6
ATTN: Library, Code 2620 6

23. Commander
Naval Oceanographic Office
Washington, DC 20390
ATTN: Code 1640 1
ATTN: Code 70 1

24. NODC/NOAA 1
Rockville, MD 20882

25. ONR Branch Office 1
1030 E. Green St.
Pasadena, CA 91106

26. Dr. Kern Kenyon 1
A-030
University of California
Scripps Institution of Oceanography
La Jolla, CA 92093

27. Prof. J. L. Reid, Jr. 1
A-030
University of California
Scripps Institution of Oceanography
La Jolla, CA 92093

28. LT W. J. Cummings, USN 1
HSL-34
NAS Norfolk
Norfolk, VA 23511

29. Dean of Research, Code 012 1
Naval Postgraduate School
Monterey, CA 93940

thesB1725
Mass, salt, and heat transport across se
3 2768 001 91209 0
DUDLEY KNOX LIBRARY